Dott. Caterina Boniello

Towards rational design of immobilized biocatalysts through consideration of mass transfer effects

DISSERTATION

Zur Erlangung des akademischen Grades einer

Doktorin der technischen Wissenschaften

erreicht an der

Technischen Universität Graz

Univ. Prof. Dr. Bernd NIDETZKY

Institut für Biotechnologie und Bioprozesstechnik

Technische Universität Graz

2010

Deutsche Fassung:
Beschluss der Curricula-Kommission für Bachelor-, Master- und Diplomstudien vom 10.11.2008
Genehmigung des Senates am 1.12.2008

EIDESSTATTLICHE ERKLÄRUNG

Ich erkläre an Eides statt, dass ich die vorliegende Arbeit selbstständig verfasst, andere als die angegebenen Quellen/Hilfsmittel nicht benutzt, und die den benutzten Quellen wörtlich und inhaltlich entnommene Stellen als solche kenntlich gemacht habe.

Graz, am …… ……..
(Unterschrift)

Englische Fassung:

STATUTORY DECLARATION

I declare that I have authored this thesis independently, that I have not used other than the declared sources / resources, and that I have explicitly marked all material which has been quoted either literally or by content from the used sources.

…… ……..
date (signature)

Acknowledgements

Most of all I would like to thank my supervisor Prof. Bernd Nidetzky for the continuous support I received during these years: plenty of time for interesting discussions, suggestions, promotion of ideas, projects and cooperation, motivation, trust, enthusiasm.

A fruitful cooperation has been established with the Institute of Analytical Chemistry and Food Chemistry: I am very grateful to Dr. Torsten Mayr and Prof. Ingo Klimant for sharing their knowledge for the development of the applied experimental procedures and for the fruitful discussions.

Thanks to Dr. Waander Riethorst, Dr. Burghard Koenig and Dr. Ferdinand Zepeck from Sandoz GmbH for the fruitful and interesting discussions during the project meetings and for financial support.

Special thanks to Dr. Peter Remler for his important support as project leader.

For financial support the former Research Centre Applied Biocatalysis (now Austrian Center of Industrial Biotechnology – ACIB) is acknowledged.

Many thanks to my colleagues for being always willing to support, to listen, to help and for the nice atmosphere at work.

Abstract

Many industrial biocatalysts are used as immobilized enzyme preparations where the protein is tethered on the surface of a porous carrier. Easy separation from solution, recovery and enhanced operational stability provided by the immobilization make the biocatalyst reusable for further reaction cycles.

Diffusion of substrates might constitute the rate-limiting step for reaction catalyzed by immobilized enzymes. Accumulation of inhibiting or acidic products in porous carriers might strongly affect enzymatic activity.

This work provides a systematic and comprehensive investigation of mass transfer aspects in the model biocatalyst Cephalosporin C amidase immobilized on epoxy-activated commercial carriers, examining enzyme kinetic and providing methodology for the evaluation of intraparticle concentration gradients (substrate and pH).

Kinetic studies gave information about magnitude of substrate diffusion limitation and magnitude of pH gradients in the immobilized biocatalyst caused by an acidic product were evaluated applying a new non-invasive detection method. A reaction-diffusion model was applied to fit the obtained experimental results leading to estimation of diffusion and kinetic parameters as well as to calculation of concentration profiles in the enzyme carrier. Proper evaluation of intraparticle diffusion as result of this work allows for formulation of particles tailored for the biocatalyst to show optimized performances and provide a methodology that might be applicable in the rational design of immobilized enzymes in which the biocatalytic conversion results in a pH change.

Zusammenfassung

Viele industrielle Biokatalysatoren werden als immobilisierte Enzympräparationen verwendet. Dabei wird das Protein an der Oberfläche eines porösen Trägermaterials gebunden. Immobilisierte Enzyme haben den deutlichen Vorteil der einfachen Abtrennbarkeit aus der flüssigen Phase sowie erhöhter Stabilität im Prozess und Wiederverwendbarkeit.

Diffusion der Substrate stellt meist den geschwindigkeitslimitierenden Schritt der Reaktion durch immobilisierte Enzyme dar und die Enzymaktivität wird stark beeinflusst durch die Akkumulierung von inhibierenden oder stark polaren Produkten, die den pH-Wert erniedrigen.

Diese Arbeit beinhaltet eine systematische und umfassende Aufarbeitung von Massentransferaspekten mit dem Modellenzym Cephalosporin C Amidase, das an Epoxy-aktivierten kommerziell erhältlichen Trägermaterialien immobilisiert wurde. Dabei wurde das Hauptaugenmerk auf die kinetische Charakterisierung sowie die Entwicklung von Methoden um den Konzentrationsgradienten von Substrat und pH innerhalb der Partikel zu verfolgen, gelegt.

Kinetische Studien liefern die Grundlage zur Bewertung von Substrat Diffusionslimitierung. Die Veränderung des pH Gradienten aufgrund von Bildung des sauren Produktes in dem immobilisierten Biokatalysator wird durch eine neue, nicht invasive Methode evaluiert. Weiters wurde ein Reaktions-Diffusions Modell entwickelt und zur Auswertung der gemessenen Parameter verwendet. Dadurch konnte eine Abschätzung der Diffusions- sowie der kinetischen Parameter gemacht werden und Konzentrationsprofile im Träger berechnet werden. Die Bewertung der Diffusion innerhalb der Partikel liefert wichtige Informationen um massgeschneiderte Biokatalysatoren mit optimierter Effizienz für die Industrie zu liefern und mit der

etabilierten Methode kann rationales Design von immobilisierten Enzymen, die mit einer pH- Wert Veränderung aufgrund von Produktbildung einhergehen, stattfinden.

Table of contents

Measurement and Modeling of Mass Transfer Effects for Rational Design of Immobilized Biocatalysts

Caterina Boniello[1,2] and Bernd Nidetzky[1,2,*]

[1] Austrian Center of Industrial Biotechnology - ACIB GmbH, Petersgasse 14, A-8010 Graz, Austria

[2] Institute of Biotechnology and Biochemical Engineering, Graz University of Technology, Petersgasse 12, A-8010 Graz, Austria

* Corresponding author

Institute of Biotechnology and Biochemical Engineering, Graz University of Technology, Petersgasse 12, A-8010 Graz, Austria

Tel. +43 316 873 8400; Fax +43 316 873 8434; E-mail: bernd.nidetzky@tugraz.at

ABSTRACT

Diffusion of substrates might constitute the limiting step for reaction catalyzed by immobilized enzymes. Accumulation of inhibiting or acidic products in porous carriers might strongly affect enzymatic activity. Although mass transfer theory in porous structure is available from decades, appropriate experimental methodology for identification of diffusion limitation and evaluation of concentration gradients in immobilized biocatalysts is nowadays still lacking and mainly based on macroscopic evidence. Investigation techniques providing information about mass transfer effects in immobilized enzymes are summarized and discussed in this summary. Proper evaluation of intraparticle diffusion should be crucial in the rational design of immobilized biocatalysts.

INTRODUCTION

Mass transfer effects are one of the main reasons of decreased enzymatic activity after immobilization [1]. The presence of the carrier influences substrate distribution in the enzyme microenvironment for two reasons: because of the formation of a boundary layer between liquid and solid phase (external diffusion) and because gradients are formed as consequence of interaction between charged groups of solutes with stationary charges of the carrier material (partitioning)[2]. These effects however can be minimized: the first by increasing the relative flow rate between particles and fluid [3], the latter employing solutions with high ionic strength [4]. A third aspect has to be considered when porous carriers are employed. Although this kind of carriers is often a preferred choice for enzyme immobilization because of their high specific surface area [5-6], pore diffusion of substrates can result to be limiting for the reaction. Inhibiting

products or generated protons can furthermore accumulate in the carrier affecting enzymatic activity. For scientific research purposes diffusion limitation is often avoided loading a small amount of enzyme on the carrier [4]; industrial applications instead require high catalytic activity per catalyst volume [7] and such solution may not be applicable.

In the development of biocatalysts a common procedure is to test many alternative formulations and the best for the specific purposes is selected [8]. Critical reviews however can provide general guidelines for the proper choice of carrier geometrical characteristics in order to favor diffusion of the chemical species [4, 9]. Recently some authors [8, 10-12] have been giving more attention to a rational design approach for the formulation of particles tailored for the biocatalyst to show optimized performances. The choice of the optimal carrier is based on the evaluation of key design parameters. This summary focuses on the evaluation of the internal diffusion as design parameter and on its impact on the catalytic efficiency of immobilized enzymatic preparations. An overview of detection methods (experimental) and computational approaches (modeling) is presented and their feasibility is discussed.

EXPERIMENTAL EVALUATION

Macroscopic Behavior

The macroscopic behavior of a biocatalyst results from both kinetic and mass-transport effects. When diffusion limitation is present, low productivity per unit biocatalyst and high (apparent) stability are observed [13]. The simplest way to express this activity loss is to calculate a stationary effectiveness factor $\eta=v_{imm}/v_{free}$, defined as the ratio between the observed initial reaction rates of immobilized (v_{imm}) and free (v_{free}) enzyme,

respectively [14]. A good estimation is given also by the Thiele modulus (Φ) that corresponds to the ratio of a reaction rate to a diffusion rate [15]. The higher Φ the more diffusion limited is the reaction. Kasche [16] calculated values of η as function of Φ, which can give a first estimation of diffusional effects for immobilized biocatalysts [14]. The same author introduced furthermore the notion of operational effectiveness factor as the ratio of the times required by immobilized and free enzyme for reaching the end point of the process. When the effectiveness factor is lower than 1, concentration gradients of substrates and products are formed in the carrier. Information about the magnitude of microscopic phenomena like intraparticle diffusion can be provided by macroscopic data derived from bulk concentration measurements. The aim of this paragraph is to give an overview on the available methodology for evaluating the presence of diffusion limitation from macroscopic measurements. A summary is reported in Table 1.

Carrier Size and Particle Disintegration

Particle diameter influences internal diffusion: it determines how far a molecule has to travel inside the carrier to reach the enzyme active site [17]. The extent of mass transfer can be evaluated measuring the apparent reaction rate of immobilized biocatalysts differing in particle size. Giordano et al. [18] observed an increase in apparent glucose-fructose isomerization rate as particle size of Maxazyme decreased from 1200 μm to 350 μm. A further particle size reduction to 150 μm did not lead to any change, suggesting that the apparent reaction rate for these smaller fraction corresponded to the intrinsic enzymatic activity deprived of diffusional effects. Valencia et al.,[19] evaluated the effect of particle size and enzyme loading on the progress curves for Penicillin G

hydrolysis and Cephalexin synthesis performed by Penicillin G acylase. Authors focused on the operation curves obtained using a coarse (R=72 µm) and a fine (R= 30 µm) biocatalyst fraction. For each fraction three preparations differing in enzyme loading were tested. Effect of enzyme loading on substrate/product profiles was observed to be more pronounced for the coarse particles.

Table 1. Macroscopic experimental evaluation of diffusion limitation

Macroscopic effect	Enzyme	Carrier	Reference
Activation Energy	Trypsin		[20]
	Pseudomonas cepacia Lipase	Polypropylene	[21]
Apparent K_M	PGA		[22]
	CCA	Sepabeads	[23]
	PGA	Glyoxyl-agarose	[19]
Proportionality activity/loading[a]	α-chymotrypsin	Polyamides, Celite	[24]
	Assemblase		[13]
	PGA	Eupergit	[25]
	Pseudomonas cepacia Lipase	Polypropylene	[21]
Active Enzyme	α-chymotrypsin	Polyamides, Celite	[24]
Linearity Eadie-Hofstee plot			[26]
	BC lipase	Mesoporous silica	[27]
Particles crushing	PGA	Eupergit	[28]
	PGA	Glyoxyl-agarose	[19]

[a] activity (µmol min^{-1} g $carrier^{-1}$); Loading (mg enzyme g $carrier^{-1}$)

Particle crushing is another way to assess the effect of the particle size [4]. Janssen et al. [28] reported that Benzylpenicillin (BP) hydrolysis activity of high loaded (0.58 µmol acive sites g^{-1}) *E. coli* Penicillin G acylase (PGA) on Eupergit C preparations increased by 65% upon particles disintegration. This was not only because of higher substrate

concentrations in enzyme proximity but also because accumulation of the product phenylacetic acid (PAA) was reduced. PAA is an inhibitor for PGA and undergoes deprotonation, causing undesirable pH gradients in the immobilized amidase (Spiess, 1999).

Estimation of Apparent K_M

Increases in K_M are often observed after enzyme immobilization. Pencreac'h et al., [21] explained this effect as consequence of three combined reasons: (1) substrate partitioning, (2) conformational changes of lipase after immobilization and (3) steric hindrance being the enzyme less accessible for the substrate. When K_M differences are observed between enzymatic preparation differing only in carrier geometrical characteristics, K_M increase denotes substrate diffusion limitation. In the analysis of Cephalosporin C amidase (CCA) immobilized on epoxy-activated Sepabeads Boniello et al., [23] observed an increase of apparent K_M after immobilization. This effect was more pronounced for the coarse (particle diameter 300-500 µm, less porous (pore diameter 30-40 nm) or high loaded fractions (70 mg/ g dry carrier). Similar effects were reported by Valencia et al.,[19] for immobilized PGA, for which the apparent K_M increased with enzyme loadings (from 8 to 30 mg/g dry) and with particle radius (from 30 µm to 72 µm) up to 4–fold for the synthesis and up to 6-fold for the hydrolysis reaction. Crushed particles showed apparent K_M values approaching the intrinsic one.

Enzyme Loading

Barros et al. [24] varied the immobilized amount of α-chymotrypsin (CT) on polyamides of different particle size and plotted the reaction rate per gram carrier versus the enzyme loading. At low loadings the dependence of the reaction rate versus the enzyme loading was linear, for higher loadings they observed a plateau, which

represent the maximum rate at which the substrate can be transported from the bulk solution to the enzyme molecules. This plateau was reached already at loadings of 10 mg CT per g carrier using a fast acyl donor. In this case a double reaction rate was observed when using particle sizes 75-106 µm instead of 300-500 µm. Van Langen et al., [29] immobilized Penicillin G acylase (PGA) from *E.Coli* on Eupergit C at various densities of protein in the carrier. Reaction rates depended strongly on the active site density: higher loadings resulted in lower catalytic conversion. Since according to active site titration, activity loss after immobilization was only 10%, authors concluded that diffusion limitation took place in the immobilized enzyme particles. On the opposite Van Roon et al., [13] excluded diffusion limitation in Assemblase (commercial immobilized PGA) observing a reaction rate value higher than 93% V_{max} in phenylglycine amide (substrate) saturating conditions (>11K_M) and linear dependence of the measured activity versus enzyme loading.

Enzymatic Activity Content at Constant Enzyme Loading

A way to estimate whether diffusion limitation is present is to compare the apparent specific activity of preparations with different immobilized activity but with the same enzyme loading; thus a certain amount of inactivated enzyme has to be co-immobilized. Barros et al. [24] tested two polyamide supports differing in particle size and total enzyme loading for evaluating the effect of the fraction of active α-chymotrypsin. Up to 10 mg protein/g dry carrier no effect of the active fraction was observed on the specific activity. High loaded preparations (100 mg/g dry carrier) showed 60% and 40% specific activity decrease for particles of 495 µm and 278 µm diameter respectively, when the active fraction of loaded enzyme increased from 5 to 100%.

Linearity of Eadie-Hofstee plot

Jaladi et al. [27] immobilized *Burkholderia cepacia* (BC) lipase on mesoporous silica beads. They extrapolated the effective diffusion coefficient (D_{eff}) for the substrate from the Eadie-Hofstee plot, following a procedure proposed by Clark and Bailey [26] for preparations of 2 and 60 μm beads respectively. For the higher particle size the plot was not linear suggesting diffusion limitation. The determined effective diffusion coefficient for the substrate in the immobilized preparations was one to two orders of magnitude lower than that in solution ($D_{eff}=61\times10^{-7}$ m^2s^{-1}) and was a function of the pore diameter of the particles, $D_{eff}=0.6\text{-}0.8\times10^{-7}$ m^2s^{-1} and $7.2\text{-}9.7\times10^{-7}$ m^2s^{-1} for 55 Å and 240 Å respectively. Lower enzyme loadings lead to higher values of D_{eff}.

Activation Energy

Temperature influences both reaction and diffusion rate but the dependence of reaction rate on temperature is higher than that of diffusion. Reaction enthalpy calculated from the slope of the curve in the Arrhenius plot are lower for reaction performed with immobilized enzyme preparations than with free enzymes because of diffusion limitation [30]. The temperature dependence of diffusion-limited enzymatic reactions was studied in detail by Buchholz and Rüth [20]. They observed that the apparent activation energy of N-α-benzoyl-L-arginine-ethyl ester (BAEE) hydrolysis by immobilized trypsin was dependent on substrate concentration, varying from a value similar to that of the free enzyme for BAEE concentrations >> K_M to much lower values. Operating at high temperature would consistently increase the reaction rate leading to reaction limited by substrate diffusion.

Intraparticle Measurements

The macroscopic behavior of immobilized enzymes can qualitatively suggest the presence of diffusion limitation. Anyway a quantification of mass transfer effects can be only performed rearranging the measured variables into a representative parameter, the Thiele modulus. For a direct and precise evaluation of the diffusion phenomena measurements of species concentration in the enzyme microenvironment are required. The knowledge of concentration gradients is necessary to quantify the local effects of the carrier on both reaction and transport kinetic [10]. Equipments for carrying out spatial and time resolved measurements are however expensive and require complicated set-ups. For this reasons there are just few works that report on measurements of concentration gradients in immobilized enzyme particles. Substrate and products in carriers are furthermore often not detectable with the common imaging techniques. In this paragraph imaging techniques available for measurements of intraparticle concentration gradients are reported and discussed.

Substrate/Products concentrations

Nuclear magnetic resonance (NMR) and Raman spectroscopy have been reported for the observation in situ of concentration gradients. These techniques have however not yet been applied for diffusion analysis in immobilized enzymes. Kuppers et al, [31] used NMR for the observation of diffusion and reaction dynamics in gel microreactors. NMR might suffer of poor resolution in case of fast changes in concentration and not be suitable to fast enzymatic conversions [10]. Raman spectroscopy is limited to certain classes of analytes that have to be present in significant concentrations. The work of Kwak and Lafleur, [32] reported an example of Raman spectroscopy applied to the

evaluation of two polyethylene glycols (PEGs) in hydrogels. The intensity of the CH stretching band was used to obtain the concentration profiles of PEGs, whereas the OH stretching band of water was used as an internal intensity standard. Fluorescence techniques like confocal laser scanning microscopy (CSLM) are powerful methods to achieve spatial and time resolved information [33] and have been used in the past for the measurements of pH gradients in immobilized enzymes (see later) or in eukaryotic cells [34]. CLSM and fluorescent-based methods in general required the analyte to be fluorescent or to be properly labeled for fluorescent detection. Light scattering and reflection however are not referenced in intensity based measurement because luminescence is measured at two wavelengths [35]. Recently Zavrel et al. [12] reported about two-photon laser scanning microscopy (LSM) applied for the spatial and time resolved detection of 3,5-dimethoxy-benzaldeyde (DMBA) in hydrogel matrix during the carboligation with (R)-3,3',5,5'-tetramethoxybenzoin (TMB). LSM is expected to provide high spatial and temporal resolution.

pH gradients

Hydrolysis of amides and esters involves products with ionizable groups [36]. Differences in pK_a dictate a net generation of protons in this conversion [7]. Concerning immobilized biocatalysts, intraparticle pH gradients constitute a relevant factor in addition to concentration profiles for substrates and product in term of activity [4, 28, 36] and stability [7]. In the last decade fluorescent based methods have been applied for pH detection in immobilized biocatalysts (Table 2).

Table 2. Available methodology for detection of pH gradients in immobilized enzymes

Method	Enzyme	Carrier	Reference
Intensity-based fluorescence	PGA/ glutaryl acylase	Eupergit C Eupergit C 250 L	[37]
Intensity based CLSM	PGA	Eupergit C Eupergit C 250 L PBA-Eupergit Trisoperl CNBrSepharose 4B	[38]
	Glucose Oxidase Catalase	N-isopropacrylamide membrane	[39]
Fluorescence lifetime	-	Hydrogel Beads	[10]
	-	Poly(ethylene) glycol	[40]
Dual lifetime referencing	CCA	Sepabeads	[23]

A first work was presented by Spiess et al. [37], who measured pH values in immobilized PGA and glutaryl acylase, following the intensity of the pH-responsive fluorophore fluorescein isothiocyanate (FITC). They observed a ΔpH between particles and bulk liquid up to 2.5 pH units. Although this approach is applicable even to stirred reactors, intensity-based measurements, might be affected by drifts in the optoelectronic setup (light sources and light detectors) and by variation of the properties of the sensor layer (dye concentration or thickness) [41]. Combining the indicator with a reference dye and measuring emission or excitation at two different wavelengths may overcome some of these drawbacks. Referenced intensity measurements were performed with a confocal laser scanning microscope by Spiess and Kasche [38] and Huang et al. [39] for determining proton concentration in biocatalytic beads and membrane respectively. The possibility to determine pH gradients in a spatial-resolved way is definitively an advantage of this method. However, light scattering and reflection are not referenced because luminescence is measured at two wavelengths [35].

Lifetime measurements of indicators that show lifetime dependence on pH are more accurate because lifetime is independent of intensity or wavelength interferences [35]. Spiess et al., [10] evaluated the diffusion of a propionic acid into hydrogels measuring the pH-dependent resorufin lifetime using CLSM and pulsar excitation. Changing in pH profile along the particle radius during the process could be monitored and obtained data used for diffusion models discrimination. Authors self remarked about the complexity of the experimentation equipment and pointed out the necessity to conduct experimental analysis to screen among experiments to perform. Kuwana and coworker [40] applied a special technique based on frequency domain proton migration (FDPM) to measure the phase shift between and thus the lifetime of a pH-sensing fluorophore, carboxy seminaphthofluorescein-1 (C-SNAFL-1) immobilized in poly(ethylene glycol) (PEG) microparticles. Lifetime measurements, in the nanoseconds order, like the case of most pH indicators, require sophisticated optoelectronic equipments [35]. In the work of Kuwana et al., [40] lifetime measurements were possible because of opportune amplification of the phase shift through multiple scattering.

Microscopy-based techniques require the investigated object to be fixed. Despite the high resolution offered, they are not suitable for measurements in batch stirred reactors, the preferred reactor choice for biocatalytic conversions [42]. Recently Boniello et al., [23] proposed a method based on dual lifetime referencing for intraparticle pH monitoring. Even though spatial resolved measurements can not be carried out so that the recorded internal pH reflects an average value along the particles radius, this method is applicable to stirred particles and overcome the mayor drawbacks of intensity based measurements thanks to internal self-referencing [35]. Dual lifetime referencing

as applied to pH detection consists in labeling the biocatalyst particles with a pH-sensitive fluorophore with lifetime in the nanoseconds range together with a reference luminophore with lifetime in the microsecond range. An overall phase shift can be recorded after excitation in the frequency domain. This phase shift is related to the proton concentration. Essential for dual lifetime referencing is that indicator and reference show overlapped excitation and emission spectra. This methodology has been applied for collection of intraparticle pH data in a time resolved way.

MODELLING

Parameter estimation

Parameters describing immobilized enzymes systems can not be obtained from macroscopic measurements. Measured apparent kinetic parameters differ from the intrinsic one because they are affected by mass transfer effects. Diffusion-reaction mathematical models are a powerful tool to evaluate separately mass transfer from kinetic effects in the study of the immobilized biocatalysts. Fitting experimental data with a model that takes into account enzyme kinetic and the governing diffusion law provide a realistic estimation of intrinsic kinetic parameters and effective diffusion coefficients. The usual approach is collect data of substrate/product concentration in the bulk liquid phase and from them through the model estimate diffusion and kinetic parameters. Polakovic et al., [43] studied the sucrose hydrolysis performed by *Saccharomices cerevisiae* cells immobilized in Ca-alginate gel particles. Fitting sucrose concentration profile in bulk with a reaction-diffusion model with Michaelis-Menten kinetic and Fick diffusion law, authors estimated the maximal reaction rate (V_{max}) and the effective diffusion coefficient (D_{eff}) for sucrose. The K_M value applied in the model was that

experimentally determined for the free cells. Berendsen et al., [44] used a similar approach to calculate intrinsic k_{cat} and K_M for the enantioselective transesterification of (R/S)-1-methoxy-2-propanol (MP) with vinyl acetate (VA) catalyzed by *Candida Antartica* Lipase B (CAL-B) using a complex kinetic expression instead of the simply Michaelis-Menten. Diffusion parameters were calculated from empirical relationships and considered known in the model. Recently Spiess et al., [10] stressed on the importance of taking into account both intraparticle and bulk concentration profiles for a proper kinetic and diffusion parameter estimation. Zavrel et al., [12] worked in this direction. Authors measured substrate concentration profiles in eight points along the particle radius. Using an optimal experimental design combined to mathematical model fitting to the measured data ten unknown parameters among enzyme kinetic, mass transfer and diffusion parameters were estimated.

Simulation

Numerical solution of partial differential equations describing diffusion and reaction in porous carriers as tool for examine particle geometrical parameters on the kinetic behavior of immobilized biocatalyst have been proposed in the last decades. In 1974 Regan et al. [45] reported about the influence of particle size, protein content, effective diffusion coefficient and Michaelis constant on the catalytic performances in terms of rate (µmol/min/mL) of a series of immobilized enzymes (Chymotripsin, lactate dehydrogenase, Alcohol dehydrogenase, penicillin amidase) bound to DEAE-cellulose. Simulated results were compared with experimental data. From then to now a large number of works dealing with developing of mathematical models supported by experimental has been published. The utility is the ability to predict the biocatalyst

behavior to screen for the optimal reaction conditions. The general approach is to estimated the unknown diffusion and/or kinetic parameter fitting the model to experimental data and then to evaluate the effect of key parameters or varied experimental conditions on the catalytic performances of the immobilized enzyme system. Berendsen et al., [44] expressed the catalytic efficiency in terms of effectiveness factor and enantiomeric performance studying the effect of the initial concentration of MP and VA as well as the effect of the enantiomeric ratio. When dealing with complex system numerical simulations lead to an improvement in understanding and control of the immobilized enzyme. Blandino et al., [46] reported about a glucose oxidase-catalase system co-encapsulated within hydrogel-membrane liquid-core capsules. The proposed model included non-uniform enzyme distribution within the carrier and deactivation of both enzymes. Authors calculated concentrations profile in both batch and continuous stirred tank reactors and found them in agreement with experimental data supporting the hypothesis of uneven enzyme distribution in the particles. Validated model can be further applied to describe the behavior of similar biocatalyst systems. Methodology for assessment of the internal biocatalyst profile is anyway available [8]. Numerical solutions should support the experimental analysis in term of prediction for appropriate experiment planning or for the knowledge of the system behavior when methodology for measurements is not available.

A third application of simulating diffusion and reaction in immobilized enzymes is the possibility to calculate concentration profiles in the enzyme microenvironment. Considering how complex intraparticle concentration measurements are, calculated results offer a solid basis in the understanding of enzymatic activity distribution in the

carrier in term of substrate availability and possible product inhibition. Halwachs et al. [47] studied the fast hydroliysis of D,L-phenylalanine methylester (DLE) to L-phenylalanine (LA) and D-phenylalanine methylesther (DE) with immobilized a-chymotrypsin. They developed a diffusion-reaction model including proton generation and the effect of pH on the maximal reaction rate. Local substrate concentration, reaction rate and pH within the particles were calculated as function of the dimensionless radial coordinate. Results show a pH gradient from pH 7.0 to pH 3.0 from the particle surface to the particle core and substrate depletion in the carrier center. These effects reflect in the reaction rate and in the fraction of carrier volume effectively utilized for the reaction to occur.

CONCLUSIONS

Research studies concerning immobilized enzymes report about diffusion limitation as one of the main reason of reduced apparent catalytic activity. Evaluation of mass transfer in biocatalyst occurs by experimental and computational way. Although theory for mass transfer in porous structure is available from decades, there are just a few works that combine information about intraparticle concentration profiles obtained by numerical calculation to experimental evidence. This is because mass transfer assessment occurs mainly through macroscopic measurements in the bulk liquid phase and methodology to detect reagent distribution in the porous structure is missing or very laborious. For a rational design approach, where mass transfer magnitude is considered a key parameter in the choice of the optimal carrier, proper evaluation of intraparticle concentration gradients is required.

REFERENCES

1. Blanch HW, Clark DS: *Biochemical Engineering.* New York: Marcel Dekker, Inc.; 1996.
2. Doran PM: *Bioprocess Engineering Principles.* London: Academic Press Limited; 1995.
3. Bird RB, Stewart WE, Lightfoot EN: *Transport Phenomena.* New York: John Wiley and Sons; 1960.
4. Tischer W, Kasche V: **Immobilized enzymes: crystals or carriers?** *Trends Biotechnol* 1999, **17:**326-335.
5. Hilterhaus L, Minow B, Muller J, Berheide M, Quitmann H, Katzer M, Thum O, Antranikian G, Zeng AP, Liese A: **Practical application of different enzymes immobilized on sepabeads.** *Bioprocess Biosyst Eng* 2008, **31:**163-171.
6. Mateo C, Abian O, Fernandez-Lorente G, Pedroche J, Fernandez-Lafuente R, Guisan JM: **Epoxy sepabeads: A novel epoxy support for stabilization of industrial enzymes via very intense multipoint covalent attachment.** *Biotechnol Progr* 2002, **18:**629-634.
7. Guisan JM, Alvaro G, Rosell CM, Fernandez-Lafuente R: **Industrial design of enzymic processes catalysed by very active immobilized derivatives: utilization of diffusional limitations (gradients of pH) as a profitable tool in enzyme engineering.** *Biotechnol Appl Biochem* 1994, **20 (Pt 3):**357-369.
8. van Roon J, Beeftink R, Schroen K, Tramper H: **Assessment of intraparticle biocatalytic distributions as a tool in rational formulation.** *Curr Opin Biotechnol* 2002, **13:**398-405.
9. Cao L: **Immobilised enzymes: science or art?** *Curr Opin Chem Biol* 2005, **9:**217-226.
10. Spiess AC, Zavrel M, Ansorge-Schumacher MB, Janzen C, Michalik C, Schmidt TW, Schwendt T, Buchs J, Poprawe R, Marquardt W: **Model discrimination for the propionic acid diffusion into hydrogel beads using lifetime confocal laser scanning microscopy.** *Chem Eng Sci* 2008, **63:**3457-3465.
11. van Roon JL, Schroen CG, Tramper J, Beeftink HH: **Biocatalysts: measurement, modelling and design of heterogeneity.** *Biotechnol Adv* 2007, **25:**137-147.
12. Zavrel M, Michalik C, Schwendt T, Schmidt T, Ansorge-Schumacher M, Janzen C, Marquardt W, Buchs J, Spiess AC: **Systematic determination of intrinsic reaction parameters in enzyme immobilizates.** *Chem Eng Sci* 2010, **65:**2491-2499.
13. van Roon JL, Joerink M, Rijkers MP, Tramper J, Schroen CG, Beeftink HH: **Enzyme distribution derived from macroscopic particle behavior of an industrial immobilized penicillin-G acylase.** *Biotechnol Prog* 2003, **19:**1510-1518.
14. Buchholz K, Kasche V, Bornscheuer UT: *Biocatalysts and enzyme technology.* Weinheim: Wiley-VCH; 2005.
15. Bailey JE, Ollis DF: *Biochemical engineering fundamentals.* New York: McGraw-Hill; 1986.

16. Kasche V: **Correlation of Experimental and Theoretical Data for Artificial and Natural Systems with Immobilized Biocatalysts.** *Enzyme and Microbial Technology* 1983, **5:**2-13.
17. Barros RJ, Wehtje E, Adlercreutz P: **Effect of mass-transfer limitations on the selectivity of immobilized alpha-chymotrypsin biocatalysts prepared for use in organic medium.** *Biotechnology and Bioengineering* 2000, **67:**319-326.
18. Giordano RLC, Giordano RC, Cooney CL: **A study on intra-particle diffusion effects in enzymatic reactions: glucose-fructose isomerization.** *Bioprocess Eng* 2000, **23:**159-166.
19. Valencia P, Wilson L, Aguirre C, Illanes A: **Evaluation of the incidence of diffusional restrictions on the enzymatic reactions of hydrolisis of penicillin G and synthesis of cephalexin.** *Enzyme and Microbial Technology* 2010, **47:**268-276.
20. Buchholz K, Ruth W: **Temperature dependence of a diffusion-limited immobilized enzyme reaction.** *Biotechnol Bioeng* 1976, **18:**95-104.
21. Pencreac'h G, Leullier M, Baratti JC: **Properties of free and immobilized lipase from Pseudomonas cepacia.** *Biotechnol Bioeng* 1997, **56:**181-189.
22. Bozhinova D, Galunsky B, Yueping G, Franzreb M, Koster R, Kasche V: **Evaluation of magnetic polymer micro-beads as carriers of immobilised biocatalysts for selective and stereoselective transformations.** *Biotechnol Lett* 2004, **26:**343-350.
23. Boniello C, Mayr T, Klimant I, Koenig B, Riethorst W, Nidetzky B: **Intraparticle concentration gradients for substrate and acidic product in immobilized cephalosporin C amidase and their dependencies on carrier characteristics and reaction parameters.** *Biotechnol Bioeng* 2010, **106:**528-540.
24. Barros RJ, Wehtje E, Adlercreutz P: **Mass transfer studies on immobilized alpha-chymotrypsin biocatalysts prepared by deposition for use in organic medium.** *Biotechnol Bioeng* 1998, **59:**364-373.
25. Van Langen LM, Janssen MH, Oosthoek NH, Pereira SR, Svedas VK, van Rantwijk F, Sheldon RA: **Active site titration as a tool for the evaluation of immobilization procedures of penicillin acylase.** *Biotechnol Bioeng* 2002, **79:**224-228.
26. Clark DS, Bailey JE: **Structure-function relationships in immobilized chymotrypsin catalysis.** *Biotechnol Bioeng* 1983, **25:**1027-1047.
27. Jaladi H, Katiyar A, Thiel SW, Guliants VV, Pinto NG: **Effect of pore diffusional resistance on biocatalytic activity of Burkholderia cepacia lipase immobilized on SBA-15 hosts.** *Chem Eng Sci* 2009, **64:**1474-1479.
28. Janssen MHA, van Langen LM, Pereira SRM, van Rantwijk F, Sheldon RA: **Evaluation of the performance of immobilized penicillin G acylase using active-site titration.** *Biotechnology and Bioengineering* 2002, **78:**425-432.
29. van Langen LM, Janssen MHA, Oosthoek NHP, Pereira SRM, Svedas VK, van Rantwijk F, Sheldon RA: **Active site titration as a tool for the evaluation of immobilization procedures of penicillin acylase.** *Biotechnology and Bioengineering* 2002, **79:**224-228.

30. Tramper J, Angelino SAGF, Muller F, Vanderplas HC: **Kinetics and Stability of Immobilized Chicken Liver Xanthine Dehydrogenase.** *Biotechnology and Bioengineering* 1979, **21:**1767-1786.
31. Kuppers M, Heine C, Han S, Stapf S, Blumich B: **In situ observation of diffusion and reaction dynamics in gel microreactors by chemically resolved NMR microscopy.** *Appl Magn Reson* 2002, **22:**235-246.
32. Kwak S, Lafleur M: **Raman spectroscopy as a tool for measuring mutual-diffusion coefficients in hydrogels.** *Appl Spectrosc* 2003, **57:**768-773.
33. Heinemann M, Limper U, Buchs J: **New insights in the spatially resolved dynamic pH measurement in macroscopic large absorbent particles by confocal laser scanning microscopy.** *J Chromatogr A* 2004, **1024:**45-53.
34. Swietach P, Zaniboni M, Stewart AK, Rossini A, Spitzer KW, Vaughan-Jones RD: **Modelling intracellular H+ ion diffusion.** *Prog Biophys Mol Bio* 2003, **83:**69-100.
35. Liebsch G, Klimant I, Krause C, Wolfbeis OS: **Fluorescent imaging of pH with optical sensors using time domain dual lifetime referencing.** *Anal Chem* 2001, **73:**4354-4363.
36. Kallenberg AI, van Rantwijk F, Sheldon RA: **Immobilization of penicillin G acylase: The key to optimum performance.** *Adv Synth Catal* 2005, **347:**905-926.
37. Spiess A, Schlothauer RC, Hinrichs J, Scheidat B, Kasche V: **pH gradients in immobilized amidases and their influence on rates and yields of beta-lactam hydrolysis.** *Biotechnology and Bioengineering* 1999, **62:**267-277.
38. Spiess AC, Kasche V: **Direct measurement of pH profiles in immobilized enzyme carriers during kinetically controlled synthesis using CLSM.** *Biotechnol Progr* 2001, **17:**294-303.
39. Huang HY, Shaw J, Yip C, Wu XY: **Microdomain pH gradient and kinetics inside composite polymeric membranes of pH and glucose sensitivity.** *Pharm Res* 2008, **25:**1150-1157.
40. Kuwana E, Liang F, Sevick-Muraca EM: **Fluorescence lifetime spectroscopy of a pH-sensitive dye encapsulated in hydrogel beads.** *Biotechnol Progr* 2004, **20:**1561-1566.
41. Vasylevska GS, Borisov SM, Krause C, Wolfbeis OS: **Indicator-loaded permeation-selective microbeads for use in fiber optic simultaneous sensing of pH and dissolved oxygen.** *Chem Mater* 2006, **18:**4609-4616.
42. Valencia P, Flores S, Wilson L, Illanes A: **Effect of particle size distribution on the simulation of immobilized enzyme reactor performance.** *Biochemical Engineering Journal* 2010, **49:**256-263.
43. Polakovic M, Kudlacova G, Stefuca V, Bales V: **Determination of sucrose effective diffusivity and intrinsic rate constant of hydrolysis catalysed by Ca-alginate entrapped cells.** *Chem Eng Sci* 2001, **56:**459-466.
44. Berendsen WR, Lapin A, Reuss M: **Investigations of reaction kinetics for immobilized enzymess - Identification of parameters in the presence of diffusion limitation.** *Biotechnol Progr* 2006, **22:**1305-1312.

45. Regan DL, Lilly MD, Dunnill P: **Influence of Intraparticle Diffusional Limitation on Observed Kinetics of Immobilized Enzymes and on Catalyst Design.** *Biotechnology and Bioengineering* 1974, **16:**1081-1093.
46. Blandino A, Macias M, Cantero D: **Modelling and simulation of a bienzymatic reaction system co-immobilised within hydrogel-membrane liquid-core capsules.** *Enzyme and Microbial Technology* 2002, **31:**556-565.
47. Halwachs W, Wandrey C, Schugerl K: Immobilized Alpha-Chymotrypsin - Pore Diffusion Control Owing to Ph Gradients in Catalyst Particles. Biotechnology and Bioengineering 1978, 20:541-554.

ARTICLE

BIOTECHNOLOGY and BIOENGINEERING

Intraparticle Concentration Gradients for Substrate and Acidic Product in Immobilized Cephalosporin C Amidase and Their Dependencies on Carrier Characteristics and Reaction Parameters

Caterina Boniello,[1] Torsten Mayr,[2] Ingo Klimant,[1,2] Burghard Koenig,[1,3] Waander Riethorst,[1,3] Bernd Nidetzky[1,4]

[1]Research Centre Applied Biocatalysis GmbH, Graz, Austria

[2]Institute of Analytical Chemistry, Graz University of Technology, Graz, Austria

[3]Department of Biocatalysis, Research and Development Anti-Infectives, Sandoz GmbH, Kundl, Austria

[4]Institute of Biotechnology and Biochemical Engineering, Graz University of Technology, Petersgasse 12, A-8010 Graz, Austria; telephone: +43-316-873-8400; fax: +43-316-873-8434; e-mail: bernd.nidetzky@tugraz.at

Received 10 November 2009; revision received 26 January 2010; accepted 2 February 2010

Published online 10 February 2010 in Wiley InterScience (www.interscience.wiley.com). DOI 10.1002/bit.22694

ABSTRACT: Cephalosporin C amidase was covalently attached using a protein loading of 7.0–200 mg protein/g dry carrier on four epoxy-activated Sepabeads differing in particle size and pore diameter. Initial-rate kinetic analysis showed that for Sepabeads with small pore diameters (30–40 nm), the apparent K_M of the amidase for hydrolysis of cephalosporin C at 37°C and pH 8.0 increased ~3-fold in response to increased particle size (~120–400 μm) and increased amount of immobilized enzyme (7.0–70 mg protein/g dry carrier) while maximum specific activity (3.2 U/mg protein; 25% of free amidase) was affected only by particle size. In contrast, for Sepabeads with wide pores (150–250 nm), the K_M was independent of the enzyme loading. Internal effectiveness factors calculated from observable Thiele modulus reflected the dependence of K_M on geometrical parameters of the particles. A new method for determination of the overall intraparticle pH was developed based on luminescence lifetime measurements in the frequency domain. Sepabeads were doubly labeled using a lipophilic variant of the pH-sensitive dye fluorescein, and Ru(II) tris(4,7-diphenyl-1,10-phenantroline) whose phosphorescence properties are independent of pH. Luminescent lifetime measurements of doubly labeled particle suspensions showed superior signal-to-noise ratio compared to fluorescence intensity-based measurements using singly labeled particles. The difference at apparent steady state (ΔpH) between bulk (external pH) and intraparticle pH (internal pH) was as large as ~0.6 units. The ΔpH was dependent on substrate concentration, particle size, and pore diameter. Therefore, these results characterize the role of carrier characteristics and reaction parameters in the formation of concentration gradients for substrate and acidic product during hydrolysis of cephalosporin C by immobilized amidase. The strong pH dependence of the immobilized amidase underscores the importance of considering intraparticle pH gradients in the design of an efficient carrier-bound biocatalyst.

Biotechnol. Bioeng. 2010;106: 528–540.

KEYWORDS: pH gradients; immobilization; porous carrier; cephalosporin C; mass transfer

Introduction

Enzyme immobilization is a key technology of biocatalytic process development (Sheldon, 2007). It is widely used in biotransformations currently performed on industrial production scale (Buchholz et al., 2005). The most commonly employed strategy for immobilization involves attachment of the enzyme on an insoluble meso- or macroporous carrier (Cao, 2005). Heterogenized catalysts are readily separated from solution and therefore support continuous bioprocessing with integrated re-use of enzyme (Buchholz et al., 2005). Enhancement of operational stability is often observed for immobilized enzymes as compared to their free counterparts (Kallenberg et al., 2005;

Correspondence to: B. Nidetzky

Contract grant sponsors: Austrian Research Promotion Agency (FFG), Styrian Business Promotion Agency (SFG), the City of Graz and Sandoz GmbH

Additional Supporting Information may be found in the online version of this article.

Mateo et al., 2007; Tischer and Kasche, 1999). This leads to an additional economic benefit given that trade off between biocatalyst lifetime and specific activity is avoided. There are three main reasons for why immobilized enzymes are usually less active than their corresponding free preparations: conformational distortion and chemical modification of the functional protein structure (Hanefeld et al., 2009), equilibrium partition of substrate and product between carrier surface and bulk solvent (Doran, 1995), and mass transfer resistances (Barros et al., 1998; Kallenberg et al., 2005; Regan et al., 1974). The effects from partition and diffusion result in the generation of concentration profiles for all compounds involved in the reaction along the characteristic dimensions of the carrier, that is, the radius in the case of spherical particles (for the general case, see Bailey and Ollis, 1986; Blanch and Clark, 1996; Buchholz et al., 2005).

Hydrolysis of amide and ester substrates is among the most widely used biotransformations in industry (Buchholz et al., 2005). Differences in pK_a for acidic groups on substrate and products usually dictate a net generation of protons in these conversions. Considering immobilized hydrolases (Janssen et al., 2002; Kallenberg et al., 2005; Tischer and Kasche, 1999), pH profiles in the intraparticle domain (i.e., internal pH), relative to the pH in bulk (i.e., external pH), constitute a potentially relevant factor in addition to concentration profiles for substrate and products. Intraparticle pH gradients could affect catalytic performances not only in terms of apparent kinetic properties of the enzyme (Bourdillon et al., 1999; Spiess and Kasche, 2001; Spiess et al., 1999) but also because of the influence of pH on protein stability (Buchholz and Kasche, 1997; Guisán et al., 1994). Although theory for coupled mass transfer and proton-forming/consuming reactions in immobilized enzyme systems has been available for decades (Byres et al., 1993; Halwachs et al., 1978; Liou and Rousseau, 1986; Ruckenstein and Rajora, 1985; Wang et al., 1995), there have been just a few studies (see below) in which biocatalyst design was based on experimental analysis of proton concentration in the carrier and its effects on enzyme activity.

Kasche and co-workers used the pH-responsive fluorophore fluorescein isothiocyanate (FITC) to measure intraparticle concentration profiles for protons in immobilized amidase. They labeled the enzyme with FITC (Spiess et al., 1999) and an additional pH-independent reference dye (Spiess and Kasche, 2001). Evidence from pH-gradient measurements and modeling of coupled diffusion and enzymatic reaction was applied to reactor design for the hydrolysis of β-lactams. The average internal pH was between 1 and 2.5 pH units lower than the external pH, a difference by far large enough to strongly affect kinetic and thermodynamic parameters of the enzymatic conversion. More recent work from Huang et al. (2008) reported on determination of pH profiles in a membrane system containing immobilized glucose oxidase. The membrane was labeled by incorporation of a FITC-dextran adduct as the pH indicator. A pH-insensitive Texas red-dextran adduct was employed as a reference. Spatial-resolved measurements of the internal membrane pH during catalytic oxidation of glucose (to gluconic acid) were obtained by laser scanning confocal microscopy. In an earlier work Spiess and Kasche (2001) have used the same technique for spatial pH mapping in a series of carriers containing immobilized amidase. These authors analyzed the pH difference, intraparticle compared to bulk, in dependence of enzyme concentration, particle size, pore size, surface modification, and matrix variation. The observed ΔpHs (differences between internal and external pH) were typically 1 pH unit or larger, and their relative magnitude was persuasively rationalized in terms of a simple reaction–diffusion model expressed in the dimensionless (squared) Thiele modulus (Eq. 1), where V_{max} is the maximum rate of the enzyme-catalyzed reaction (mM/s), K_M is the Michaelis constant (mM), R is the particle radius (m), and D_{eff} is the effective diffusion coefficient (m^2/s). Smaller pores lead to smaller values of D_{eff} (see later)

$$\Phi^2 = \frac{V_{max} R^2}{K_M D_{eff}} \tag{1}$$

Considering that stirred tanks often constitute the preferred choice of enzyme reactor for conversions necessitating pH control, it is a clear limitation of the previously described methods of intraparticle pH determination that they are based on the measurement of fluorescence intensities. Precise intensity measurements are compromised by a strong fluctuation of the recorded signal of the suspended particles. We propose here a new approach that is based on *dual luminescence lifetime referencing* (DLR) and allows to work independently of the density of the particle suspension and hence of stirring conditions. Considering complications possibly arising from chemical modification of the enzyme by the luminophores used for DLR, we chose to label the particles prior to attachment of the enzyme. An industrially used cephalosporin C amidase (CCA) from *Pseudomonas* sp. SE83 (Scheme 1) was covalently bound on a series of epoxy-activated polymethacrylate carriers (Sepabeads) featuring a representative variation in pore as well as particle diameters. The reason to work with Sepabeads was that these carriers have been well characterized and are widely employed in scientific community for enzyme immobilization (Hilterhaus et al., 2008; Mateo et al., 2002). The immobilized amidase preparations were examined with respect to kinetic effectiveness and formation of intraparticle pH gradients during hydrolysis of cephalosporin C. The results allow for the design of particles tailored for the biocatalyst to show optimized performances and provide a methodology that might be widely applicable to immobilized enzyme systems in which the biocatalytic conversion results in a pH change.

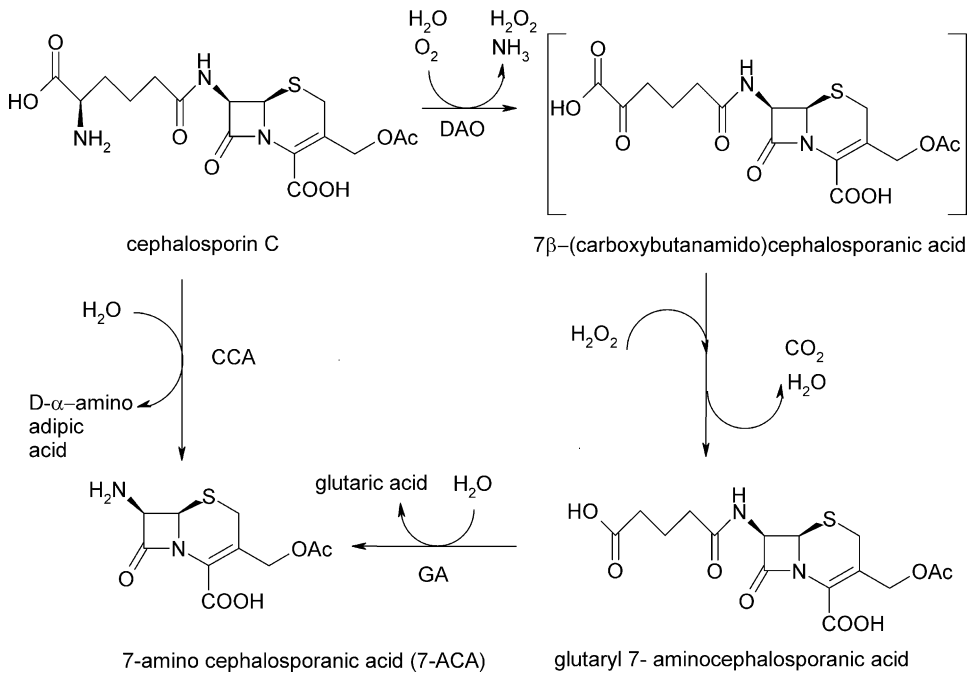

Scheme 1. Single-step amidase-catalyzed conversion of cephalosporin C to 7-aminocephalosporanic acid as compared to the classical two-step chemo-enzymatic transformation using D-amino acid oxidase (DAO) and glutaryl acylase (GA).

Materials and Methods

Chemicals

Cephalosporin C (sodium salt; CC-Na) (87.1% purity) and 7-aminocephalosporanic acid (7-ACA) were kind gifts from Sandoz GmbH (Kundl, Austria). *p*-Dimethylaminobenzaldehyde (pDAB) was from Sigma–Aldrich (Vienna, Austria). Lipophilic fluorescein (LP-FLU) and ruthenium(II)tris(4,7-diphenyl-1,10-phenanthroline di(trimethylsilylpropan sulfonate) (Ru(dpp)) were synthesized according to Weidgans et al., 2004 and Borisov and Klimant, 2009, respectively. Sepabeads EXE096 (standard grade), EXE096/M (coarse grade), EXE096/SS (fine grade), and EXE030 (high porosity grade) were kind gifts from Resindion (Milano, Italy). Table I lists relevant properties of the carriers used. All other reagents were of analytical grade and obtained from Sigma-Aldrich or Roth (Karlsruhe, Germany).

Enzyme Immobilization

An engineered cephalosporin C amidase (EC 3.5.1.93) from *Pseudomonas* sp. SE83 was obtained as a partially purified protein preparation from Sandoz GmbH. The enzyme is a functional heterodimer with a molecular weight of 83,000 (α-unit 24,720, β-unit 58,131) (Shin et al., 2005). The sixfold mutant (Val121α replaced by Ala, Gly139α by Ser, Phe58β by Asn, Ile75β by Thr, Ile176β by Val, Ser471β by Cys) was obtained from the *acyII* gene identified by Matsuda et al. (1987) (GenBank M18278), as reported in Shin et al. (2005). On an SDS–polyacrylamide gel, the protein preparation appeared to be ~75% pure and was used without further purification. The protein stock solution had a concentration of ~7 mg/mL in 20 mM potassium phosphate buffer (PPB), pH 7.5. It was kept at −20°C, and no loss of the original specific activity (~10 U/mg; see later) was observed during about 6 months of storage.

Table I. Physical parameters of the enzyme carriers and analysis of substrate diffusion of the enzymatic reaction rate.

Sepabeads	Particle size range (μm)	Pore size range (nm)	Observable modulus[a]	Internal effectiveness factor[b]
Standard grade EXE096	150–300	30–40	1.94	0.60
Coarse grade EXE096/M	250–550	30–40	2.85	0.45
Fine grade EXE096/SS	75–175	30–40	0.69	0.90
High porosity grade EXE030	100–300	150–250	0.33	0.98

[a]Obtained using Equation (2) and data reported in text and Table S2.
[b]From the reported relationship of η_i (internal effectiveness factor) and Φ_{obs} (observable modulus) for spherical particles under conditions when $S_0/K_M = 5$ applies (Bailey and Ollis, 1986).

For immobilization, we adopted the method of Mateo et al. (2002), with some simplifications. The enzyme solution was diluted with 1.5 M PPB, pH 7.5, in order to obtain a buffer concentration of 0.75 M PPB, pH 7.5. About 0.4 g of dry Sepabeads was suspended in 10 mL of enzyme solution and incubated at 18°C using gentle mixing in an end-over-end rotator (~10 rpm). Samples were withdrawn at different times, and protein content and CCA activity remaining in the supernatant were measured. After 24 h, the immobilized CCA was first washed twice with 20 mM PPB, pH 7.5, then recovered using a 0.20-μm membrane filter and finally stored at 4°C until further use.

Assays

CCA activity was measured using a reported spectrophotometric assay (Patett and Fischer, 2006) with some modifications. A reaction mixture containing 500 μL of 40 mM CC-Na and 500 μL of enzyme solution (both in 0.1 M PPB, pH 8.0) was incubated at 37°C in Eppendorf tubes using agitation at 350 rpm in a Thermomixer (Eppendorf, Hamburg, Germany). A 120 μL sample was taken after 15 min and transferred into a disposable cuvette. Then, 720 μL of colorant solution containing 0.5% (w/v) pDAB in MeOH, 50 mM NaOH, and 20% (v/v) aqueous acetic acid in a volumetric ratio of 1:2:4 was added to stop the reaction. Absorbance at 414 nm was read 3 min after reagent addition using a DU 800 UV-vis spectrophotometer (Beckman Coulter, Inc., Fullerton, CA, USA). Suitable controls lacking the enzyme were always performed. Reported enzymatic rates are corrected for relevant blank readings. A calibration curve with known 7-ACA concentrations was obtained using 120 μL of 7-ACA in 0.1 M PPB, pH 8.0, after incubation for 15 min at 37°C, instead of the sample from the reaction mixture. One unit (U) of activity corresponds to the release of 1 μmol of 7-ACA per minute under assay conditions.

The activity assay for immobilized CCA was performed in a 15-mL vessel containing typically about 25 mg of wet carrier. Three milliliters of 0.1 M PPB, pH 8.0, was added to suspend the carrier. Another 3 mL of the same buffer containing 80 mM CC-Na was added to start the reaction, which was conducted for 15 min at 37°C in an orbital shaker (Certomat, Sartorius, Goettingen, Germany) at 250 rpm. A carrier-free sample (120 μL) was withdrawn from the supernatant and analyzed as described for the free enzyme.

Protein was measured using the Bio-Rad assay referenced against known concentrations of BSA in the range of 0.10–1.0 mg/mL.

Dual Luminescence Labeling of Sepabeads

The lipophilic luminescent dyes were non-covalently immobilized on the carrier surface. About 0.4 g dry Sepabeads was weighed in a 15-mL vessel (covered with aluminum foil for protection against light) and successively, 9.5 mL of 0.1 M PPB, pH 7.2, and 0.5 mL of LP-FLU stock solution (2 mg/mL in ethanol) was added. The suspension was incubated at room temperature overnight using mixing at 15 rpm with an end-over-end rotator. The labeled carrier was washed twice with 0.1 M PPB, pH 7.2, and with deionized water until the filtrate was colorless. Prior to proceed with enzyme immobilization, as described in the enzyme immobilization paragraph, the carrier was additionally washed with 1.5 M PPB, pH 7.5, to remove non-bound luminescent dye. Then, after immobilization, the resulting immobilized CCA was washed twice (0.1 M PPB, pH 7.2) and incubated (10 min, room temperature, end-over-end rotation at 15 rpm) in the presence of 10 mL reagent solution which contained 1 mL of Ru(dpp) (2 mg/mL) dissolved in EtOH and 9 mL of 0.1 M, PPB, pH 7.2. The last wash was done with 0.1 M PPB, pH 8.5, and the dual-labeled immobilized CCA was recovered by suction of the supernatant. The total amount of luminescent dye offered per gram dry carrier was 2.5 mg for LP-FLU and 5 mg for Ru(dpp). It was verified that this derivatization of Sepabeads did not affect the specific activity of the immobilized CCA.

We also prepared singly labeled particles in which 5-aminofluorescein was covalently attached via its amino group to Sepabeads EXE096. The procedure was analogous to that used for the non-covalent incorporation of LP-FLU into the carriers. The resulting beads were used as reference material in a comparison with the dual labeled particles.

Measurement of External and Internal pH During Hydrolysis of Cephalosporin C

A cylindrical vessel with a working volume of about 2 cm^3 (4 mm radius, 40 mm height) was used. It was equipped with a magnetic stirrer (stirring at 270 rpm) and placed in a water bath for temperature control at 37°C. It was confirmed by visual inspection that despite stirring, the particles were not mechanically disintegrated during the course of the experiment (~30 min). Figure S1 in Supporting Information shows results of an analysis by confocal laser scanning microscopy in which particles before and after performing a

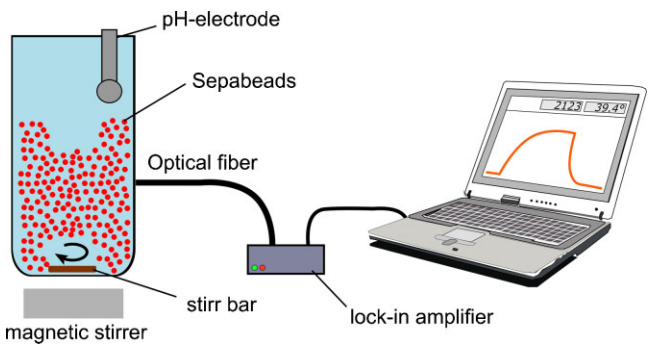

Scheme 2. Set-up for measurement of internal particle pH.

reaction are compared. A pH electrode (Minitrode, Hamilton, Bonaduz, Switzerland), interfaced to a laptop computer, was used for bulk pH measurement (Scheme 2). The luminescence signal of the labeled particles was detected by phase-shift measurements with a miniaturized lock-in amplifier (pH-Mini, PreSens GmbH, Regensburg, Germany) equipped with a 2-mm optical fiber. Measurements were carried out at a modulation frequency of 45 kHz. For each batch of labeled particles, a suitable calibration of fluorescence signal against bulk pH was obtained under conditions in which no enzymatic reaction took place. When particles derivatized with 5-aminofluorescein were employed, measurement of the internal pH required that fluorescence intensities were recorded. This was done using same pH-Mini instrument, applying analogous conditions for excitation and detection. An analogous procedure for calibration was applied.

Hydrolysis experiments were performed using 1 mL of 100 mM PPB, pH 8.5, containing a suitable amount of immobilized enzyme, typically ~3 U of activity. The pH in bulk and the fluorescence from the particles were recorded continuously. The reaction was started by the addition of CC-Na once a stable signal from each sample was obtained. It was monitored for typically 25 min.

Results

Method Development for Internal pH Measurement in Suspended Particles

Fluorescein derivatives are useful pH indicators because they can be applied in the neutral pH range and show high quantum yields. A previously developed method called DLR (Huber et al., 2001; Mayr et al., 2002), which enables the conversions of fluorescence intensities signals into phase shifts, was applied to measure the internal pH of particles containing immobilized CCA (see Scheme 2). In the system presented here, LP-FLU is used as the pH indicator and Ru(dpp) as reference luminophore. LP-FLU shows a luminescence decay time in the nanoseconds range, while the luminescence of Ru(dpp) decays in microseconds. The selected luminophores show overlapped excitation spectra and their emission can be detected at a common band of wavelengths with a single photodetector. The pH-dependent fluorescence of LP-FLU is converted into a phase shift that depends on the ratio of intensities of indicator and reference. Because the reference intensity is invariant with pH, the measured phase shift can be directly related to the proton concentration (for details of DLR, see Huber et al., 2001; Mayr et al., 2002). Note that Ru(dpp) is sensitive to oxygen. However, measurements were carried out under constant oxygen concentrations in air-saturated samples. Figure 1A shows a calibration curve relating the measured phase shifts for LP-FLU to external pH values in a suspension of doubly labeled Sepabeads EXE096. Using the chosen combination of luminophores, a representative pH range from 5.0 to 8.5 in which many enzymes are optimally active and stable, can be covered. Figure 1B displays time course data for external and internal pH determined in a hydrolysis experiment where conversion of CC-Na by CCA immobilized on Sepabeads EXE096 was carried out in the absence of pH control in liquid bulk. The results show that the average internal pH (solid phase) quickly dropped below the external pH (bulk phase) once substrate was added to

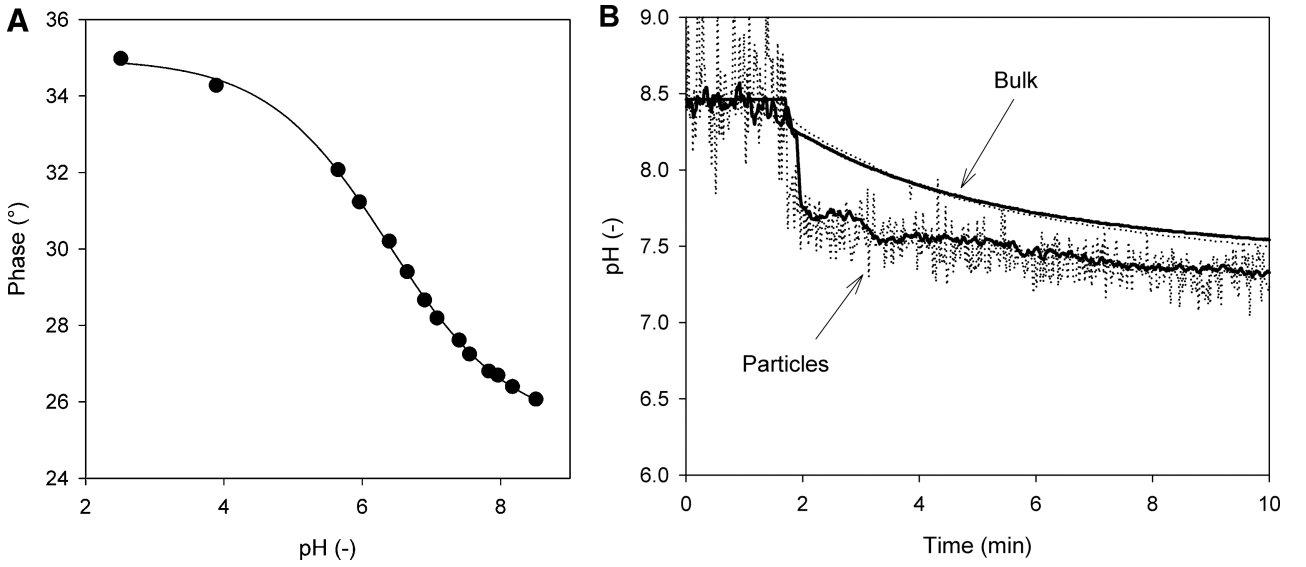

Figure 1. Internal pH measurements for Sepabeads EXE096 suspended in PPB. **A**: Calibration curve using the DLR system. **B**: Time course for the internal and external pH during hydrolysis of CCA determined by DLR (solid line) or using fluorescence intensity-based data (dotted line). In panel A, (●) indicates the data and the line is their fit with a four-parameter sigmoidal function.

the system. Despite the gradual decrease in the external pH as the reaction progressed, a negative ΔpH remained throughout the entire course of hydrolysis. Figure 1B compares internal pH data obtained using DLR and fluorescence intensity-based measurements. The results are clear in showing a dramatic enhancement in signal stability achieved through incorporation of a reference luminophore into the labeled particles. Furthermore, internal pH measurements using singly labeled 5-amino-fluorescein beads were afflicted with a large standard error (data not shown) that was conveniently overcome by employing the DLR approach.

Immobilization of CCA on Different Sepabeads

CCA was immobilized on four types of Sepabeads offering the same surface chemistry but differing in pore size and particle diameter. Immobilization was monitored by measuring residual protein concentration and volumetric enzyme activity in the supernatant as a function of incubation time in the presence of carrier. Binding of CCA activity (pDAB assay) was parallel to binding of protein (Bio-Rad assay) and complete after ~20 h. However, a typical time course of CCA adsorption was characterized by a fast initial phase (<5 h) in which about 85% of the total amount of bound protein became attached to the carrier. This was followed by a much slower phase of binding in which the remainder of the respective protein was adsorbed. These two phases probably express (see Mateo et al., 2002) that immobilization occurs in two steps where rapid physical adsorption between protein and carrier is followed by a slower covalent reaction between different protein groups (amino, thiol, and phenolic) and the epoxy groups of the carrier. After 1 h of incubation no elution of protein occurred upon transfer of the resulting beads into 1 M NaCl suggesting that the immobilization of CCA had taken place via coupled adsorption and covalent attachment. Figure 2 compares protein immobilization on the four carriers under various conditions of offered protein amount per gram dry carrier. Sepabeads EXE030, which according to technical data provided by the supplier, have only half of the specific surface area (40 m^2/g dry carrier) and one-third of the reactive oxirane content (120 μmol/g dry carrier) as compared to Sepabeads EXE096 (90 m^2/g dry carrier and 350 μmol/g dry carrier, respectively) showed the lowest binding capacity among the carriers tested. Using three sieve fractions of Sepabeads EXE096 having large (M), intermediate (standard grade), and small (SS) diameter (Table I), we found that contrary to our expectation for carriers of spherical geometry, there was only a fairly modest effect of particle size on protein binding capacity. However, because Sepabeads EXE096 have relatively small mesopores (diameter 30–40 nm), it is possible that a substantial fraction of the total surface area is unavailable for the enzyme. Despite this, from the crystal structure of a class I cephalosporin amidase (Kim et al., 2000) it is estimated that CCA has a maximum characteristic length of ~7 nm. Carrier pores should thus be large enough to let CCA diffuse into these pores and bind evenly distributed onto the available surface of the carrier.

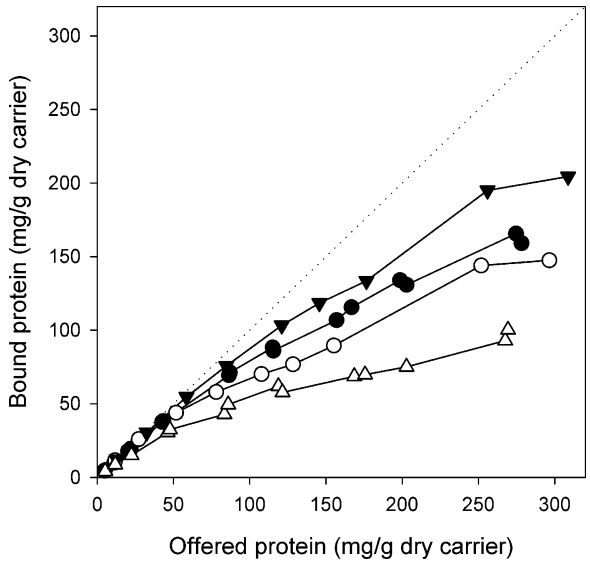

Figure 2. Immobilization of CCA on different types of Sepabeads. (●) Standard Grade EXE096, (Δ) high porosity grade EXE030, (○) coarse grade EXE096/M, and (▼) fine grade EXE096/SS. The concentration of beads was 0.01–0.04 g dry carrier/mL.

Characterization of Immobilized CCA Preparations

A preparation of CCA immobilized on Sepabeads EXE096, containing ~70 mg bound protein per gram dry carrier, was used to obtain a comparison of the catalytic properties of free and immobilized CCA. It was observed that the apparent activity of the immobilized enzyme was dependent on the orbital shaking velocity (in the range 200 rpm and lower) applied in the assay. To ensure the absence of limitation of the overall enzymatic rate by external (liquid-to-solid) mass transfer, we performed all further assays at a shaking velocity of 250 rpm.

The specific activity of this immobilized CCA preparation was one-fourth of that of the free enzyme. The optimum temperature for both immobilized and free CCA was 50°C. Arrhenius plots constructed from temperature dependencies of the enzyme activities were linear in the range 20–50°C (Fig. 3A) and yielded similar activation free energies for CC-Na hydrolysis 45 kJ/mol (free enzyme) and 38 kJ/mol (immobilized enzyme). The pH dependencies of immobilized and free CCA are compared in Figure 3B. A decrease in pH from 8.5 to 7.0 caused a ~7-fold drop in activity for the free enzyme, whereas immobilized CCA was clearly less sensitive than the free CCA. The stability of free CCA was affected by pH (Fig. S2 of the Supporting Information). Assuming a first-order decay of enzyme activity, we can calculate that the half-life time of CCA was increased two-

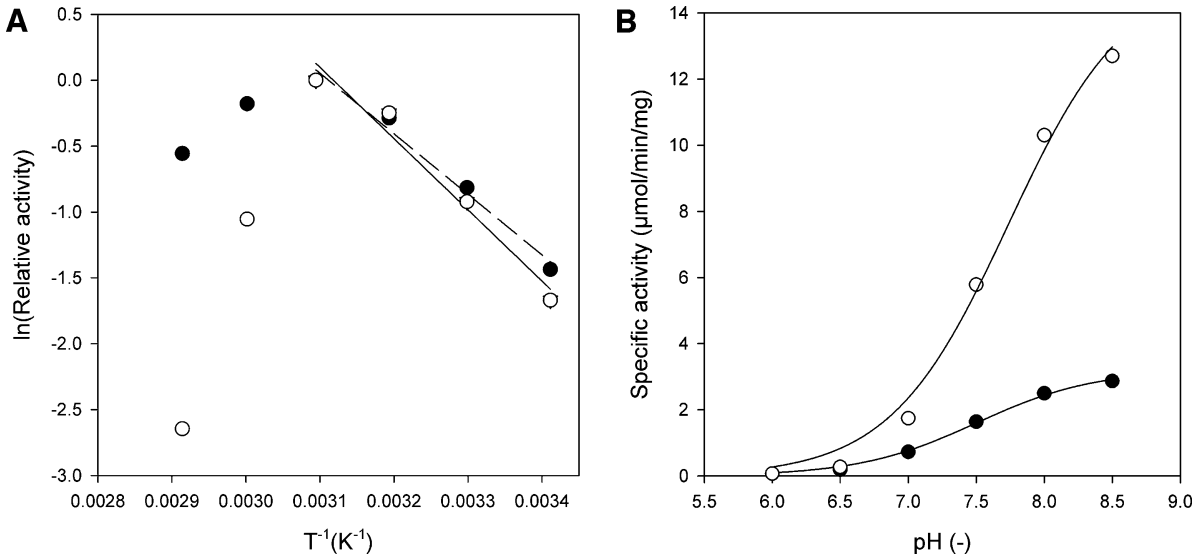

Figure 3. Temperature (**A**) and pH dependencies (**B**) of the activities of free CCA and enzyme immobilized on Sepabeads EXE096. A: 15 mM CC-Na; pH 8.0, (●) CCA immobilized on standard grade EXE096, 0.06 mg protein/mL; (○) free CCA, 0.01 mg protein/mL. B: 38 mM CC-Na; 37°C, (●) CCA immobilized on standard grade EXE096, 0.08 mg protein/mL; (○) free CCA, 0.01 mg protein/mL.

and fourfold at pH 7.5 and 6.5, respectively, as compared to the half-life time at pH 8.5. A decrease in pH, therefore, has opposite effects on activity (decrease; Fig. 3B) and stability (increase; Fig. S2).

Steady-State Kinetic Analysis

Initial rates of hydrolysis of CC-Na catalyzed by different preparations of free and immobilized CCA were determined at seven or more substrate concentrations in the range 0.5–35 mM. Kinetic parameters (V_{max}, K_M) were obtained using nonlinear fits of the Michaelis–Menten equation to the data. They are summarized in Table S1 of the Supporting Information. Figure 4 is an Eadie–Hofstee representation of results obtained through variation of the carrier type using a constant (intermediate) protein loading of 60–70 mg protein/g dry carrier. Small particle diameters (as in Sepabeads EXE096/SS) and large pore sizes (as in Sepabeads EXE030) appear to be correlated with a relatively high V_{max} and a low K_M.

Using the values of V_{max} (=13.2 U/mg) and a V_{max}/K_M (=4.00 U/mg mM) of the free CCA as the reference, we calculated two types of stationary effectiveness factor (η) for the different immobilized enzyme preparations, η (V_{max}) and η (V_{max}/K_M), where η is the ratio of the rate parameters for immobilized to free enzyme. η (V_{max}) and η (V_{max}/K_M) refer to reaction conditions at which the substrate is saturating and limiting, respectively. Figure 5A shows the effect of enzyme loading on η (V_{max}) and η (V_{max}/K_M) for CCA immobilized on Sepabeads EXE096 and EXE030. η (V_{max}) was consistently higher than η (V_{max}/K_M), and effectiveness factors for the carrier with wide pores (EXE030) exceeded those for the carrier with narrow pores (EXE096). η (V_{max}/K_M) decreased with increasing enzyme loading irrespective of carrier pore size. Interestingly, while η (V_{max}) for Sepabeads EXE030 showed a similar dependence on enzyme loading as the corresponding η (V_{max}/K_M), the η (V_{max}) for Sepabeads EXE096 was independent of the

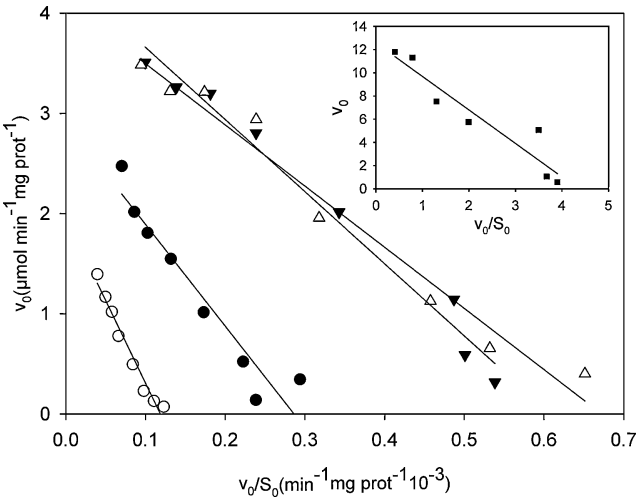

Figure 4. Eadie–Hofstee plots of initial-rate data obtained for different preparations of CCA. Reactions were performed at pH 8.0 and 37°C with agitation at 250 rpm in an orbital shaker. CC-Na concentration was varied from 0.6 to 35 mM. (●) Standard grade EXE096, 0.06 mg protein/mL; (Δ) high porosity grade EXE030, 0.05 mg protein/mL; (○) coarse grade EXE096/M, 0.06 mg protein/mL; (▼) fine grade EXE096/SS, 0.06 mg protein/mL. Inset: (■) free enzyme, 0.006 mg/mL; agitation at 350 rpm in a thermomixer.

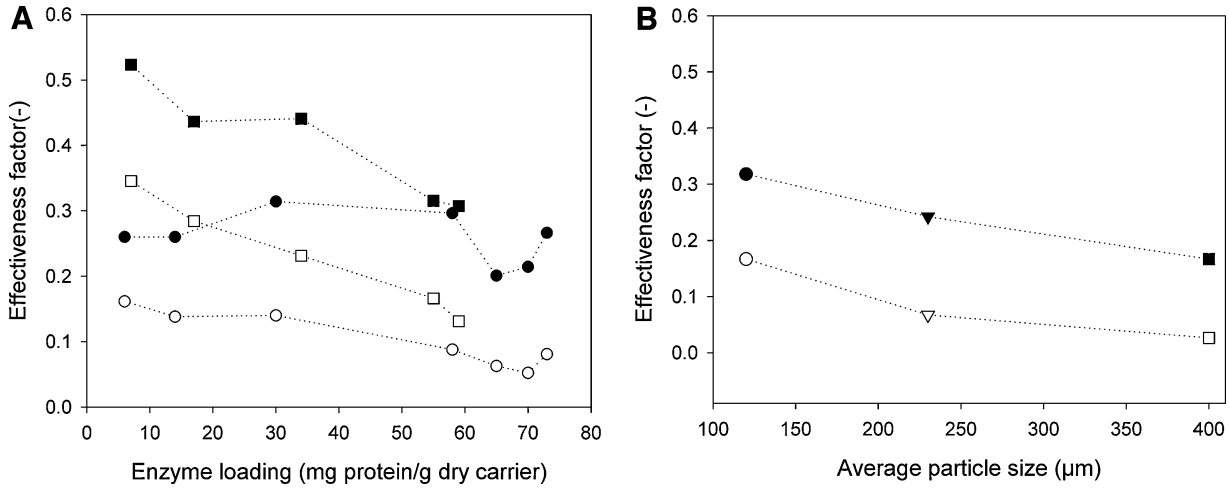

Figure 5. Stationary effectiveness factors for immobilized CCA in dependence of enzyme loading (**A**) and carrier size (**B**). Full symbols η (V_{max}); open symbols η (V_{max}/K_M) (A) (●) standard grade EXE096; (■) high porosity grade EXE030. B: (●) Fine grade EXE096/SS; (▼) standard grade EXE096; (■) coarse grade EXE096/M.

amount of protein bound/g dry carrier in the range tested. Elimination of an enzyme loading dependence on η by offering a saturation concentration of CC-Na suggests that pore diffusion of substrate becomes increasingly rate determining for V_{max}/K_M when a large amount of enzyme (70 mg/g dry carrier) is immobilized on Sepabeads EXE096. Figure 5B shows that η (V_{max}/K_M) and η (V_{max}) for CCA immobilized on Sepabeads EXE096 decreased as the particle size of the carrier was increased. Therefore, this result implies that substrate diffusional resistance was clearly not the sole reason for the decrease of η at high enzyme loading. It is consistent with the finding in Figure 5A that wider pores (EXE030 relative EXE096) appear to contribute to re-establishment of the dependence of η (V_{max}) on enzyme loading. The ΔpH (intraparticle compared with bulk) could contribute to the observed dependence of η (V_{max}) on reaction conditions.

Dependence of Intraparticle pH Gradients on Carrier and Reaction Parameters

The course of internal and external pH was measured as a function of reaction time during hydrolysis of CC-Na catalyzed by different preparations of the immobilized CCA (Fig. 6, panels A–D). There was a maximum in ΔpH immediately after the addition of substrate because of the almost instantaneous drop of the internal pH. However, the ΔpH reached a constant value after a few minutes of reaction. Figure 6A shows for CCA immobilized on Sepabeads EXE096 that ΔpH prior to and in the steady state increased as the initial concentration of CC-Na was increased. The effect of the initial substrate concentration on ΔpH was markedly alleviated when using Sepabeads EXE030 instead of Sepabeads EXE096 (Fig. 6B). The difference in carrier characteristics in Sepabeads EXE030 as compared to Sepabeads EXE096 was associated with a strong reduction of ΔpH formation, (i.e., the rate with which the internal pH decreased relative to the external pH) during the initial phase of the reaction (<1 min). Figure 6C shows that rate of ΔpH formation in Sepabeads EXE030 was dependent on the initial substrate concentration and typically just about half of that in Sepabeads EXE096. Variation in the particle size of Sepabeads EXE096 caused a clear change in steady-state ΔpH when Sepabeads EXE096 and EXE096/M are compared (Fig. 6D). However, the results do not support a simple generalization that larger beads lead to more substantial ΔpH. The ΔpH for Sepabeads EXE096/SS was nearly identical to that observed for Sepabeads EXE096.

Discussion

7-ACA is an important intermediate for the industrial production of a whole series of cephem antibiotics obtained by fermentation and hydrolysis of cephalosporin C. The classical enzymatic route occurred by a multi-step chemo-enzymatic transformation, in which two biocatalysts were required, as shown in Scheme 1 (Buchholz et al., 2005; López-Gallego et al., 2004; Monti et al., 2000). Identification of enzymes capable of hydrolyzing cephalosporin C in one enzymatic step (Fritz-Wolf et al., 2002; Kim et al., 2000; Lopez-Gallego et al., 2005; Oh et al., 2003; Otten et al., 2007; Pollegioni et al., 2005) has promoted implementation of a simpler route of biocatalytic processing on manufacturing scale. Process technology developed for the hydrolysis of glutaryl-7-ACA is applied in the conversion of cephalosporin C. This involves the use of carrier-bound enzyme in stirred tank reactors at pH ≥8 where the reaction equilibrium favors product yields of 95% or greater. Short

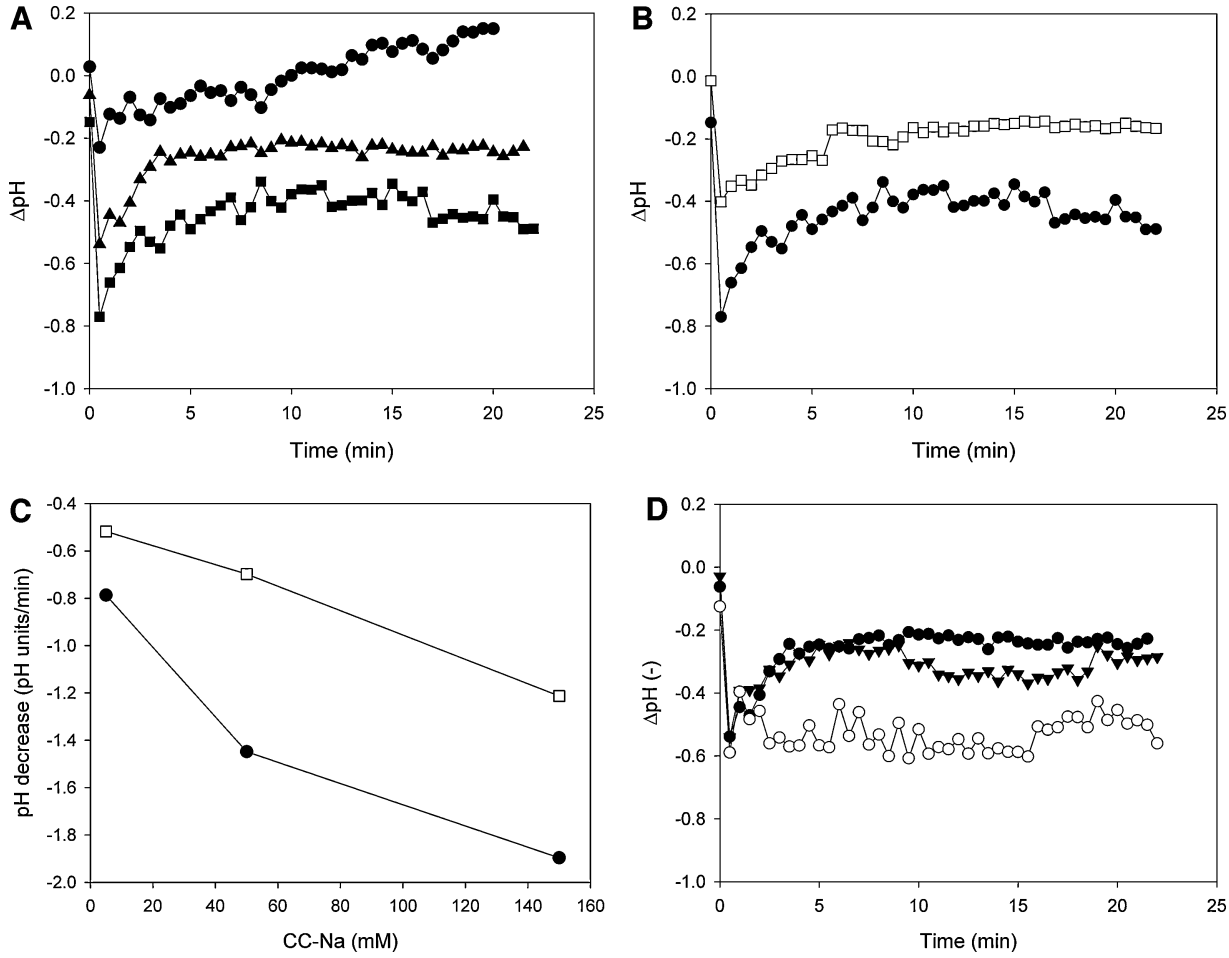

Figure 6. Difference between external and internal pH (ΔpH) during hydrolysis of CC-Na by different preparations of immobilized CCA. One hundred millimolar PPB, pH 8.5; 37°C; 270 rpm. **A**: Effect of substrate concentration on ΔpH for CCA immobilized on Sepabeads EXE096. (●) 5 mM CC-Na, (▲) 50 mM CC-Na, (■) 150 mM CC-Na, Sepabeads EXE096 70 mg protein/g dry carrier; 1 mg protein/mL. **B**: Comparison of CCA immobilized on Sepabeads EXE096 and EXE-030; 150 mM CC-Na. (●) Sepabeads EXE096, 70 mg protein/g dry carrier; (□) Sepabeads EXE030, 60 mg protein/g dry carrier. **C**: Rate of ΔpH formation in Sepabeads EXE096 and EXE-030. (●) Sepabeads EXE096, 70 mg protein/g dry carrier; (□) Sepabeads EXE030, 60 mg protein/g dry carrier. **D**: Effect of particle size on ΔpH. (▼) Sepabeads EXE096/SS, 67 mg protein/g dry carrier, 50 mM CC-Na. (●) Sepabeads EXE096, 70 mg protein/g dry carrier; (○) Sepabeads EXE096/M, 47 mg protein/g dry carrier.

hydrolysis times (≤30 min) are preferred to avoid 7-ACA loss due to intermolecular condensation reaction (Buchholz et al., 2005). Design of the immobilization such that the resulting CCA preparation is optimally active and stable would present a useful improvement in the new process. This article describes for the first time a detailed characterization of immobilized CCA, focusing on intra-particle concentration gradients for substrate and the proton formed in the reaction. From analysis of the dependence of these gradients on structural properties of the carriers and reaction conditions, important criterions for carrier selection are derived.

Immobilization of CCA

By comparison with relevant literature on other amidases and esterases (Basso et al., 2007; Mateo et al., 2002; Pollegioni et al., 2008), attachment to epoxy-activated Sepabeads is a useful method of immobilization of CCA. There is only a one carbon atom spacer between the reactive epoxy group and the particle surface in these carriers. Consistent with literature (Mateo et al., 2002), it is assumed, therefore, that the enzyme is bound through multi-point covalent attachment, presumably contributing to the observed stabilization of immobilized CCA at elevated temperature (see Fig. 3A). The binding capacity for carriers of the EXE096 type was greater than or equal to 150 mg bound protein/g dry carrier; that of Sepabeads EXE030 was ~100 mg/g dry carrier. The larger amount of specific surface in EXE096 as compared to EXE030 probably explains why more protein could be loaded on the former carrier. Interestingly, however, despite the fact that the density of epoxy groups per area (~3.5 μmol/m^2) was similar in the two carriers, the amount of protein bound per m^2 was higher in EXE030 (~2.5 mg/m^2) than EXE096 (1.7 mg/m^2). EXE030 could thus be considered more efficient than

EXE096 in the exploitation of available surface area for protein binding.

Even when working at high protein loadings (200–300 mg offered protein/g dry carrier), the immobilization yield (=100% × (offered protein − unbound protein)/offered protein) was still around 50% for EXE096 and 30% for EXE030. Immobilized CCA retained between 20% and 50% specific amidase activity of the free enzyme preparation, depending on the type of carrier and the enzyme loading used (see later). Both free and immobilized CCA were best active at the highest pH employed herein (pH 8.5). However, the activity of the immobilized preparation displayed a twofold attenuated response, as compared to that of the free CCA, to a drop of pH to a value of 7.0 or lower, which may occur during the biocatalytic process. While both enzyme preparations share the same optimum temperature of 50°C, the loss of activity above 50°C was much more dramatic for the free CCA, suggesting that covalent immobilization on Sepabeads enhanced resistance to thermal-induced denaturation.

Kinetic Evidence for Substrate Concentration Gradients in Immobilized CCA Particles

Calculation of the Thiele modulus (Eq. 1) requires knowledge of intrinsic kinetic parameters for the immobilized enzyme. As these parameters were not available for CCA, the observable modulus Φ_{obs} (Eq. 2; Bailey and Ollis, 1986; Blanch and Clark, 1996) was used to assess the magnitude of diffusional limitation during hydrolysis of CC-Na using immobilized CCA preparations

$$\Phi_{obs} = \frac{(R/3)^2 v_{obs}}{(D_{eff} S_0)} \quad (2)$$

In Equation (2), v_{obs} is the observed rate (mol/m^3 s), and S_0 (mol/m^3) is the initial substrate concentration in liquid bulk. The enzymatic reaction is kinetically controlled for $\Phi_{obs} < 0.3$ and diffusion limited for $\Phi_{obs} > 3$. D_{eff} for cephalosporin C was estimated using Equation (3) (Bailey and Ollis, 1986)

$$D_{eff} = D\frac{\varepsilon}{\tau}(1 - r_{molecule}/r_{pore})^4 \quad (3)$$

where D is the substrate diffusivity in bulk liquid (m^2/s), ε is the support porosity, τ is the pore tortuosity, $r_{molecule}$ (m) and r_{pore} (m) are the substrate molecular radius and characteristic pore radius, respectively. Considering the similarity of the reaction systems used $r_{molecule}$ was approximated using reported values for benzylpenicillin and glutaryl-7-aminocephalosporanic acid ($r_{molecule} = 1.2$ nm) (Spiess et al., 1999). The molecular diffusivity D of cephalosporin C in water was estimated according to Wilke-Chang (Perry et al., 1997)

$$D = 7.4 \times 10^{-8} \frac{(\Phi M_B)^{1/2}}{(\eta_B V_A^{0.6})} \quad (4)$$

where M_B is the molecular weight of the solvent, T the absolute temperature (K), η_B the viscosity of the solvent (cp), and Φ a dimensionless association factor of solvent (2.26 for water). The value of V_A, the molar volume of cephalosporin C at its normal boiling temperature was estimated from the Schroeder's group contributions method (Reid et al., 1987) to be 385 cm^3/mol. At 37°C D was 5.95×10^{-10} m^2/s.

Using data in Table S2 for average porosity and a particle density of 1.14 g dry carrier/mL, ε was calculated as 0.27 for Sepabeads EXE096, EXE096/SS, and EXE096/M, and 0.70 for Sepabeads EXE030. The average r_{pore} was assumed to be the midpoint of the r_{pore} range provided by the supplier that is 17.5 nm for Sepabeads EXE096 and 100 nm for Sepabeads EXE030. τ was calculated according to Beekman (Shen and Chen, 2007) as reported in Table S2. Using these data and applying Equation (3), D_{eff} for Sepabeads EXE096 was just one-fourth of that of Sepabeads EXE030 (Table S2).

The Φ_{obs} values summarized in Table I suggest that, in substrate saturating conditions, reactions catalyzed by CCA immobilized on Sepabeads EXE096 became increasingly limited by diffusion as the particle radius R was increased. The reaction catalyzed by CCA on Sepabeads EXE030, by contrast, was limited by enzymatic conversion. A more direct quantification of diffusion limitation is given by the internal effectiveness factor (η_i) which is the ratio between

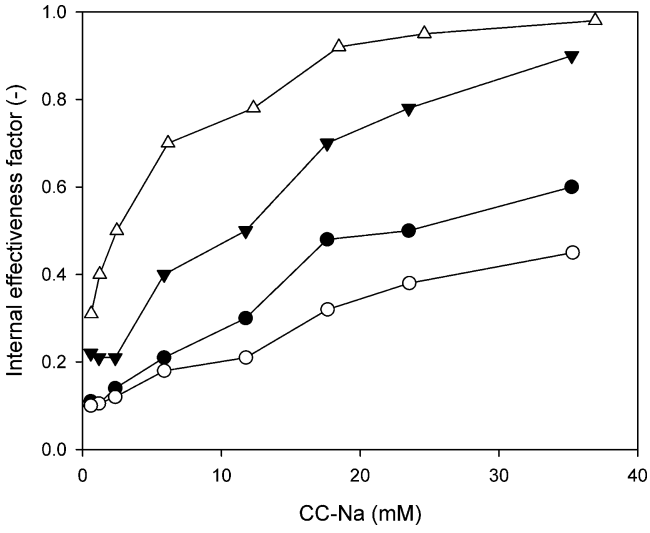

Figure 7. Internal effectiveness factors for immobilized CCA in dependence of substrate concentration: (●) standard grade EXE096 (72 mg protein/g dry carrier), (Δ) high porosity grade EXE030 (55 mg protein/g dry carrier), (○) coarse grade EXE096/M (64 mg protein/g dry carrier), (▼) fine grade EXE096/SS (73 mg protein/g dry carrier).

ν_{obs} and the reaction rate that would result if the entire interior surface were exposed to external pellet surface conditions. Considering spherical carrier geometry and the chosen reaction conditions where $S_0/K_M = 5$, we used reported dependencies of η_i on Φ_{obs} (Bailey and Ollis, 1986) to obtain effectiveness factors for the different immobilized CCA preparations (Table I). Figure 7 shows a plot of η_i versus substrate concentration indicating that the internal effectiveness decreased when the substrate concentration was decreased, with a marked drop of η_i being observed at substrate concentrations lower than K_M. The increase in apparent K_M for immobilized CCA preparations (Table S1), relative to the K_M for the free enzyme (3.3 ± 0.7 mM), appears to reflect the variation of η_i in response to changes in pore and particle size as well as enzyme loading. However, Figure 5 reveals that η values derived from experimental kinetic parameters, while generally following the overall trend expected from Table I, are substantially lower than is explicable by substrate diffusional effects alone (η_i). We show that accumulation of acidic product in the enzyme microenvironment probably accounts for additional lowering of η (V_{max}/K_M) and, noteworthy, η (V_{max}). Effects of immobilization on the protein structure (as relevant for CCA activity) were not pursued.

Method for Determining Internal pH in Suspended Biocatalytic Particles

Measurement of intraparticle pH using the DLR method eliminated a major disadvantage of earlier analytical approaches (Huang et al., 2008; Spiess and Kasche, 2001; Spiess et al., 1999) that were not applicable to suspended carriers in stirred or fluidized-bed systems. Phase-shift measurements are, however, independent of particle density and are therefore relatively insensitive to particle movements in solution (Kuwana et al., 2004; Mayr et al., 2002). Internal pH measurement under process-near mixing conditions and at different scales of operation is thus supported. Although not specifically examined for this purpose (see Fig. 6), collection of internal pH data in a time-resolved manner could provide a useful, hitherto unexploited parameter for on-line control of the biocatalytic process. Importantly, therefore, the phase-shift signal was very stable, resulting in a pH response that was much more accurate than the corresponding pH response obtained by fluorescence intensity-based measurements.

Because particle labeling was achieved through direct adsorption of the two luminophores by the carriers, we believe that the labeling procedure is independent of the enzyme chosen and should also be applicable to methacrylate carriers other than Sepabeads. The DLR method should be likewise compatible with different surface functionalities as it avoids chemical modification of carrier as well as of enzyme. Using more specialized techniques like confocal laser scan microscopy (see Huang et al., 2008; Spiess and Kasche, 2001; Spiess et al., 2008), it could certainly be adopted for spatial resolved measurements of intraparticle pH.

Dependence of Intraparticle pH Gradients on Reaction Conditions and Carrier Characteristics

The difference between internal and external pH (ΔpH) at steady state increased in response to substrate concentration. Using CC-Na concentrations higher than 50 mM, ΔpH was as large as $\sim$0.5. Considering the pH-activity profile (Fig. 3B) for CCA immobilized on Sepabeads EXE096, the observed pH decrease could cause about twofold reduction in enzymatic activity and would hence significantly affect η (V_{max}). Widening the carrier pores in Sepabeads EXE030 as compared to Sepabeads EXE096 resulted in a relatively smaller ΔpH at steady state (ΔpH $\sim$ 0.3; Fig. 6B) and a slower rate of initial pH drop (Fig. 6C), all consistent with the idea that internal diffusion of acidic product was facilitated as r_{pore} of the carrier increased. The marked effect of r_{pore} on internal pH was also noted by Spiess and Kasche (2001) studying amidase-catalyzed hydrolysis of penicillin G. Particle size did affect ΔpH, the overall trend being as expected that larger carriers (EXE096/M compared to EXE096) resulted in enhanced pH gradients. However, there was only little difference between Sepabeads EXE096 and Sepabeads EXE096/SS in our experiments. The change in particle size range from 150–300 μm (EXE096) to 75–175 nm (EXE096/SS) may be simply too small to a produce detectable response. Analysis of the distribution of bound protein in these two carriers could provide further insight. Interestingly, Van Roon et al. (2005) demonstrated intraparticle enzyme heterogeneity for an industrial immobilized penicillin G acylase.

Conclusions

Our study provides methodology for measurement of intraparticle pH gradients and guides carrier selection for preparation of immobilized CCA in order to achieve optimum performance with respect to activity and stability. Facilitated diffusion of substrate and in particular of an acidic product is a clear advantage of Sepabeads EXE030 over Sepabeads EXE096. A higher V_{max} and a lower K_M are obtained for comparable, yet technologically relevant enzyme loadings ($\geq$50 mg protein/g dry carrier) when using CCA bound to Sepabeads EXE030 as compared to the Sepabeads EXE096. Improved enzyme kinetic efficiency may thus compensate for the lower protein binding capacity (in terms of mg per g dry carrier) of Sepabeads EXE030 as compared to Sepabeads EXE096. The pore size of Sepabeads EXE030 is within practical limits for enzyme carriers (r_{pore} = 40–80 nm; Buchholz and Kasche, 1997). The particle size range of Sepabeads EXE096 particles (150–300 μm) was suitable, and carriers of larger size are not recommended. We believe that the findings for CCA in combination with

the methodology developed are useful for others working with immobilized amidase and esterase systems.

The Oesterreichische Austrian Research Promotion Agency (FFG), the Province of Styria, the Styrian Business Promotion Agency (SFG), the city of Graz, and Sandoz GmbH are acknowledged for financial support. We are grateful to Dr. Paolo Caimi (Resindion Srl) for supplying Sepabeads resins. Dr. Massimiliano Cardinale (Institute for Environmental Biotechnology, TU Graz) is thanked for performing microscopic analysis of the carriers used.

References

Bailey JE, Ollis DF. 1986. Biochemical engineering fundamentals. New York: McGraw-Hill, p 202–227.

Barros RJ, Wehtje E, Adlercreutz P. 1998. Mass transfer studies on immobilized α-chymotrypsin biocatalyst prepared by deposition for use in organic medium. Biotechnol Bioeng 59:365–373.

Basso A, Braiuca P, Cantone S, Ebert C, Linda P, Spizzo P, Caimi P, Hanefeld U, Degrassi G, Gardossi L. 2007. In silico analysis of enzyme surface and glycosylation effect as a tool for efficient covalent immobilization of CalB and PGA on Sepabeads®. Adv Synth Catal 349:877–886.

Blanch HW, Clark DS. 1996. Biochemical engineering. New York: Marcel Dekker, Inc., p 127–137.

Borisov S, Klimant I. 2009. Luminescent nanobeads for optical sensing and imaging of dissolved oxygen. Microchim Acta 164:7–15.

Bourdillon C, Demaille C, Moiroux J, Savéant J-M. 1999. Analyzing product inhibition and pH gradients in immobilized enzyme films as illustrated experimentally by immunologically bound glucose oxidase electrode coatings. J Phys Chem B 103:8532–8537.

Buchholz K, Kasche V. 1997. Biokatalysatoren und Enzymtechnologie. Weinheim: Wiley-VCH, p 146, 251.

Buchholz K, Kasche V, Bornscheuer UT. 2005. Biocatalysts and enzyme technology. Weinheim: Wiley-VCH, p 244, 262–275, 340–343, 381–392.

Byres JP, Shah MB, Fournier RL, Varanasi S. 1993. Generation of a pH gradient in an immobilized enzyme system. Biotechnol Bioeng 42:410–420.

Cao L. 2005. Carrier-bound immobilized enzymes principles, applications and design. Weinheim: Wiley-VCH, p 169–170.

Doran PM. 1995. Bioprocess engineering principles. London: Academic Press Limited, p 298–299.

Fritz-Wolf K, Koller KP, Lange G, Liesum A, Sauber K, Schreuder H, Aretz W, Kabsch W. 2002. Structure-based prediction of modifications in glutarylamidase to allow single-step enzymatic production of 7-aminocephalosporanic acid from cephalosporin C. Protein Sci 11:92–103.

Guisán JM, Alvaro G, Rossel CM, Fernandez-Lafuente R. 1994. Industrial design of enzymic processes catalysed by very active immobilized derivatives: Utilization of diffusional limitations (gradients of pH) as a profitable tool in enzyme engineering. Biotechnol Appl Biochem 20:357–369.

Halwachs W, Wandrey C, Schügerl K. 1978. Immobilized α-chymotrypsin: Pore diffusion control owing to pH gradients in the catalyst particles. Biotechnol Bioeng 20:541–554.

Hanefeld U, Gardossi L, Magner E. 2009. Understanding enzyme immobilisation. Chem Soc Rev 38:453–468.

Hilterhaus L, Minow B, Mueller J, Berheide M, Quitmann H, Katzer M, Thum O, Antranikian G, Zeng AP, Liese A. 2008. Practical application of different enzymes immobilized on sepabeads. Bioprocess Biosyst Eng 31:163–171.

Huang HY, Shaw J, Yip C, Wu XY. 2008. Microdomain pH gradient and kinetic inside composite polymeric membranes of pH and glucose sensitivity. Pharm Res 25:1150–1157.

Huber C, Klimant I, Krause C, Wolfbeis OS. 2001. Dual lifetime referencing as applied to a chloride optical sensor. Anal Chem 73:2097–2103.

Janssen MHA, van Langen LM, Pereira SRM, van Rantwijk F, Sheldon RA. 2002. Evaluation of the performance of immobilized penicillin G acylase using active-site titration. Biotechnol Bioeng 78:425–432.

Kallenberg AI, van Rantwijk F, Sheldon RA. 2005. Immobilization of penicillin G acylase: The key to optimum performance. Adv Synth Catal 347:905–926.

Kim Y, Yoon K-I, Khang Y, Turley S, Hol WGJ. 2000. The 2.0 Å crystal structure of cephalosporin acylase. Structure 8:1059–1068.

Kuwana E, Liang F, Sevick-Muraca EM. 2004. Fluorescence lifetime spectroscopy of a pH-sensitive dye encapsulated in hydrogel beads. Biotechnol Prog 20:1561–1566.

Liou JK, Rousseau I. 1986. Mathematical model for internal pH control in immobilized enzyme particles. Biotechnol Bioeng 28:1582–1589.

Lopez-Gallego F, Betancor L, Hidalgo A, Mateo C, Fernandez-Lafuente R, Guisan JM. 2005. One-pot conversion of cephalosporin C to 7-amicephalosporanic acid in the absence oh hydrogen peroxide. Adv Synth Catal 347:1804–1810.

López-Gallego F, Betancor L, Hidalgo A, Mateo C, Guisán JM, Fernandez-Lafuente R. 2004. Optimization of an industrial biocatalyst of glutaryl acylase: Stabilization of the enzyme by multipoint covalent attachment onto new amino-epoxy Sepabeads. J Biotechnol 111:219–227.

Mateo C, Abian O, Fernandez-Lorente G, Pedroche J, Fernandez-Lafuente R, Guisan JM, Tam A, Daminati M. 2002. Epoxy Sepabeads: A novel epoxy support for stabilization of industrial enzymes via very intense multipoint covalent attachment. Biotechnol Prog 18:629–634.

Mateo C, Palomo JM, Fernandez-Lorente G, Guisan JM, Fernandez-Lafuente F. 2007. Review. Improvement of enzyme activity, stability and selectivity via immobilization techniques. Enzyme Microb Technol 40:1451–1463.

Matsuda A, Toma K, Komatsu KI. 1987. Nucleotide sequences of the genes for two distinct cephalosporin acylases from a *Pseudomonas* strain. J Bacteriol 169:5821–5826.

Mayr T, Klimant I, Wolfbeis OS, Werner T. 2002. Dual lifetime referenced optical sensor membrane for the determination of copper (II) ions. Anal Chim Acta 462:1–10.

Monti D, Carrea G, Riva S, Baldaro E, Frare G. 2000. Characterization of an industrial biocatalyst: Immobilized glutaryl-7-ACA acylase. Biotechnol Bioeng 70:239–244.

Oh B, Kim M, Yoon J, Chung K, Shin Y, Lee D, Kim Y. 2003. Deacylation activity of cephalosporin acylase to cephalosporin C is improved by changing the side-chain conformations of active-site residues. Biochem Biophys Res Commun 3120:19–27.

Otten LG, Sio CF, Reis CR, Koch G, Cool RH, Quax WJ. 2007. A highly active adipyl-cephalosporin acylase obtained via rational randomization. FEBS J 274:5600–5610.

Patett F, Fischer L. 2006. Spectrophotometric assay for quantitative determination of 7-aminocephalosporanic acid from direct hydrolysis of cephalosporin C. Anal Biochem 350:304–306.

Perry RH, Green DW, Maloney JO. 1997. Perry's chemical engineers' handbook. New York: McGraw-Hill, p 5–51.

Pollegioni L, Lorenzi S, Rosini E, Marcone GL, Molla G, Verga R, Cabri W, Pilone MS. 2005. Evolution of an acylase active on cephalosporin C. Protein Sci 14:3064–3076.

Pollegioni L, Pilone M, Molla G, Cucchetti E, Verga R, Cabri W. 2008. Cephalosporin C acylases. Patent No.: US 73996424 B2.

Regan DL, Lilly MD, Dunnill P. 1974. Influence of intraparticle diffusional limitation on the observed kinetics of immobilized enzymes and on catalyst design. Biotechnol Bioeng 16:1081–1093.

Reid RC, Prausnitz JM, Poling BE. 1987. The properties of gases and liquids. New York: McGraw-Hill.

Ruckenstein E, Rajora P. 1985. Optimization of the activity in porous media of proton-generating immobilized reactions by weak acid facilitation. Biotechnol Bioeng 27:807–817.

Sheldon RA. 2007. Enzyme immobilization: The quest for optimum performance. Adv Synth Catal 349:1289–1307.

Shen L, Chen Z. 2007. Critical review of the impact of tortuosity on diffusion. Chem Eng Sci 62:3748–3755.

Shin YC, Jeon J, Jung KH, Mark MR, Kim Y. 2005. Cephalosporin C acylase mutant and method for preparing 7-ACA using same. WO 2005/014821 A1.

Spiess AC, Kasche V. 2001. Direct measurement of pH profiles in immobilized enzyme carriers during kinetically controlled synthesis using CLSM. Biotechnol Prog 17:294–303.

Spiess A, Schlothauer RC, Hinrichs J, Scheidat B, Kasche V. 1999. pH gradients in immobilized amidases and their influence on rates and yields of β-lactam hydrolysis. Biotechnol Bioeng 62:267–277.

Spiess AC, Zavrel M, Ansorge-Schumacher MB, Janzen C, Michalik C, Schmidt TW, Schwendt T, Büchs J, Poprawe R, Marquardt W. 2008. Model discrimination for the propionic acid diffusion into hydrogel beads using lifetime confocal laser scanning microscopy. Chem Eng Sci 63:3457–3465.

Tischer W, Kasche V. 1999. Immobilized enzymes: Crystals or carriers? Tibtech 17:326–335.

Van Roon JL, Groenendijk E, Kieft H, Schroen CGPH, Tramper J, Beeftink HH. 2005. Novel approach to quantify immobilized-enzyme distributions. Biotechnol Bioeng 89:660–669.

Wang H, Seki M, Furusaki S. 1995. Mathematical model for analysis of mass transfer for immobilized cells in lactic acid fermentation. Biotechnol Prog 11:558–564.

Weidgans BM, Krause C, Klimant I, Wolfbeis OS. 2004. Fluorescent pH sensors with negligible sensitivity to ionic strength. Analyst 129:645–650.

SUPPORTING INFORMATION

Intraparticle Concentration Gradients for Substrate and Acidic Product in Immobilized Cephalosporin C Amidase and Their Dependencies on Carrier Characteristics and Reaction Parameters

Caterina Boniello, Torsten Mayr, Ingo Klimant, Burghard Koenig, Waander Riethorst, and Bernd Nidetzky

Table S1. Kinetic parameters for different immobilized CCA preparations

Sepabeads	*Loading (mg protein/g dry carrier)*	*V_{max} (U/mg protein)*	*K_M (mM)*
EXE096	73	3.5±0.1	10.8±0.6
EXE096	70	2.9±0.2	13.5±1.9
EXE096	65	2.7±0.2	10.6±1.7
EXE096	58	3.9±0.1	11.1±1.0
EXE096	30	4.1±0.1	7.4±0.3
EXE096	14	3.4±0.2	6.2±1.2
EXE096	6	3.4±0.1	5.3±0.7
EXE030	59	4.1±0.1	7.7±0.4
EXE030	55	4.2±0.1	6.3±0.7
EXE030	34	5.8±0.2	6.3±0.8
EXE030	17	5.8±0.2	5.1±0.5
EXE030	7	6.9±0.1	5.0±0.2
EXE096/SS	73	4.2±0.3	6.4±1.3
EXE096/M	64	2.2±0.4	20.9±5.5

Table S2 Carrier characteristics and reaction conditions applied in the calculation of the observable modulus

Sepabeads	*Average particle radius*[a] *(m)*	*Average porosity*[b] *(mL/ g dry)*	*Tortuosity*[c] *(-)*	D_{eff} *(m^2 s^{-1})*[d]	v_{obs} *(mol s^{-1} m^{-3})*[e]	S_0 *(mol m^{-3})*
Standard Grade EXE096	1.15×10^{-4}	0.32	1.65	7.25×10^{-11}	3.38	35.2
Coarse Grade EXE096/M	2.00×10^{-4}	0.32	1.65	7.25×10^{-11}	1.64	35.3
Fine Grade EXE096/SS	0.60×10^{-4}	0.32	1.65	7.25×10^{-11}	4.44	35.2
High Porosity Grade EXE030	0.90×10^{-4}	2.00	1.46	2.70×10^{-10}	3.62	36.9

[a] Provided by the supplier.

[b] Provided by the supplier.

[c] According to Beekman $\tau^2=\varepsilon/(1-(1-\varepsilon)^{1/3})$ as remarked in Shen and Chen (2007) for heterogeneous catalysts.

[d] Obtained using Eq. 3 and data reported in text and this Table.

[e] Obtained as product of enzyme loading (mg protein/g dry carrier), the immobilized enzyme specific activity (μmol product s^{-1} (mg protein)$^{-1}$), and the particle density (g dry carrier/mL carrier).

FIGURES

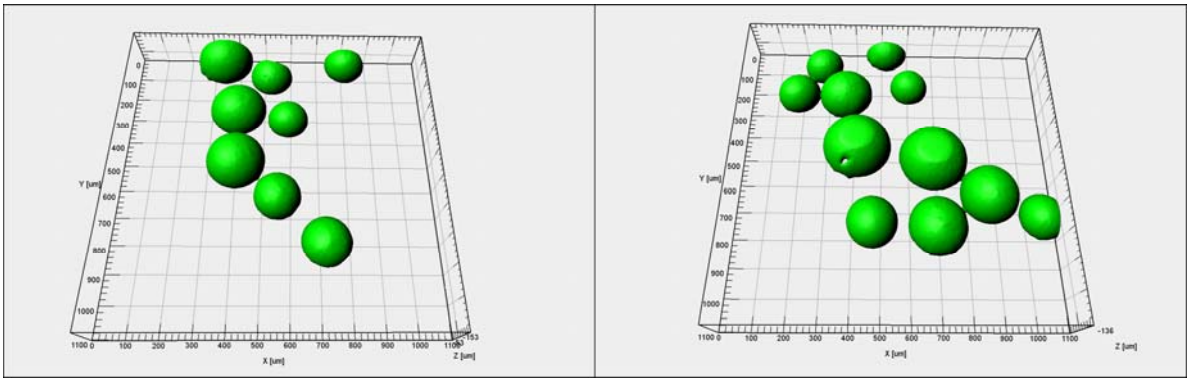

Figure S1. Confocal laser scanning microscopic analysis of Sepabeads EXE096 before (left) and after (right) reaction stirring. Confocal stacks were recorded with a Leica TSC SP (Leica Microsystems GmbH, Germany) equipped with a 10X objective (NA: 0.3), using a Z-step of 4 µm. Three-dimensional reconstructions were created with the software Imaris 6.4.0 (Bitplane, Switzerland).

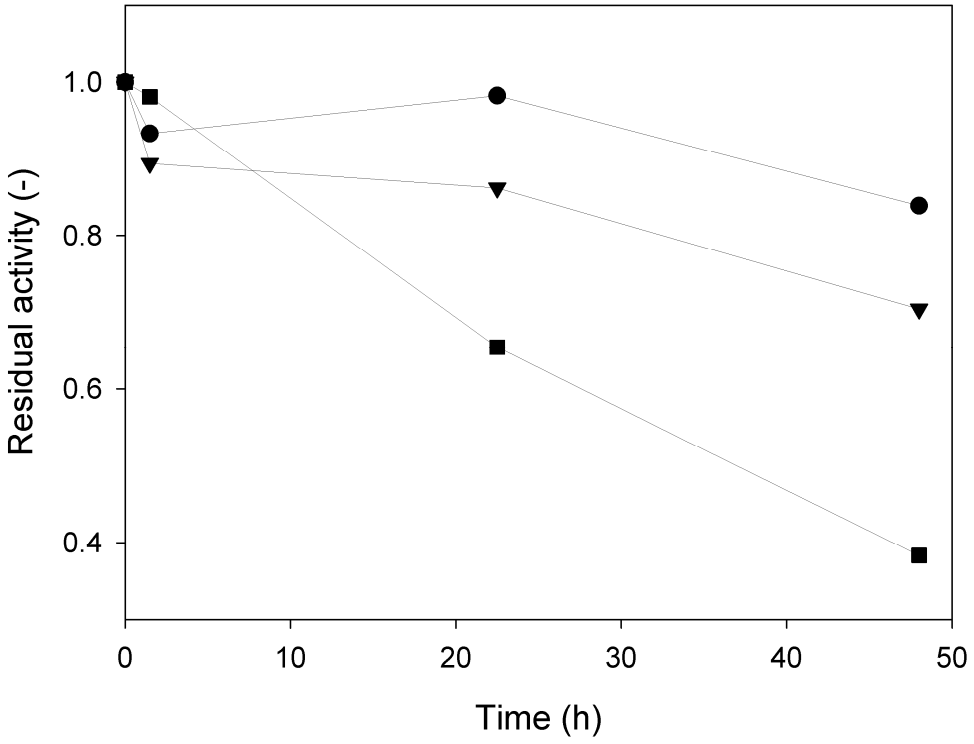

Figure S2. Residual activity of free CCA after incubation in thermomixer at 37°C and 350 rpm in 0.1 M PPB (●) pH 6.5, (▼) pH 7.5, (■) pH 8.5. Residual activity is the ratio between the activity (U/mL) at the current time and the activity (U/mL) at the initial time measured at pH 8.0 and 37°C as described for the standard assay.

Acidic Product Accumulation in Immobilized Cephalosporin C Amidase Characterized By Experiment and Modeling: Implications For Optimal Carrier Selection

Caterina Boniello[1,2] and Bernd Nidetzky[1,2,*]

[1] Austrian Center of Industrial Biotechnology - ACIB GmbH, Petersgasse 14, A-8010 Graz, Austria

[2] Institute of Biotechnology and Biochemical Engineering, Graz University of Technology, Petersgasse 12, A-8010 Graz, Austria

* Corresponding author

Institute of Biotechnology and Biochemical Engineering, Graz University of Technology, Petersgasse 12, A-8010 Graz, Austria

Tel. +43 316 873 8400; Fax +43 316 873 8434; E-mail: bernd.nidetzky@tugraz.at

Running title: pH gradients in immobilized Cephalosporin C amidase

Abbreviations used: 7-ACA, 7-amino cephalosporanic acid; DAAA, D-α-amino adipic acid; CephC, cephalosporin C; CephC-Na, sodium salt of CephC

Abstract. A reaction-diffusion model was developed describing the catalytic performance of a cephalosporin C amidase immobilized on a series of insoluble carriers (epoxy-activated Sepabeads) that differ in particle or pore diameter. The model was applied to fit experimental time courses of net proton formation during cephalosporin C conversion into 7-amino cephalosporanic acid (7-ACA) and D-α-amino adipic acid (DAAA), monitored both inside the carrier and in bulk liquid. This provided estimates for the maximal intrinsic reaction rate unmasked from diffusional and carrier acidification effects (V_{max}) as well as for the effective proton diffusion coefficient ($D_{eff,H+}$). The $D_{eff,H+}$ estimate (≈ 1 – 2 × 10^{-10} m^2/s) was about one order of magnitude lower than expected for proton diffusion in such porous structures, suggesting a role for co-diffusion of the proton and the corresponding DAAA anion in decreasing the proton diffusivity. Using $D_{eff,H+}$ as a constant, time courses of product formation in bulk were also fitted with the model, and the resulting V_{max} estimates showed that carrier-bound amidase had lost 20 – 50% of activity of the free enzyme due to the immobilization. Comparison of experimentally determined maximum rates (V_{obs}) to V_{max} revealed that in carriers with standard pore diameter (30 – 40 nm), diffusional resistance and the intraparticle pH gradient associated with it resulted in an additional, up to 40% reduction of the intrinsic activity of the immobilized enzyme, depending on the amount of amidase loaded on the carrier. In carriers having large pore diameter (150 – 250 nm), V_{obs}/V_{max} had a value near unity at all enzyme loadings tested (7 – 55 mg protein/dry carrier). Modeling was used to characterize the influence of geometrical characteristics of the carrier on distribution of substrate and products in the pore, and it is shown how these intraparticle concentration gradients affect enzyme performance under simulated process conditions.
Key words: pH gradients; reaction-diffusion modeling; immobilized cephalosporin C amidase; porous carrier optimization

INTRODUCTION

Enzymes bound on insoluble porous carriers represent the most prevalent catalysts used in biotransformations currently performed at industrial production scale (Buchholz et al. 2005). Unfortunately, despite significant research efforts over many decades (Cao 2005), development of these enzyme preparations remains a largely empirical endeavour. Design of the immobilization for optimum biocatalyst performance is restricted by limited understanding of consequences that result from physico-chemical attachment of enzyme to carrier (Sheldon 2007). Firstly, the overall specific activity of the enzyme is likely to become negatively affected upon immobilization, reflecting conformational distortion and other alterations of the native protein structure in the carrier-bound enzyme. Non-productive orientation of the enzyme on the carrier surface can likewise cause activity loss (Hanefeld et al. 2009). Secondly, mass transfer resistances and the resulting concentration gradients between liquid bulk and solid carrier can also adversely impinge on the activity (Doran 1995). The key problem in practice is to determine how these two principal effects of the immobilization combine to lower the specific activity of the free enzyme to the observed specific activity of the immobilized enzyme preparation (Sheldon 2007). Relevant evidence would provide guidance for selecting suitable surface chemistry and morphological characteristics of the carrier. Trying to eliminate all mass transfer resistance in the enzyme immobilizate is a potentially useful approach (Tischer and Kasche 1999). However, it is also laborious and restricts one to optimization of geometry at given surface property of the carrier. Application of reaction-diffusion models in a combined experimental and modeling approach presents a powerful and flexible strategy for characterizing and optimizing immobilized enzyme preparations (Berendsen et al. 2006; Spiess et al. 1999; Valencia et al. 2010; Zavrel et al. 2010). It is used here to advance immobilization of an amidase

(EC 3.5.1.93) that is applied in the industrial conversion of cephalosporin C into 7-amino-cephalosporanic acid (7-ACA) and α-amino adipic acid (DAAA) (Scheme 1). 7-ACA is the key intermediate in the production of a whole series of semisynthetic cephem antibiotics (Barber et al. 2004).

Before a reaction-diffusion model can be applied for simulation and optimization purposes, its diffusional and kinetic parameters must be determined. This is usually done by measuring the concentrations of relevant reaction species in bulk liquid and fitting the model to the experimental time-course data (Berendsen et al. 2006; Giordano et al. 2000). Recently some authors stressed on the importance of additional measurements inside the carrier for proper estimation of reaction and transport parameter (Spiess et al. 2008; Zavrel et al. 2010). Zavrel et al. (2010) estimated enzyme kinetic, mass transfer and diffusion parameters for a reactive biphasic system where the carboligation of 3,5-dimetoxy-benzaldehyde with (R)-3,3′,5,5′-tetramethoxy-benzoin using benzaldehyde lyase in hydrogel beads takes place. Concentration measurements in the beads were performed applying two-photon laser scanning microscopy (LSM) and the diffusion-reaction model was fitted to experimental data at 8 different radial positions. Enzymatic hydrolysis of cephalosporin C presents a special case that is however typical of biocatalytic conversion of numerous amide and ester substrates in that it produces a net increase in the proton concentration as products are formed (Boniello et al. 2010; Kallenberg et al. 2005; Spiess et al. 1999; Tischer and Kasche 1999). Diffusional resistance will cause development of a pH gradient along the characteristic dimension of the carrier (e.g. the radius of a spherical particle), and the resulting pH conditions may not be suitable for the enzymatic reaction. A reaction-diffusion model for immobilized CephC amidase, therefore, must consider D_{eff} for the proton ($D_{eff,H+}$).

Previous studies have shown that $D_{eff,H+}$ in porous carriers is not just a function of pore geometry (Ruckenstein and Sasidhar 1984). It displays a complex dependence on the presence of fixed and mobile buffers (Junge and Mclaughlin 1987) and can be strongly affected by co-diffusion of the anion of the proton-releasing species (e.g. DAAA) (Bailey and Chow 1974). Therefore, treating $D_{eff,H+}$ as a constant may be invalid and evidence from literature strongly supports the suggestion that $D_{eff,H+}$ should be determined as parameter of the reaction-diffusion model. However, proton concentration data from bulk solution alone may be insufficient to obtain a reliable estimate of the diffusion parameter (Spiess et al. 2008) and measurement of the pH gradient between carrier and bulk liquid is therefore a likely requirement to determine $D_{eff,H+}$ in a given enzyme immobilizate.

In a recent paper (Boniello et al. 2010) we have presented a method for time-resolved determination of the internal pH in CephC amidase immobilized on epoxy-activated Sepabeads and applied the method to delineate the role of carrier characteristics (e.g. particle size, pore diameter) and other reaction parameters (e.g. substrate concentration) on the development of differences in the (average) proton concentration in carrier and bulk liquid during the amidase-catalyzed conversion of CephC. It was pointed out in the paper that prevention of intraparticle pH gradient formation is an important criterion for choosing a suitable carrier for the immobilization. We have continued this work with the aim of providing a quantitative basis for optimal carrier selection and would like to report here on the application of reaction-diffusion modeling to time-course data for intraparticle and external pH, monitored during CephC hydrolysis by the previously described Sepabeads immobilizates of CephC amidase. The carriers used were different in average diameter of the particle or in pore diameter. From fits of experimental data with the model, we have determined $D_{eff,H+}$ and obtained estimates for the maximum specific initial rate of immobilized amidase (V_{max}), unmasked from all

diffusional effects. We show that about one half of the observed decrease of V_{max} in immobilized enzyme as compared to soluble amidase results from inactivation processes caused by tethering of the enzyme onto the carrier surface. The remainder is ascribed to the effect of carrier acidification on enzyme activity. Simulation was used to characterize the role of intraparticle concentration gradients on the performance of different enzyme immobilizates under process-near reaction conditions. The results could be of significant interest to others working with immobilized amidases and esterases.

REACTION-DIFFUSION MODEL FOR IMMOBILIZED AMIDASE

The following assumptions were made to develop a reaction-diffusion model for the enzymatic conversion shown in Scheme 1. (1) Particles are spherical, and immobilized enzyme is uniformly distributed inside the carrier. (2) Conversion of CephC-Na takes place only inside the carrier. (3) No enzyme deactivation occurs during the course of the reaction. (4) The bulk concentration of CephC-Na is uniform and external mass transfer neglected due to efficient mixing (Sh ≈ 10). (5) Diffusion of all reactants is described by Fick's law whereby the effective diffusion coefficient replaces molecular diffusivity. With these assumptions, the complete mass balance for each chemical species (subscript i) in the reaction, that is CephC-Na, 7-ACA, and DAAA, is given by Equations 1 – 6 where $c_{b,i}$ and $c_{p,i}$ stand for concentrations in bulk and particle, respectively.

In bulk liquid:

$$\frac{\partial c_{b,i}}{\partial t} = -\frac{A_p}{V_{liq}} D_{eff,i} \left.\frac{\partial c_{p,i}}{\partial r}\right|_{r=R} \tag{1}$$

$$A_p = \frac{3}{R} V_p = \frac{3}{R} \frac{1-\varepsilon_b}{\varepsilon_b} V_{liq} \tag{2}$$

In the intraparticle fluid:

$$\varepsilon \frac{\partial c_{p,i}}{\partial t} = D_{eff,i} \frac{1}{r^2} \frac{\partial}{\partial r}\left(r^2 \frac{\partial c_{p,i}}{\partial r} \right) - v_i \qquad (3)$$

Initial conditions are:

$$t = 0, \qquad c_{b,i} = c_{b0,i}; \quad c_{p,i} = c_{p0,i} \qquad (4)$$

Boundary conditions are:

$$r = 0 \qquad \frac{\partial c_{p,i}}{\partial r} = 0 \qquad (5)$$

$$r = R \qquad c_{b,i} = c_{p,i}\Big|_{r=R} \qquad (6)$$

In Equation 2 R is the particle radius (m), A_p is the total particles external surface area (m^2) and V_p is the total volume of the particles in reactor (m^3). ε_b designate the bulk porosity that is expressed by the fraction of the liquid volume (V_{liq}) in relation to the total reactor volume ($V_{liq} + V_P$). In Equation 3 ε is the particle porosity and $D_{eff,i}$ ($m^2 s^{-1}$) is the effective diffusion coefficient of the specie i in the particle pore. The volumetric reaction rate v_i (mol m^{-3} s^{-1}) in Equation 3 refers to biocatalytic particle volume. It is related to specific activity of the immobilized enzyme (v_s; μmol min^{-1} mg^{-1}) through Equation 7:

$$v_i = v_s E \rho_p (1-\varepsilon)/60 \qquad (7)$$

where E is the enzyme loading (mg g dry^{-1}) and ρ_p is the material density (mg mL^{-1}).

A minimal mathematical model was chosen to describe the kinetics of CephC amidase (see later). It assumes irreversible conversion of CephC-Na and Michaelis-Menten dependence of v_i on the substrate concentration, implying the parameters V_{max} and K_M. Of the two, only V_{max} is assumed to display significant pH-dependence. The acidic limb of this pH-dependence is known from experiments to be well described by Equation 8. Considering reported pK_a values of 4.42 and 5.42 for the carboxylic groups of DAAA (Martell and Smith 1976), we assume that the DAAA produced in the enzymatic reaction at slightly alkaline pH is completely dissociated. 7-ACA does not undergo

protonation/deprotonation under the conditions used. Therefore, one proton is released for each CephC-Na converted. pH is calculated using an expanded Henderson-Hasselbach relationship that includes buffering effect from the phosphate buffer (Equation 9). The concentrations of phosphate monoanion and dianion at the start of the reaction were calculated from initial pH. c_H is the concentration of protons generated by enzymatic reaction and has a value of zero at t = 0.

$$V_{\max} = \frac{V^*_{\max}}{1+10^{pK-pH}} \quad (8)$$

$$pH = pK_a + \log\frac{\left[HPO_4^{2-}\right]_0 - c_H}{\left[H_2PO_4^-\right]_0 + c_H} \quad (9)$$

MATERIALS AND METHODS

Materials, Chemicals, and Assays

The carriers used for immobilization were kind gifts of Resindion (Milano, Italy): Sepabeads EXE096 (standard grade), EXE096/M (coarse grade), EXE096/SS (fine grade) and EXE030 (high porosity grade). Table I summarizes relevant characteristics of these carriers. CephC-Na (87.1% purity), 7-ACA, and CephC amidase were kind gifts from Sandoz GmbH (Kundl, Austria). All other materials were reported elsewhere. The CephC amidase was described previously and its immobilization on Sepabeads was done by a reported protocol. Assays for enzyme activity measurement were previously reported (Boniello et al. 2010).

Reaction Time Course Monitoring Using pH Measurement

pH profiles in bulk and in particles were recorded for 30 min during the conversion of 50 mM CephC-Na by immobilized CephC amidase. CephC amidase was covalently bound on epoxy-activated Sepabeads (50-70 mg/g dry carrier), differing in particle and pore diameter as indicated in Table I. CC-Na hydrolysis was performed in a 2 mL-cylindrical

vessel, with controlled temperature (37°C, water bath) and constant stirring (270 rpm, magnetic stirrer). Each reaction batch was loaded with about 0.02 g dry immobilized CephC amidase, (≈3 U) suspended in 1 mL 100 mM PPB pH 8.5. To start the reaction 100 µL 550 mM CC-Na pH 8.5 were added. pH in the bulk liquid was recorded using a glass pH electrode (Minitrode, Hamilton, Germany). pH in immobilized CephC amidase was monitored using a method based on dual lifetime referencing (Boniello et al. 2010). Indicators as well labeling procedure were the same as described in the cited paper.

Reaction Time Course Monitoring Using 7-ACA Detection

7-ACA detection was based on derivatization with p-dimethylamino-benzaldehyde (pDAB) that leads to imine formation of its amino functionality (Patett and Fischer 2006). Assays were conducted as reported in (Boniello et al. 2010). Different experiments were carried out varying initial CephC-Na concentration from 0.5 to 35 mM. For each experiment 7-ACA concentration was measured after 15 min for seven or more initial substrate concentrations. The intermediate product concentrations at 3, 6, 9 and 12 minutes respectively were extrapolated linearly between the measured concentrations at 0 and 15 minutes.

pH Effect on Reaction Rate

Initial rates of CC-Na hydrolysis were measured in substrate saturating conditions (40 mM CephC-Na) for the free CephC amidase. 500 µL CephC-Na and 500 µL enzyme solution (both in 0.1 M PPB) were incubated at 37°C in Eppendorf tubes (37°C, 350 rpm). Buffer pH was varied from 6.0 to 9.0. Obtained reaction rates were normalized to the value measured at pH 9.0. The dependence of the relative activity vs pH was fit with a single pK curve (Equation 8) using the enzyme kinetic tool of the software Sigma Plot 11.0.

Modeling and Simulation Tools

Equations expressing mass balances in the bulk liquid phase (Equation 1) and in the intraparticle fluid (Equation 3) for CephC-Na, 7-ACA, DAAA and proton, are solved simultaneously using the software package Athena Visual Workbench v 12.3 (Stewart and Associates Engineering Software, Inc). Initial and boundary conditions were assigned as indicated by Equations 4 and Equations 5-6, respectively. Since reaction rate pH dependence (Equation 8) and the Henderson-Hasselbach equation (Equation 9) were included in the system, the implemented equation system resulted constituted both by algebraic and partial differential equations. Equations were numerical integrated using the software tool for mixed systems with diagonal matrix, where the diagonal elements of this matrix represent the numerical coefficients of the mass balances time derivatives. In our case all coefficients were unitary. The space domain was described in spherical coordinates, where the particle radius denoted the x coordinate. Particle radius was discretized using the central finite differences scheme with twenty discretization points applying second order approximation on both boundaries.

Parameter Estimation

Parameter estimation was preformed fitting experimental data by employing the non-linear least squares method.

From time-resolved pH in the bulk liquid and time-resolved pH in particles two parameters, V_{max} and $D_{eff,H+}$, were contemporaneously estimated. These two pH profiles constitute two responses for the model. The first (bulk pH) is the pH value on the particle surface, the second (particles pH) expresses pH at r=R/2. pH values calculated at r=R/2 and r=R through Equation 9 were contemporaneously fitted to experimental data. Note that because mixing and substrate chemical self-hydrolysis it was necessary to shift the initial reaction time of a couple of seconds, correcting the initial substrate concentration,

calculating the amount of self-hydrolyzed substrate on the basis of the occurred pH change.

From time-resolved 7-ACA concentrations V_{max} was estimated. 7-ACA time-profile constitutes one response for the model. The seven or more formation curves, obtained starting from seven or more different initial substrate concentrations were fitted contemporaneously for each immobilized CephC amidase preparation. This was possible in Athena including to the model two more experimental settings (initial substrate concentration and reactor porosity) that were assigned singularly for each experiment. The value of $D_{eff,H+}$ applied in the model, was that obtained from the fit of pH profiles data of the correspondent carrier used. All other parameters were considered known and independent of reaction conditions and are listed in table I.

RESULTS AND DISCUSSION

Reaction-Diffusion Model for Immobilized CephC Amidase

All of the assumptions made for model development are supported by direct evidence for immobilized CephC amidase (Boniello et al. 2010) and literature precedent on other carrier-bound enzymes. Application of Fick's law to describe diffusion of charged species is also reasonable (Bailey and Chow 1974; Ruckenstein and Rajora 1985; Spiess et al. 1999). Table II summarizes all non-adjustable model parameters and describes the procedures used to obtain them. The model applied to express the kinetics of CephC amidase is made very simple for practical reasons. However, we are fully aware that in order to represent the full course of the enzymatic conversion, at least, it would have to be expanded by kinetic terms for the reverse reaction. Notwithstanding, validity of the conceptual approach reported herein does not depend on the complexity of the enzyme kinetic model used. It was further assumed, in line with the widely held idea of carrier-bound enzymes and supported by results of steady-state

kinetic characterization of different CephC amidase immobilizates, that the intrinsic K_M for the CephC substrate does not change substantially as result of immobilization of the amidase. Because substrate was nearly saturating under most of the experimental conditions applied, a possible pH dependence of K_M was not considered. Data concerning the pH-profile for the reaction rate of the free enzyme as reported in our previous work (Boniello et al. 2010) were normalized to highest value (correspondent to pH 9.0) and fitted with Equation 8. The resulting pK is reported in Table I.

Determination of $D_{eff,H+}$

Figure 1 shows experimental time courses for the pH change inside the porous biocatalytic carrier and in the bulk liquid phase, obtained under conditions in which different immobilizates of CephC amidase were applied for hydrolysis of CephC. The fit of the reaction-diffusion model having V_{max} and $D_{eff,H+}$ as adjustable parameters is superimposed on the measured data in Figure 1. The comparison reveals that the model provides good representation of the experimental situation both inside the carrier and in bulk liquid. Enzymatic reaction went along with a fast drop of internal pH to generate a substantial pH gradient (ΔpH = external pH – internal pH) between the bulk phase and the carrier. The observed ΔpH varied in the range 0.3 - 0.8, depending on the carrier used. As noted in the previous paper (Boniello et al. 2010), the ΔpH magnitude increased with decreasing pore diameter (panel A,B) and increasing particle size (panels A,C,D) of the carrier. Figure 1 also shows that after the initial “burst” of ΔpH formation that was complete within just a few seconds, both the internal and external pH decreased slowly over time.

Data recorded to reaction times exceeding the 10-min time span indicated in Figure 1 were applied for parameter estimation. The observed trend was that quality of the

overall fit, expressed by the R-square value from regression analysis, decreased in response to an increase in reaction time from 10 to 20 min. It was typical for extended reaction times that the model predicted a drop in pH for bulk liquid that was substantially faster than the corresponding pH drop measured experimentally (data not shown). This discrepancy was not unexpected, considering the aforementioned limitations of the simple Michaelis-Menten model used. Changes in the time range used lead to differences in the estimated values for V_{max} and $D_{eff,H+}$ of about 20%.

Table II summarizes estimates for $D_{eff,H+}$ and V_{max} obtained from fits of the data in Figure 2. Both parameters have useful relative S.D. of 2% or smaller and are therefore considered to be statistically well determined. However, it should be noted that a substantial degree of linear correlation (≤ -0.6) generally exists between the $D_{eff,H+}$ and V_{max} estimate, except for the case of using EXE096/M as carrier. Values of V_{max} differed by about 2.5-fold across the series of carriers used and possible reasons for this variation will be discussed below in more detail. The values of $D_{eff,H+}$ determined for the different carriers span about 2-fold. The diffusion coefficient for the proton in water (D_{H+}) at 37 °C was reported as 7.83×10^{-9} m^2s^{-1} (Perry et al. 1997). The relationship proposed by (Bailey and Ollis 1986) for the effective diffusion coefficient in porous structures (Equation 10)

$$D_{eff,i} = D_i \, \varepsilon/\tau \, (1-r_m/r_p)^4 \qquad (10)$$

was applied to obtain values of 1.27×10^{-9} m^2s^{-1} and 3.75×10^{-9} m^2s^{-1} for $D_{eff,H+}$ in standard porosity carriers (EXE096, EXE096/M, EXE096/SS) and the high porosity carrier EXE030, respectively. The calculated values for $D_{eff,H+}$ exceed the $D_{eff,H+}$ estimates in Table III by an order of magnitude or more. We therefore considered a co-diffusion model (Equation 11) described by (Bailey and Chow 1974) in which $D_{eff,H+}$ is affected by diffusion of the corresponding anion from the protic acid (D_B).

$$D_{eff,H+} = \frac{2D_A D_B}{D_A + D_B} \qquad (11)$$

Applying effective diffusion coefficients for proton and DAAA, calculated with Equation 10 for EXE096 and EXE030, we can use Equation 11 to obtain values of 1.37×10^{-10} m^2s^{-1} and 5.04×10^{-10} m^2s^{-1} for $D_{eff,H+}$ in carriers having standard (EXE096) and large (EXE030) pores, respectively. The calculated $D_{eff,H+}$ for EXE096 is in excellent agreement with the averaged $D_{eff,H+}$ estimate of 1.63×10^{-10} m^2s^{-1} for this type of carrier that was obtained from the data in Table II. There is not as good, however still useful consistency between the theoretical $D_{eff,H+}$ in EXE030 and the corresponding $D_{eff,H+}$ derived from the experimental data.

A possible role for fixed and mobile buffers on altering $D_{eff,H+}$ has been discussed in literature (Junge and Mclaughlin 1987; Swietach et al. 2003). However, observation that the $D_{eff,H+}$ estimate for standard grade carriers of the EXE096 type was not dependent on the amount of CephC amidase loaded on the carrier in the range 7 - 60 mg protein/g dry Sepabeads (data not shown) supports the idea that in the system studied, proton effective diffusivity is not affected by a fixed buffer effect in which ionizable protein groups that are attached to the surface of the carrier slow down diffusion of the proton. We therefore think that the co-diffusion model represented by Equation 11 provides a useful description of effective proton diffusivity in immobilized CephC amidase and the data in Table II are applicable for the simulation of intraparticle pH-gradient formation during enzymatic hydrolysis of CephC.

Intrinsic V_{max} of Immobilized CephC Amidase

The V_{max} of free CephC amidase at pH 8.0 and 37 °C had a value of 7.8 ± 0.2 U/mg that serves as reference for evaluating the immobilized enzyme preparations used. A two-step procedure was applied for determination of V_{max} in immobilized CephC amidase.

V_{max} thus obtained is meant to be unmasked from effects of diffusion and carrier acidification. Therefore, the true loss of catalytic activity that results from fixation of the enzyme on the carrier can be determined. A first estimate of V_{max} was obtained from fit of the reaction-diffusion model to data in Figure 2. Results are shown in Table II. In the second step, experimental time courses of 7-ACA formation in bulk liquid (Figure S4) obtained with carriers containing varied amount of bound CephC amidase were fitted with the reaction-diffusion model whereby V_{max} was the adjustable parameter and $D_{eff,H+}$ was a constant from Table II. Results are summarized in Table III.

Table II shows that V_{max} estimates for enzyme immobilized on EXE096 were decreased in comparison to free amidase. By contrast, enzyme immobilized on EXE030 displayed a V_{max} comparable to that of the free amidase. Considering the common material basis of all carriers used in this work, variation of V_{max} across the series of EXE096 and EXE030 immobilizates was not clear, especially because effects of changes in carrier size (EXE096) and pore diameter (EXE096, EXE030) had already been eliminated in the estimate for the intrinsic activity of the immobilized enzyme. However, aside from the possible error contained in the V_{max} estimate (Table III), we cannot exclude the possibility that batch-to-batch variability in the carrier samples used is a relevant source of the observed variation in V_{max}. It was our own experience with different samples of EXE030 that the experimentally determined specific activity of immobilized CephC amidase could change by as much as twofold depending on the batch of carrier used.

The results in Table III provide a detailed analysis of V_{max} in CephC amidase immobilizates. V_{max} estimates obtained at high enzyme loading (≥ 30 mg protein/dry carrier) reveal that except for coarse grade EXE096/M where both experimental and calculated V_{max} were unexpectedly low, immobilizates of the enzyme express between 55 and 75% of the intrinsic activity of the free amidase. Comparison of the observed

V_{max} with the V_{max} estimate shows that standard porosity carriers (EXE096) had lower effectiveness factors (η) of ~0.7 than the high porosity carrier EXE030 for which η was unity at all enzyme loadings examined. In EXE096, η had a value of 1 only at low enzyme loading and it decreased as the enzyme loading was raised. We conclude from Table III that product diffusion and carrier acidification contribute to a reduction of V_{max} by about 30 – 40%. The loss of enzyme activity resulting from attachment of CephC amidase onto the insoluble carrier is of a similar magnitude (25 – 45%).

Simulation of Intraparticle Concentration Profiles

Using values for $D_{eff,H+}$ (Table II) and V_{max} (data for highest enzyme loading in Table III), we employed the reaction-diffusion model to simulate concentration gradients for CephC, DAAA and the proton along the internal radius of the different carriers. Results are displayed for varied reaction time in Figures S1 (CephC), S2 (DAAA) and S3 (pH) of the Supporting Information. An initial CephC concentration of 35 mM was assumed that represents the maximum level of substrate used for analysis of time courses of 7-ACA formation (Table III).

In the high-porosity carrier EXE030 (panels B in Figures S1 – S3), CephC was almost evenly distributed inside the carrier. There was little accumulation of DAAA in the center of the carrier and consequently, a modest pH gradient of maximally –0.25 pH units developed relative to the pH in bulk liquid. In standard-grade EXE096, by contrast, the available CephC was completely exhausted already at a position corresponding to about half of the particle radius (Panels A in Figures S1 – S3), resulting in a high internal concentration of DAAA and a large pH gradient of up to –0.5 pH units. As expected, the effect of substrate depletion along the radial dimension of EXE096 carriers was a maximum in coarse grade particles. Using fine grade EXE096/SS, about 10 mM of CephC substrate were still available for enzymatic reaction in the center of the particle.

In other words, enhanced diffusional resistance resulting from having wider pores in EXE030 as compared to EXE096 can be partly compensated by decreasing the diameter of the carrier particles.

Figure 2 depicts the combined effects of substrate depletion and pH drop due to internal product accumulation on formation of a reaction rate gradient along the radius of the carrier. Only in EXE030 is it possible to utilize all of the immobilized amidase effectively. In standard grade and coarse grade EXE096 where the reaction rate vanishes at slightly below and above half the radial distance, just about 60% and 40% of the particle volume are exploited for biocatalytic conversion, respectively. Reduction in particle size as in fine grade EXE096 alleviates the effect on the reaction rate real though utilization of the overall carrier volume for enzymatic conversion is still lower than in EXE030.

Simulation of Performance of Mixed Batch Reactor with pH Control

Typically, on industrial scale, Cephalosporin C hydrolysis is carried out in stirred batch reactors with controlled pH in bulk, performed by addition of a base like sodium hydroxide or ammonia, to neutralize the generated acid. Here we simulate the behavior of the four enzymatic preparations, described in the previous paragraph, in a stirred batch reactor with controlled pH in bulk under typical assay conditions. The model is modified for the right boundary condition of the proton mass balance, to assure that there is no pH change in the bulk solution. Figure 3 shows for EXE030 the highest catalytic performances and pH in particles that remained almost constant during substrate conversion. EXE030 showed furthermore the lowest ΔpH. In all the “low porous” carriers pH in particles increased with reaction proceeding and the ΔpH increased increasing particle size. The small difference in internal pH between EXE096 and EXE096/SS was probably due to the fact that the smaller particles were higher catalytically active.

CONCLUSIONS

The theoretical analysis carried out through the development of a mathematical model describing the behavior in reactor of CephC amidase immobilized on epoxy-activated Sepabeads, where diffusion and reaction in the carrier are treated separately, lead to conclude that mass transfer effects and enzyme deactivation after carrier attachment contributed with similar magnitude (30-40%) to the observed loss of enzyme activity. To make this deduction a proper estimation of the proton effective diffusion coefficient was performed, dictating $D_{eff,H+}$ the magnitude of ΔpH between bulk and particles. Together with the possibility of evaluating otherwise unknown parameters, reaction modeling provided information about concentration profiles inside the carrier and allowed for evaluation of carrier characteristics in experimental conditions differing from that employed as well for the choice of an optimal carrier. Results emerging from this analysis confirmed the experimental results obtained in our previous work (Boniello et al. 2010). Geometrical characteristics of Sepabeads EXE030 showed to favor diffusion of substrate and product, being they evenly distributed in the whole particles and being their concentration similar to that of the bulk solution. These facts lead to a less pronounced carrier acidification and to almost constant reaction rate value along the particle radius, showing that enzyme worked in the same conditions independently of its position in the particles. Reduced porosity, which is the case of EXE096, dramatically hindered species diffusion. A reduction of the particle size like in Sepabeads EXE096/SS alleviated effects on the reaction rate but an internal particle core, where enzyme was not active or working in substrate limiting conditions still remained.

AKNOWLEDGEMENTS

The Austrian Research Promotion Agency (FFG), the Province of Styria, the Styrian Business Promotion Agency (SFG), the city of Graz, and Sandoz GmbH are

acknowledged for financial support. We are grateful to Dr. Paolo Caimi (Resindion Srl) for supplying Sepabeads resins and to Dr. Pavel Acai for the support in developing the model with Athena Visual Studio.

NOMENCLATURE

A_p Total particle external surface area (m^2)

$c_{b,i}$ Concentration in the bulk ($mol \cdot m^{-3}$)

$c_{p,i}$ Concentration in the particles ($mol \cdot m^{-3}$)

D_A Diffusion coefficient of proton in pores ($m^2 \cdot s^{-1}$)

D_B Diffusion coefficient of the anion from the protic acid in pores ($m^2 \cdot s^{-1}$)

$D_{eff,i}$ Effective diffusion coefficient ($m^2 \cdot s^{-1}$)

D_{H+} Proton diffusion coefficient in water ($m^2 \cdot s^{-1}$)

D_i Diffusion coefficient in water ($m^2 \cdot s^{-1}$)

E Enzyme loading ($mg \cdot g\ dry\ carrier^{-1}$)

K_M Michaelis constant ($mol\ m^{-3}$)

R Particle radius (m)

r Radial distance in the particle (m)

r_m Molecular radius (m)

r_p Pore radius (m)

t Time (s)

v_i Volumetric reaction rate ($mol \cdot m^{-3} \cdot s^{-1}$)

V_{liq} Bulk volume (m^3)

V_{max} Maximal reaction rate: volumetric($mol \cdot m^{-3} \cdot s^{-1}$), specific ($\mu mol\ min^{-1}\ mg^{-1}$)

V_{max*} Maximal reaction rate reached if all the enzyme is in catalytically active form: volumetric ($mol \cdot m^{-3} \cdot s^{-1}$), specific ($\mu mol\ min^{-1}\ mg^{-1}$)

V_p Total particles volume (m^3)

v_s Specific reaction rate ($U \cdot mg^{-1}$)

Greek letters

ε Particle porosity (-)

ε_b Bulk porosity $V_{liq}/(V_{liq}+V_p)$ (-)

ρ_p Material density ($g \cdot mL^{-1}$)

τ Pore tortuosity (-)

REFERENCES

Bailey JE, Chow MTC. 1974. Immobilized Enzyme Catalysis with Reaction-Generated pH Change. Biotechnology and Bioengineering 16(10):1345-1357.

Bailey JE, Ollis DF. 1986. Biochemical engineering fundamentals. New York: McGraw-Hill.

Barber MS, Giesecke U, Reichert A, Minas W. 2004. Industrial enzymatic production of cephalosporin-based beta-lactams. Molecular Biotechnology of Fungal Beta-Lactam Antibiotics and Related Peptide Synthetases 88:179-215.

Berendsen WR, Lapin A, Reuss M. 2006. Investigations of reaction kinetics for immobilized enzymess - Identification of parameters in the presence of diffusion limitation. Biotechnology Progress 22(5):1305-1312.

Boniello C, Mayr T, Klimant I, Koenig B, Riethorst W, Nidetzky B. 2010. Intraparticle concentration gradients for substrate and acidic product in immobilized cephalosporin C amidase and their dependencies on carrier characteristics and reaction parameters. Biotechnol Bioeng 106(4):528-40.

Buchholz K, Kasche V, Bornscheuer UT. 2005. Biocatalysts and enzyme technology. Weinheim: Wiley-VCH.

Cao L. 2005. Carrier-bound immobilized enzymes: principles, applications and design. Weinheim: Wiley-VCH.

Doran PM. 1995. Bioprocess Engineering Principles. London: Academic Press Limited.

Giordano RLC, Giordano RC, Cooney CL. 2000. A study on intra-particle diffusion effects in enzymatic reactions: glucose-fructose isomerization. Bioprocess Engineering 23(2):159-166.

Hanefeld U, Gardossi L, Magner E. 2009. Understanding enzyme immobilisation. Chemical Society Reviews 38(2):453-468.

Junge W, Mclaughlin S. 1987. The Role of Fixed and Mobile Buffers in the Kinetics of Proton Movement. Biochimica Et Biophysica Acta 890(1):1-5.

Kallenberg AI, van Rantwijk F, Sheldon RA. 2005. Immobilization of penicillin G acylase: The key to optimum performance. Advanced Synthesis & Catalysis 347(7-8):905-926.

Martell A, Smith R. 1976. Critical Stability Constants. New York:: Plenum Press.

Patett F, Fischer L. 2006. Spectrophotometric assay for quantitative determination of 7-aminocephalosporanic acid from direct hydrolysis of cephalosporin C. Analytical Biochemistry 350(2):304-306.

Perry RH, Green DW, Maloney JO. 1997. Perry's chemical engineers' handbook. New York: McGraw-Hill.

Ruckenstein E, Rajora P. 1985. Optimization of the Activity in Porous-Media of Proton-Generating Immobilized Enzymatic-Reactions by Weak Acid Facilitation. Biotechnology and Bioengineering 27(6):807-817.

Ruckenstein E, Sasidhar V. 1984. Acid Generating Immobilized Enzymic Reactions in Porous Media-Activity Control Via Augmentation of Proton Diffusion by Weak Acids. Chemical Engineering Science 39(7-8):1185-1200.

Sheldon RA. 2007. Enzyme immobilization: The quest for optimum performance. Advanced Synthesis & Catalysis 349(8-9):1289-1307.

Spiess A, Schlothauer RC, Hinrichs J, Scheidat B, Kasche V. 1999. pH gradients in immobilized amidases and their influence on rates and yields of beta-lactam hydrolysis. Biotechnology and Bioengineering 62(3):267-277.

Spiess AC, Zavrel M, Ansorge-Schumacher MB, Janzen C, Michalik C, Schmidt TW, Schwendt T, Buchs J, Poprawe R, Marquardt W. 2008. Model discrimination for the propionic acid diffusion into hydrogel beads using lifetime confocal laser scanning microscopy. Chemical Engineering Science 63(13):3457-3465.

Swietach P, Zaniboni M, Stewart AK, Rossini A, Spitzer KW, Vaughan-Jones RD. 2003. Modelling intracellular H+ ion diffusion. Progress in Biophysics & Molecular Biology 83(2):69-100.

Tischer W, Kasche V. 1999. Immobilized enzymes: crystals or carriers? Trends in Biotechnology 17(8):326-335.

Valencia P, Flores S, Wilson L, Illanes A. 2010. Effect of particle size distribution on the simulation of immobilized enzyme reactor performance. Biochemical Engineering Journal 49:256-263.

Zavrel M, Michalik C, Schwendt T, Schmidt T, Ansorge-Schumacher M, Janzen C, Marquardt W, Buchs J, Spiess AC. 2010. Systematic determination of intrinsic reaction parameters in enzyme immobilizates. Chemical Engineering Science 65(8):2491-2499.

Table I. Model parameters used for fitting time-resolved pH profiles curves in bulk and particles (Figure 1)

Parameter	Value	Units	Equations
R (EXE096)	[a] 1.15×10^{-4}	m	(2), (6)
R (EXE030)	[a] 0.90×10^{-4}	m	(2), (6)
R (EXE096/SS)	[a] 0.60×10^{-4}	m	(2), (6)
R (EXE096/M)	[a] 2.00×10^{-4}	m	(2), (6)
r_p (EXE096, EXE096/M, EXE096/SS)	[b] 17.5	nm	(10)
r_p (EXE030, EXE096/M, EXE096/SS)	[b] 100	nm	(10)
ε (EXE096, EXE096/M, EXE096/SS)	[c] 0.27	-	(3), (7)
ε (EXE030)	[c] 0.70	-	(3), (7)
ρ_p	[d] 1.14	g cm^{-3}	(7)
$D_{eff,S}$ (EXE096, EXE096/M,EXE096/SS)	[e] 7.25×10^{-11}	m^2 s^{-1}	(1), (3)
$D_{eff,S}$ (EXE096)	[e] 2.70×10^{-10}	m^2 s^{-1}	(1), (3)
K_M	[f] 4.54	Mol m^{-3}	(3)
pK	[g] 7.7	-	(8)

[a] Averaged particle radius as provided by the supplier

[b] Pore radius calculated as middle point in the range provided by the supplier

[c] Carrier porosity calculated as reported in Boniello et al., 2010

[d] Carrier density as provided by the supplier

[e] Effective diffusion coefficients for CephC were calculated using Equation 10 as reported in Boniello et al., (2010)

[f] K_M for the used free CephC amidase preparation

[g] pK for free CephC amidase as calculated fitting pH profiles data with Equation 8

Table II. Estimated parameters and fit goodness

Sepabeads	$D_{eff,H+}$ ($m^2\ s^{-1}$)	SD ($m^2\ s^{-1}$)	V_{max} ($U\ mg^{-1}$)	SD ($U\ mg^{-1}$)	Correlation	R-square
Standard Grade EXE096	1.63×10^{-10}	1.11×10^{-12}	3.37	0.02	-0.710	0.9594
High Porosity Grade EXE030	1.81×10^{-10}	2.07×10^{-12}	7.24	0.06	-0.799	0.9297
Fine Grade EXE096/SS	9.66×10^{-11}	6.99×10^{-13}	6.40	0.05	-0.621	0.9491
Coarse Grade EXE096/M	1.25×10^{-10}	1.30×10^{-12}	2.79	0.05	-0.392	0.9239

Table III. Calculated and apparent maximal reaction rate as depending on carrier characteristics and enzyme loading

Sepabeads	Enzyme Loading (mg g dry^{-1})	V_{max} (U mg^{-1})	V_{obs} (U mg^{-1})	V_{obs}/V_{max} (-)
EXE096	72	4.8	3.3	0.69
EXE096	58	5.9	3.9	0.66
EXE096	30	5.7	4.1	0.73
EXE096	14	3.6	3.4	0.95
EXE096	6	3.3	3.4	1.05
EXE030	55	4.2	4.2	0.98
EXE030	34	5.9	5.8	0.99
EXE030	17	5.6	5.8	1.03
EXE030	7	6.3	6.9	1.09
EXE096/SS	73	5.8	4.2	0.73
EXE096/M	64	3.7	2.2	0.59

FIGURES

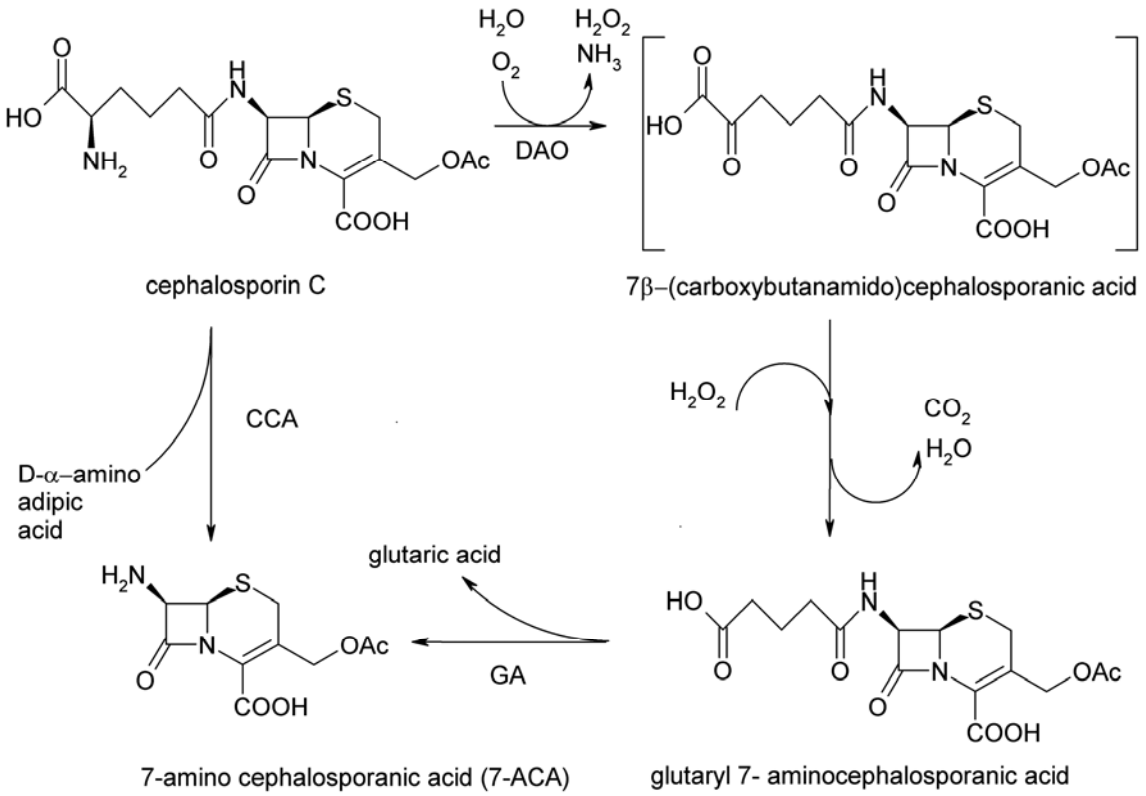

Scheme 1. Single-step amidase-catalyzed conversion of cephalosporin C to 7-aminocephalosporanic acid as compared to the classical two-step chemo-enzymatic transformation using D-amino acid oxidase (DAO) and glutaryl acylase (GA).

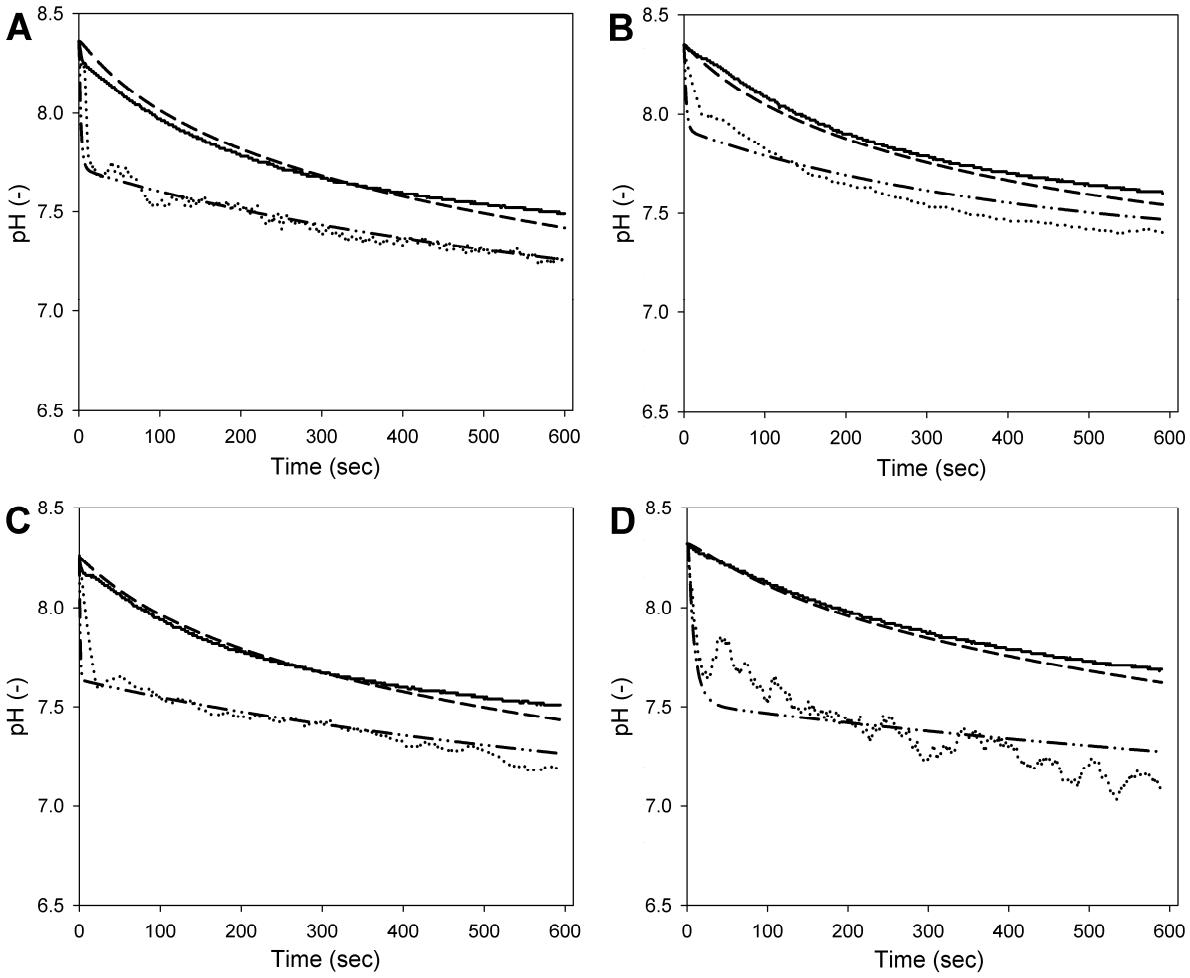

Figure 1. Experimental and calculated pH in bulk and in particles. Solid line: experimental bulk pH; Dash line: calculated bulk pH; Dotted line: experimental particles pH; Dash-dot-dot line: calculated particles pH. **Panel A. EXE096; Panel B. EXE030; Panel C. EXE096/SS; Panel D. EXE096/M.**

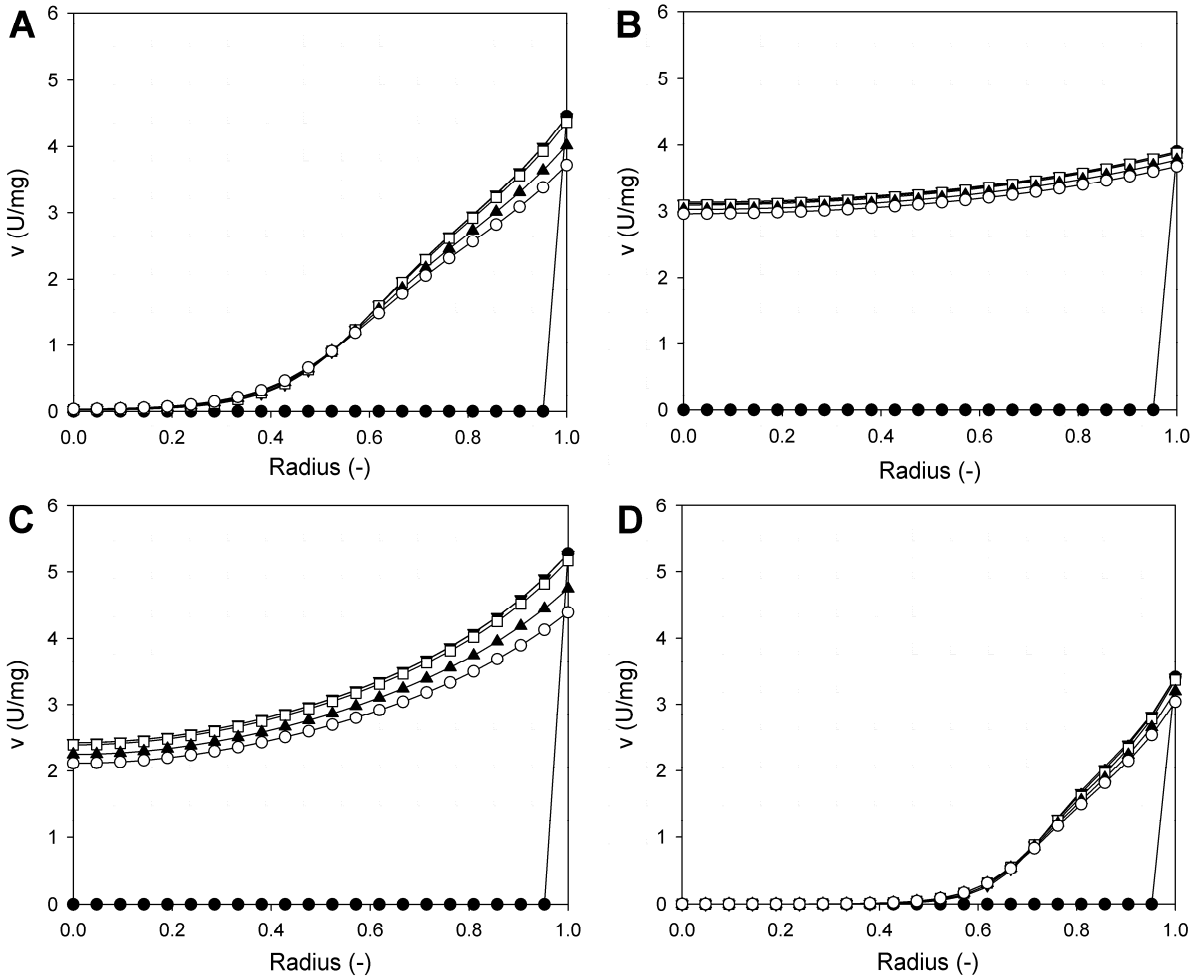

Figure 2. Calculated reaction rate in immobilized CephC amidase preparations. (●) 0 sec; (●) 10 sec; (▼) 15 sec; (□) 100 sec; (▲) 500 sec; (○) 900 sec. Panel A. EXE096; Panel B. EXE030; Panel C. EXE096/SS; Panel D. EXE096/M.

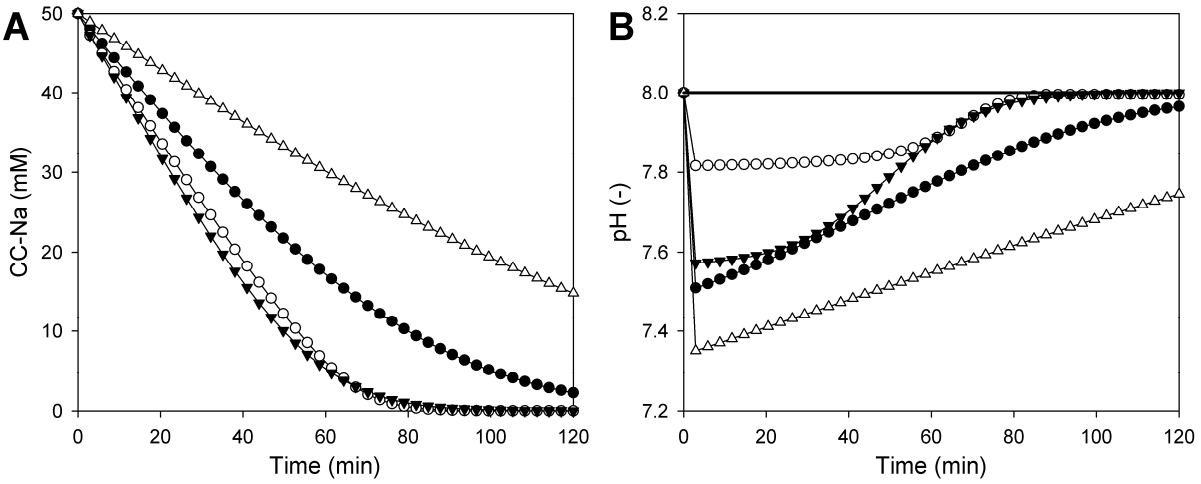

Figure 3. Calculated CephC-Na conversion (Panel A) and internal pH at r=R/2 (Panel B) for immobilized CephC amidase preparations in stirred batch reactor with controlled pH in bulk. 50 mM CC-Na; 100 mM PPB pH 8.0; 37°C; 11 mg protein/assay; 50 mL (●) EXE096 72 mg protein/g dry; (○) EXE030 55 mg protein/ g dry; (▼) EXE096/SS 73 mg protein/ g dry; (∆) EXE096/M 64 mg protein/ g dry.

SUPPORTING INFORMATION

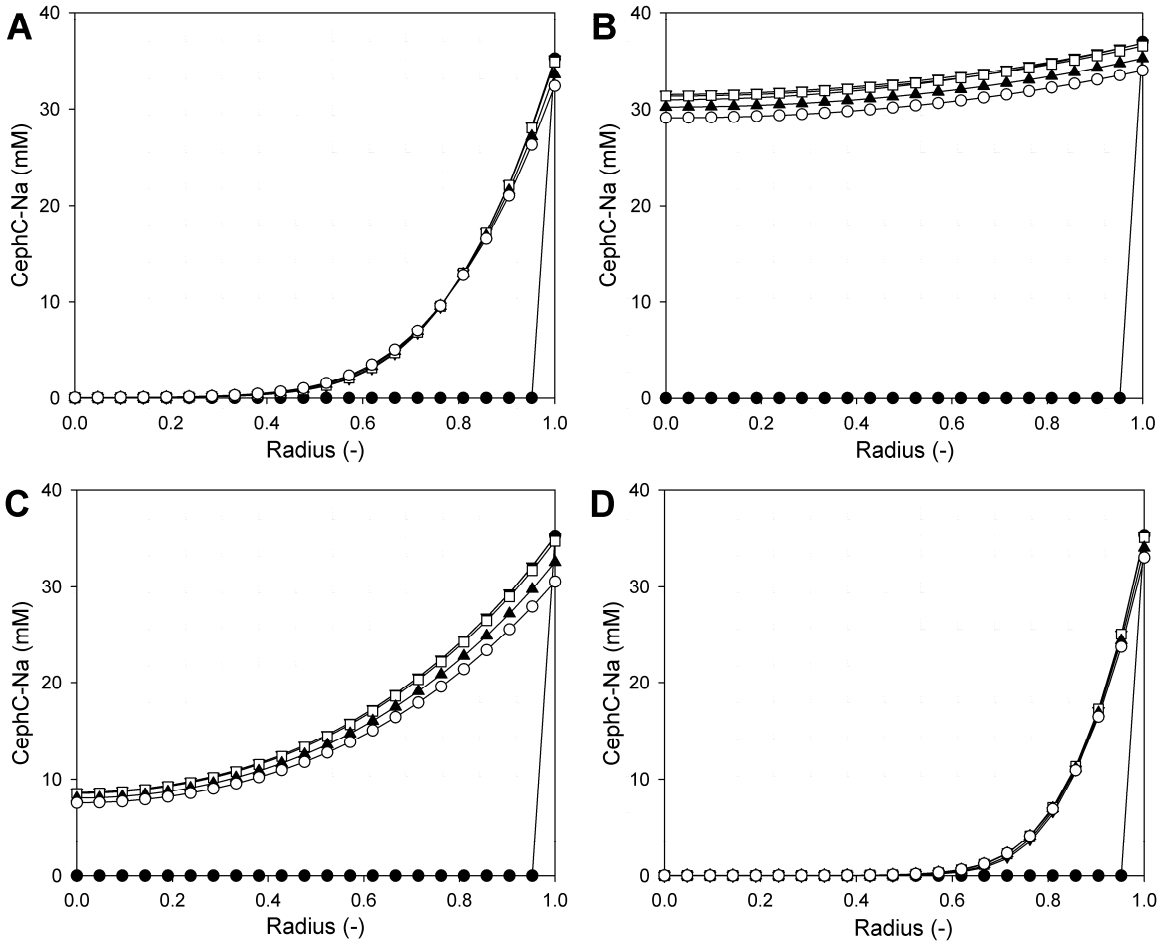

Figure S1. **Calculated CephC-Na concentrations in immobilized CephC amidase preparations.** (●) 0 sec; (·) 10 sec; (▼) 15 sec; (□) 100 sec; (▲) 500 sec; (○) 900 sec. Panel A. EXE096; Panel B. EXE030; Panel C. EXE096/SS; Panel D. EXE096/M.

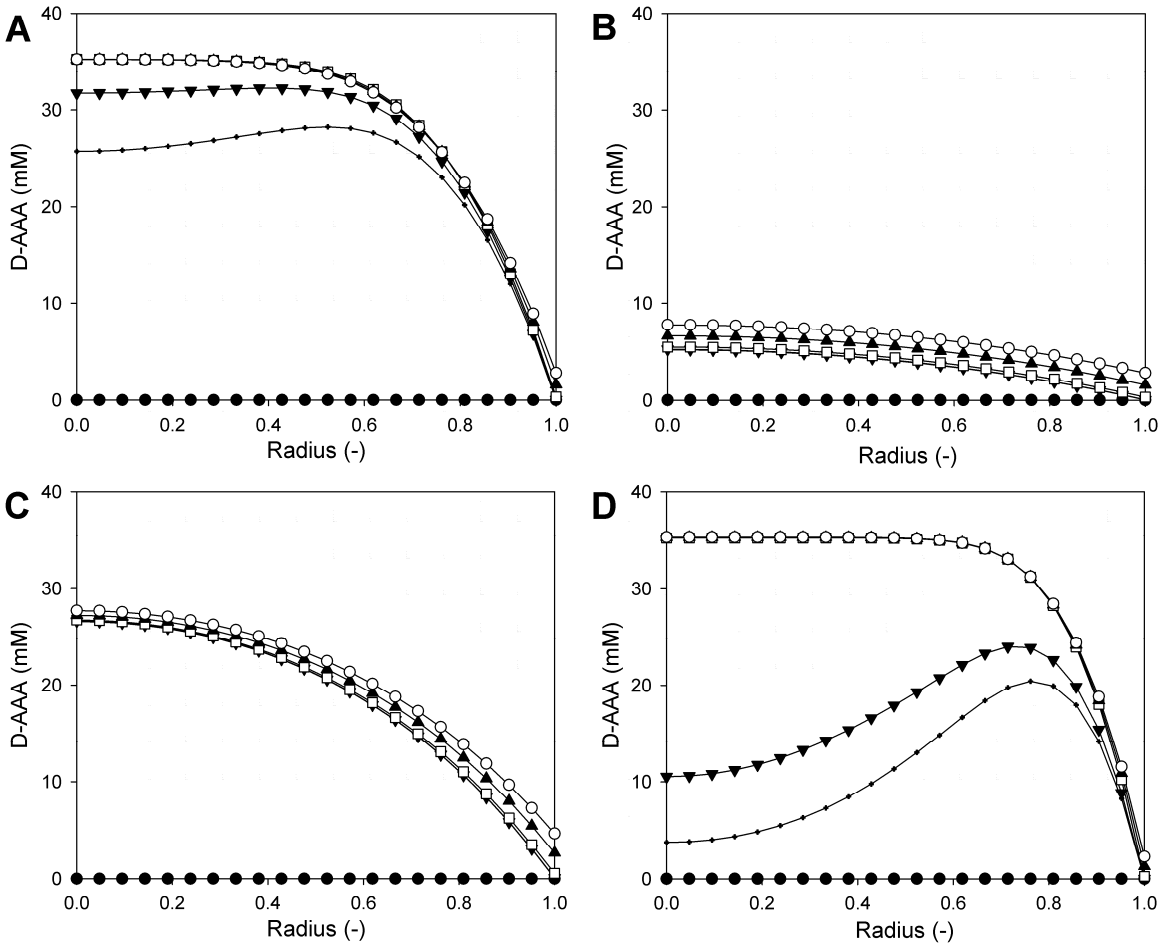

Figure S2. **Calculated D-AAA concentrations in immobilized CephC amidase preparations**. (●) 0 sec; (·) 10 sec; (▼) 15 sec; (□) 100 sec; (▲) 500 sec; (○) 900 sec. Panel A. EXE096; Panel B. EXE030; Panel C. EXE096/SS; Panel D. EXE096/M.

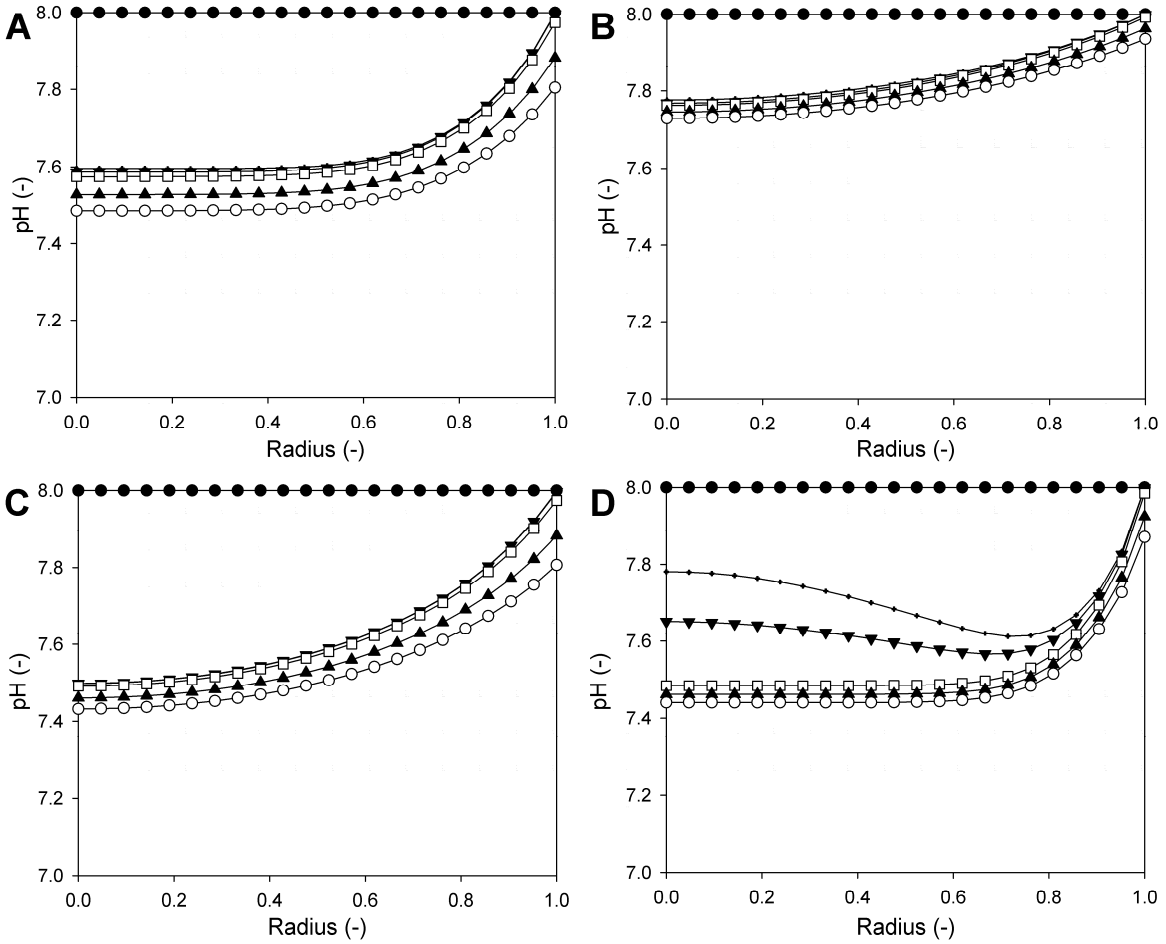

Figure S3. **Calculated pH in immobilized CephC amidase preparations**. (●) 0 sec; (●) 10 sec; (▼) 15 sec; (□) 100 sec; (▲) 500 sec; (○) 900 sec. Panel A. EXE096; Panel B. EXE030; Panel C. EXE096/SS; Panel D. EXE096/M.

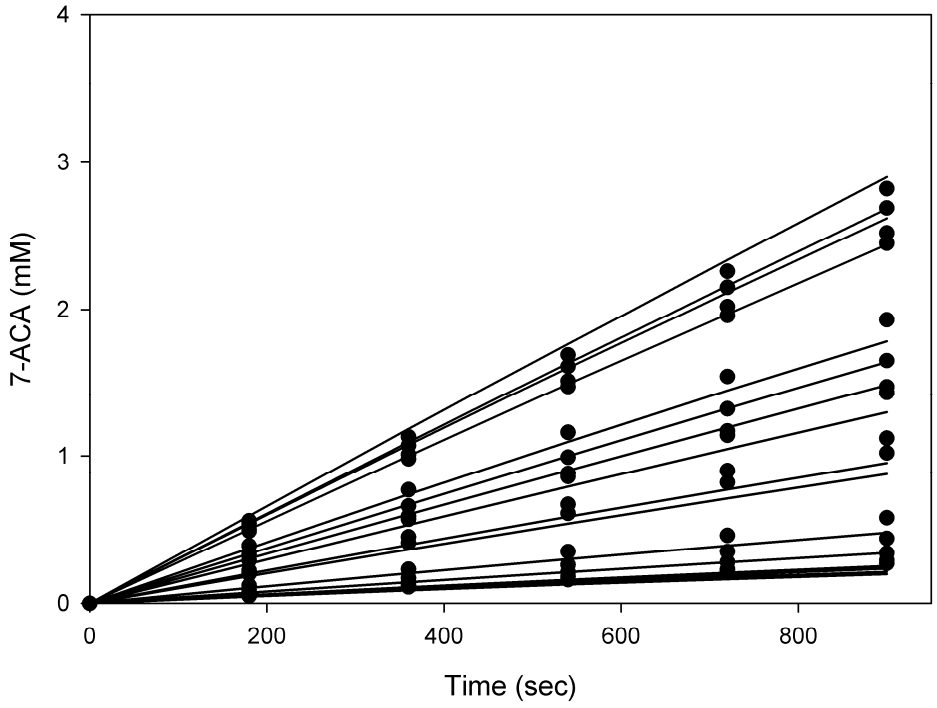

Figure S4. Experimental (●) and calculated (-) 7-ACA concentrations

Dual-lifetime referencing (DLR) for on-line monitoring of immobilized enzymes microenvironmental pH in stirred batch reactors

Caterina Boniello[1,2], Torsten Mayr[3] and Bernd Nidetzky[1,2,*]

[1] Austrian Center of Industrial Biotechnology - ACIB GmbH, Petersgasse 14, A-8010 Graz, Austria

[2]Institute of Biotechnology and Biochemical Engineering, Graz University of Technology, Petersgasse 12, A-8010 Graz, Austria

[3]Institute of Analytical Chemistry and Food Chemistry, Graz University of Technology, Technikerstraße 4, A-8010 Graz, Austria

* Corresponding author

Short title: pH monitoring in immobilized amidase

Email addresses:

CB: caterina.boniello@tugraz.at

TM: torsten.mayr@tugraz.at

BN: bernd.nidetzky@tugraz.at

Abstract

Background

pH changes in enzyme microenvironment have important influence on the charge distribution of the protein molecule. The reactivity of the active site groups and substrate binding are modified with considerable effects on enzymatic activity and structural stability. Many industrial biocatalysts are used as immobilized enzyme preparations. Near positive aspects like easy catalyst recovery, reusability and protein-free products, some effects related to the modification of the enzyme microenvironment due to the carrier have to be taken into account. In case of microporous supports, often preferred for covalent enzyme attachment, reactants have to diffuse from carrier surface to the enzyme active site and vice versa and may accumulate in the carrier itself. When reactions lead to formation of protons, the knowledge of pH profiles in the carrier microdomain becomes necessary to optimize biocatalysts performances.

Results

A simple and non-invasive method based on dual-lifetime referencing (DLR) for pH monitoring in immobilized biocatalysts is presented. The fluorescence intensities of two luminophores (fluorescein as pH indicator and Ru(II) tris(4,7-diphenyl-1,10-phenantroline) Ru(dpp) as reference) are converted in an overall phase shift that is recorded in a time-resolved way. Using the chosen combination of luminophores a pH range from 5.0 to 8.0 could be covered. Internal pH of immobilized Cephalosporin C amidase (CCA) was followed during Cephalosporin C hydrolysis in a stirred batch reactor under controlled pH conditions in the bulk liquid phase. A pH difference of about 1 unit between particles and bulk was observed after substrate addition, then pH in particles increased up to reaching equilibrium with the bulk in correspondence to the reaction to go to completion. Labeling of the biocatalyst did not affect protein loading and only slightly (lower than 10%) enzymatic activity.

Conclusions

The combined knowledge of carrier acidification and immobilized enzyme activity is crucial in the evaluation of the performances of immobilized CCA and other biocatalysts, which catalyze the formation of acidic products. The proposed methodology enables on-line monitoring on both variables also in stirred reactors and can be applied as valuable tool for efficient selection of carrier optimal geometrical characteristics.

Background

Enzyme immobilization, where the protein is tethered on the surface of an insoluble porous carrier, is often necessary for industrial application. It enables biocatalyst recovering and reuse and can prolong enzyme operational stability. [1] Carrier binding might anyway strongly influence the catalytic efficiency of an enzyme preparation. The properties of immobilized enzymes are in this case dictated by both enzyme and carrier and their interactions to each other [2] An accurate choice of the immobilization method and carrier characteristics becomes necessary to obtain optimal catalytic performances [2].

Hindered diffusion of reactants is one of the main reasons, why a loss in specific activity is often observed after enzyme immobilization, because of substrate depletion and product accumulation in the carrier [3]. When the biocatalytic reaction involves generation of an acidic product, a pH gradient may establish in the carrier, affecting enzyme activity, stability and reaction equilibrium [4].

Evaluation of diffusion limitation in porous catalyst is often performed through estimation of the Thiele modulus that expresses a ratio between a reaction rate and a diffusion rate [5]. Since carrier geometrical characteristics as well as reactant size are taken into account in this estimation, useful information for optimal carrier selection may be provided by this analysis.

Carrier acidification results as combination of the amount of generated product that is the enzymatic activity loaded on the carrier and hindered product diffusion because of carrier characteristics [6-7]. Experimental methods based on biocatalyst labeling with fluorescent pH indicators have been proposed in literature for evaluating the magnitude of pH gradients during the course of proton generating enzymatic reactions. The simplest way is to evaluate luminescence intensity changes of the pH indicator in response to increases in proton concentration. Spiess et al. [4] measured pH in biocatalytic particles in a stirred batch reactor, following the intensity of the pH-responsive fluorophore fluorescein isothiocyanate (FITC). Intensity-based measurements, anyway, are affected by drifts in the optoelectronic setup (light sources and light detectors) and by variation of the properties of the sensor layer (dye concentration or thickness) [8]. Combining the indicator with a reference dye and measuring emission or excitation at two different wavelengths may overcome some of these drawbacks. Referenced intensity measurements were performed with a confocal laser scanning microscope by Spiess and Kasche [9] and Huang et al. [6] for determining proton concentration in biocatalytic beads and membrane respectively. The possibility to determine pH gradients in a spatial-resolved way is definitively an advantage of this method. However, light scattering and reflection are not referenced because luminescence is measured at two wavelengths [10]. Equipment is furthermore expensive and not suitable for stirred reactors.

Lifetime measurements of indicators that show lifetime dependence on pH are more accurate because lifetime is independent of intensity or wavelength interferences [10]. Spiess et al. [11] evaluated the diffusion of a propionic acid into hydrogels measuring the pH-dependent resorufin lifetime using CLSM and pulsar excitation. Kuwana and coworker [12] applied a frequency domain proton migration (FDPM) technique to measure the phase shift and thus the lifetime of a pH-sensing fluorophore, carboxy seminaphthofluorescein-1 (C-SNAFL-1) immobilized in

poly(ethylene glycol) (PEG) microparticles. However, lifetime measurements in the nanoseconds range of fluorescent pH indicators, require sophisticated optoelectronic equipment [10] .

Hydrolysis of ester and amide is among the most important industrial enzymatic conversions. Considering the influence of carrier costs on biocatalyst production, the choice of a carrier tailored for the biocatalyst becomes a priority. The goal of this work is to propose an effective method for bioreactor monitoring that takes into account biocatalyst activity and at the same time the established pH in the immobilized enzyme microenvironment. As model biocatalyst we chose Cephalosporin C amidase (CCA) immobilized on epoxy-activated Sepabeads. This enzyme is responsible for the direct hydrolysis of cephalosporin C into 7-amino cephalosporanic acid (7-ACA) and D-α-amino adipic acid (DAAA). Product determination can be preformed by titration with an opportune base like NaOH. pH detection in the carrier has to be performed in stirred tank reactors, has to be detected in a time resolved-way and instrumentation must be cheap and easy to handle. The above reported methods are not applicable for these purposes or when they are, they might be too inaccurate, like the case of intensity-based measurements or require sophisticated equipments. Here we apply a pH detection method based on dual lifetime referencing (DLR) [13-14]. Combining a pH indicator with a reference standard, which shows similar excitation and emission spectra to the sensitive fluorophore, fluorescence intensity is converted into a phase shift [14]. The result is self-referenced measurements, not influenced by optical system interferences and relative independent of particle movements.

Results and discussion

Internal pH detection: choice of materials and sensor calibration

Dual lifetime referencing has been applied for opto-chemical sensor sensor for pH, oxygen, chloride, copper and ammonia [7, 9, 12-16]. In this work we apply DLR for pH detection in

immobilized biocatalysts, for monitoring acidification in immobilized CCA as consequence of DAAA and 7-ACA generation during cephalosporin C (sodium salt; CC-Na) hydrolysis.

To apply DLR for our purposes a pH-sensitive fluorophore with a fluorescence lifetime in the nanoseconds range is combined with a reference phosphore, which lifetime is in the microseconds range. Both are simultaneously excited at a common wavelength. After excitation in the frequency domain, their fluorescence intensities are converted in an overall phase shift that is related to the proton concentration. Essential for indicator and reference luminophores is to show overlapping excitation and emission spectra. Fluorescein and Ru(dpp) respond to these requisites [8, 10]. In order to attach these luminophores to the carrier without involving its functional groups necessary to enzyme immobilization, we opted for the more lipophilic variants 5(6)-N-octadecyl-carboxamidofluorescein and ruthenium(II)tris(4,7-diphenyl-1,10-phenanthroline di(trimethylsilylpropan sulfonate) respectively. This lipophilic dyes could be physically immobilized on the porous methacrylic polymer matrix of epoxy-activated Sepabeads.

Labeled biocatalyst particles were excited with a blue LED light at a wavelength of 470 nm. The excitation light was modulated sinusoidally with a frequency of 45 kHz.

In defined reaction conditions for each Fluorescein/Ru(dpp) ratio the detected phase shift depends only on the proton concentration. Note that Ru(dpp) is oxygen sensitive and the pH response depends on the oxygen partial pressure Therefore, measurements were performed under constant oxygen concentrations (air-saturation). The system is cross-sensitive to ionic strength and temperature. Calibration was performed in the same conditions as the sample.

Since the overall phase shift depends on the relative intensity of the two luminophores [14], decreasing the offered amount of Ru(dpp) in relation to fluorescein, will result in a lower phase shift. Indicator concentration effect on phase shift is reported in Figure 1. The higher the ratio between Ru(dpp) and fluorescein the higher the phase shift at a certain pH. In the applied working conditions, the chosen amounts of luminophores to label the carrier (fluorescein 2.5 mg

per gram dry carrier; Ru(dpp) 5 mg per gram dry carrier) lead to phase values between about 21° at pH 8.5 and 30° at pH 3.0 (Figure 2B) and were optimal to get the best phase resolution using the applied frequency.

Figure 2A shows how calibration was performed. Starting from pH 8.6, phase shift changes were recorded as response to bulk pH decrease by titration with suitable amounts (50-100 µL) of 1.2 M HCl. In correspondence to the each applied pH phase shift was recorded for 1 minute and an average value was calculated. Average values resulting from two independent titrations are plotted versus pH in figure 2B and fitted with a four parameters sigmoidal curve according to Equation 1 (R^2=0.9983) [15].

$$\Phi = \frac{A_{max} - A_{min}}{1 + 10^{(pH - pK_a')/x}} + A_{min} \qquad (1)$$

where Φ is the overall phase shift. A_{max} and A_{min} are values of the phase shift of the sample in fully protonated state (A_{min}) and fully deprotonated state (A_{max}). x is a numerical coefficient related to the slope of the curve. pK_a' is the apparent pK_a for the indicator/reference dye system immobilized on the enzyme carrier. In the applied working conditions (50 mM PPB) the pK_a' was calculated to be 5.80±0.05. Values for pK_a' as well for A_{max} and A_{min} and x resulting from fit are reported in Table 1.

On-line monitoring of internal pH and product formation

Internal particles pH was monitored for 1 hour during the biocatalytic conversion of 50 mM CC-Na performed by immobilized CCA. For each reaction batch (liquid volume 8.8 mL) 0.3 g wet biocatalyst were used, which correspond to an enzyme concentration of 0.65 mg/mL. First the immobilized enzyme was suspended in 8 mL 50 mM PPB pH 8.0. Phase shift at pH 8.0 was recorded for about 2 minutes before adding 800 µl 550 mM CC-Na to start the reaction (it was checked that the added liquid did not influence the recorded phase shift using buffer instead of substrate). Phase shift of the labeled biocatalytic particles was then converted in pH using the

calibration curve (Figure 2B). Figure 3A shows time-course of pH in bulk and in particles. In the bulk liquid phase pH was kept constant by titration of the generated acid with 0.1 M NaOH. pH in particles decreased fast upon substrate addition from pH 8.0 to approximately pH 6.9, showing acidic product accumulation in the carrier itself. During the catalytic reaction, pH in particles increased, reflecting the fact that the relative rate of reaction to diffusion decreased as consequence of substrate consumption, leading to equilibrium between internal and external pH approaching reaction completion.

The volume of titrating agent added for controlling bulk pH expresses acidic product concentration in the bulk liquid phase. Using the chosen enzyme and substrate concentrations, substrate conversion reached 60% after 1 hour. From the slope of the initial part of the curve (between 100 and 600 seconds), where the product dependence is linear versus time, enzymatic activity was calculated. For the 4 experiments reported in Figure 3B specific activity referred to the amount of bound protein was 1.48±0.02 U/mg. This result is in accord to the activity measured with the spectrophotometric assay in the same reaction conditions (1.45±0.01 U/mg).

Effect of labeling on protein loading and enzymatic activity

Fluorescein and Ru(dpp) were physically attached to the Sepabeads. Because of their lipophilic characteristics they could be adsorbed without involving the functional groups of the carrier, which remained available for enzyme immobilization. Comparison of protein loadings for fluorescence labeled and untreated carrier confirmed that the applied treatment did not influence enzyme binding (Table 2). On the other side, introducing indicator molecules in the enzyme microenvironment might alter the catalytic activity of immobilized CCA when interactions between indicators and protein occur [18]. However no effect on the specific reaction rate was observed as consequence of fluorescein labeling. The presence of Ru(dpp) caused a decrease of about 10% in the catalytic activity (Table 2).

Reproducibility and applicability

Figure 3A and 3B show pH and product time course obtained from three independent experiments. pH standard deviation was in the range of (0.10 pH units) at the beginning of the reaction and increased to 0.20 pH units after 1 hour. This increase is assumed to pH approaching 8.0 that corresponds to work far from pK_a' of the indicators system, at the boundary of the linear range of the sigmoidal curve (Figure 2B), where a certain phase perturbation results in higher changes in pH response.

On the other side reproducibility of product measurement was good as indicated in Figure 3B. Relative standard deviation calculated upon the four independent experiments was 4%.

A signal drift was observed that is assumed to leaching or photobleaching of indicator dye molecules. These effects result in losses in intensities of the luminophores contributing to the phase signal and are not referenced in DLR [10]. In order to avoid leaching we washed properly the labeled beads after each treatment, with 100 mM PPB pH 7.2, with deionized water and finally with the buffer used in the next step. A phase drift of 2.5° in 1 hour (equivalent to 1.5 pH units) was observed when sampling was performed every second. This increase in phase shift denotes decomposition of the pH indicator and is caused by singlet oxygen generation by the reference dye in the presence of molecular oxygen [15]. Lower phase drifts (1.8° in 1 hour equivalent to 1.2 pH units) were observed when sampling was performed every 5 seconds but signal resolution was not satisfactory, because it was not possible to apply a dynamic averaging of the collected values. Our attempts to lower the light intensity to decrease photo-bleaching by applying 10% of the available LED intensity did not improve the phase drift.

To overcome the problem of signal drift, a blank experiment was performed (Figure 4). The recorded phase values of the blank experiment were subtracted from the phase signals when measurements were performed.

Note that higher signal intensities on other hand are expected to increase the amplitude of the signal leading to more stable values, higher resolution and thus to smoother responses. Higher amplitude values and thus improved signal stability can be achieved increasing particle density. We adopted a compromise between enzyme concentration and labeled particles density.

Substrate auto-hydrolysis

In alkaline conditions and higher temperature CC-Na undergoes self-hydrolysis. Experimental set-up requires that enzyme has to be suspended first in the reactor to get an initial phase shift value at pH 8.0 and CC-Na has to be added at a second time to the reaction mixture to start the reaction. In order to cause as small as possible volume changes, the amount of added CC-Na did not exceeded 10% of the reaction volume. CC-Na solution was prepared at high concentration (550 mM) and its pH adjusted to 8.0 with 1 M KOH. In order to prevent self-hydrolysis of the CC-Na stock solution it was kept at 4°C until use checking pH correctness before conducting reactions. Anyway when substrate was added to the reactor a fast decrease in pH was observed, likely due to temperature increase (37°C). NaOH titration curves for the enzymatic reactions were thus corrected with a blank obtained titrating substrate in absence of enzyme. Figure 5 shows that after an initial fast hydrolysis self-hydrolysis proceeded linearly versus time. Self-hydrolysis rate was calculated to be 0.68 μmol per minute.

Conclusions

Dual lifetime referencing, an established method in opto-chemical sensors, is here applied to internal pH monitoring of stirred biocatalyst particles. This method allows pH monitoring in moving particles improving the signal quality of intensity based-measurement and overcoming the limit of microscopic techniques that require the use of fixed bad reactors or membranes for the sample to be analyzed. This is definitely an advantage for bioreactor monitoring being batch reactors the preferred choice for biocatalytic conversions. Considering the lipophilic character of

the chosen luminophores the proposed labeling methodology is applicable to a variety of hydrophobic carriers independently of their functional activation. Reproducibility of results was satisfactory. The observed drift in the phase signal due to photobleaching could compensated by calibration. The use of recently developed red light-excitable pH sensing materials [17], which exhibit chemical and photochemical robustness and are not affected by oxygen, could overcome this disadvantage.

Methods

Dual luminescence labeling

A stock solution of fluorescein (2 mg/mL in ethanol) was prepared and successively diluted with 100 mM PPB pH 7.2 (5% (v/v)). 1.6 g dry Sepabeads were incubated with 40 mL of this solution at room temperature (mixing overnight; 15 rpm; end-over-end rotator). After opportune washing (100 mM PPB pH 7.2, deionized water and 1.5 M PPB pH 7.5) CCA was immobilized (see later) on the labeled beads. After enzyme immobilization and opportune washing, beads were incubated for 10 min (room temperature, 15rpm, end-over-end reactor) with 40 mL of a solution constituted by 10% (v/v) Ru(dpp) (2 mg/mL in ethanol) and 90% (v/v) 100 mM PPB pH 7.2. The last wash was performed with 50 mM PPB pH 8.0. Beads were finally recovered by filtration through a 0.20 μm membrane filter.

Measurement of internal pH

Phase shift measurements were performed with a lock-in amplifier (pH-mini, PreSens GmbH, Germany). This apparatus consists in a blue LED light source (excitation frequency at 470 nm), a 2-mm polymer optical fiber as transducer with a polished distal tip and a photodetector (emission is collected after filtering at 550 nm). Measurements were carried out in the frequency domain, adjusting the modulation frequency to the decay time of Ru(dpp) (modulation frequency of 45 kHz). Time-resolved recorded phase shift was than converted in pH through the calibration curve.

Experimental set-up

CC-Na hydrolysis was carried out in a 20 mL batch reactor equipped with an overcoat for temperature control. About 0.3 g wet biocatalyst were suspended in 8 mL 50 mM PPB pH 8.0. If necessary was adjusted with pretitration with 0.1 M NaOH. A titrator (T-50, Mettler Toledo, Greifensee, Switzerland) equipped with a pH electrode (Minitrode, Hamilton, Bonaduz, Switzerland) was used for stirring and pH control in bulk. Stirring rate was set at 10%. The hydrolytic reaction was started adding 800 µl 550 mM CC-Na pH 8.0 previously kept at 4°C. pH-sta (pH 8.0) was performed by addition of 0.1 M NaOH (Roth, Germany). Temperature was kept at 37°C by circulation in the reactor overcoat of a preheated fluid.

For phase shift detection of the labeled particles the 2-mm polymer optical fiber connected to pH-mini was fixed inside the reactor in correspondence of the pH-electrode.

Enzyme Immobilization

An engineered CCA from Pseudomonas sp. SE83 (more details on this enzyme were previously reported [19]) was covalently immobilized on standard grade epoxy-activated Sepabeads (Resindion, Milan, Italy). The protein was obtained from Sandoz GmbH (Kundl, Austria) as partially purified preparation (4.5 U/mg, 60% purity). Protein concentration was 36.5 mg/mL. For immobilization we adopted the method of Mateo et al. [20] with some simplifications. A solution constituted by 3.5 mL enzyme stock solution, 16.5 mL 20 mM PPB pH 7.5 and 20 mL 1.5 mM PPB pH 7.5 was added to 1.6 g dry labeled Sepabeads. The 50 mL vessel containing the suspension was incubated at 18°C using gentle mixing (5 rpm) in an end-over-end rotator. After 24 hours the immobilized CCA was washed twice with 20 mM PPB pH 7.5 and recovered using a 0.20 µm membrane filter and stored at 4°C until further use.

Protein and activity assay

Protein was measured using the Bio-Rad assay referenced against known concentrations of BSA in the range of 0.10 - 1.0 mg/mL.

Activity measurements of free and immobilized CCA were performed using a reported spectrophotometric assay [21] with some modifications as previously described [19].

Authors' contributions

CB, TM and BN designed research; CB performed experiments and analyzed data; CB, TM and BN wrote the paper.

Acknowledgements

The Austrian Research Promotion Agency (FFG), the Province of Styria, the Styrian Business Promotion Agency (SFG), the city of Graz, and Sandoz GmbH are acknowledged for financial support. We are grateful to Dr. Paolo Caimi (Resindion Srl) for supplying Sepabeads resins.

References

1. Buchholz K, Kasche V, Bornscheuer UT: *Biocatalysts and enzyme technology.* Weinheim: Wiley-VCH; 2005.
2. Tischer W, Kasche V: **Immobilized enzymes: crystals or carriers?** *Trends Biotechnol* 1999, **17:**326-335.
3. Kallenberg AI, van Rantwijk F, Sheldon RA: **Immobilization of penicillin G acylase: The key to optimum performance.** *Adv Synth Catal* 2005, **347:**905-926.
4. Spiess A, Schlothauer RC, Hinrichs J, Scheidat B, Kasche V: **pH gradients in immobilized amidases and their influence on rates and yields of beta-lactam hydrolysis.** *Biotechnology and Bioengineering* 1999, **62:**267-277.
5. Bailey JE, Ollis DF: *Biochemical engineering fundamentals.* New York: McGraw-Hill; 1986.
6. Huang HY, Shaw J, Yip C, Wu XY: **Microdomain pH gradient and kinetics inside composite polymeric membranes of pH and glucose sensitivity.** *Pharm Res* 2008, **25:**1150-1157.
7. Janssen MHA, van Langen LM, Pereira SRM, van Rantwijk F, Sheldon RA: **Evaluation of the performance of immobilized penicillin G acylase using active-site titration.** *Biotechnology and Bioengineering* 2002, **78:**425-432.

8. Vasylevska GS, Borisov SM, Krause C, Wolfbeis OS: **Indicator-loaded permeation-selective microbeads for use in fiber optic simultaneous sensing of pH and dissolved oxygen.** *Chem Mater* 2006, **18:**4609-4616.
9. Spiess AC, Kasche V: **Direct measurement of pH profiles in immobilized enzyme carriers during kinetically controlled synthesis using CLSM.** *Biotechnol Progr* 2001, **17:**294-303.
10. Liebsch G, Klimant I, Krause C, Wolfbeis OS: **Fluorescent imaging of pH with optical sensors using time domain dual lifetime referencing.** *Anal Chem* 2001, **73:**4354-4363.
11. Spiess AC, Zavrel M, Ansorge-Schumacher MB, Janzen C, Michalik C, Schmidt TW, Schwendt T, Buchs J, Poprawe R, Marquardt W: **Model discrimination for the propionic acid diffusion into hydrogel beads using lifetime confocal laser scanning microscopy.** *Chem Eng Sci* 2008, **63:**3457-3465.
12. Kuwana E, Liang F, Sevick-Muraca EM: **Fluorescence lifetime spectroscopy of a pH-sensitive dye encapsulated in hydrogel beads.** *Biotechnol Progr* 2004, **20:**1561-1566.
13. Huber C, Klimant I, Krause C, Wolfbeis OS: **Dual lifetime referencing as applied to a chloride optical sensor.** *Anal Chem* 2001, **73:**2097-2103.
14. Mayr T, Klimant I, Wolfbeis OS, Werner T: **Dual lifetime referenced optical sensor membrane for the determination of copper(II) ions.** *Anal Chim Acta* 2002, **462:**1-10.
15. Kocincova AS, Borisov SM, Krause C, Wolfbeis OS: **Fiber-optic microsensors for simultaneous sensing of oxygen and pH, and of oxygen and temperature.** *Anal Chem* 2007, **79:**8486-8493.
16. Kocincova AS, Nagl S, Arain S, Krause C, Borisov SM, Arnold M, Wolfbeis OS: **Multiplex bacterial growth monitoring in 24-well microplates using a dual optical sensor for dissolved oxygen and pH.** *Biotechnology and Bioengineering* 2008, **100:**430-438.
17. Borisov SM, Gatterer K, Klimant I: **Red light-excitable dual lifetime referenced optical pH sensors with intrinsic temperature compensation.** *Analyst* 2010, **135:**1711-1717.
18. Weidgans BM, Krause C, Klimant I, Wolfbeis OS: **Fluorescent pH sensors with negligible sensitivity to ionic strength.** *Analyst* 2004, **129:**645-650.
19. Boniello C, Mayr T, Klimant I, Koenig B, Riethorst W, Nidetzky B: **Intraparticle concentration gradients for substrate and acidic product in immobilized cephalosporin C amidase and their dependencies on carrier characteristics and reaction parameters.** *Biotechnol Bioeng* 2010, **106:**528-540.
20. Mateo C, Abian O, Fernandez-Lorente G, Pedroche J, Fernandez-Lafuente R, Guisan JM: **Epoxy sepabeads: A novel epoxy support for stabilization of industrial enzymes via very intense multipoint covalent attachment.** *Biotechnol Progr* 2002, **18:**629-634.
21. Patett F, Fischer L: **Spectrophotometric assay for quantitative determination of 7-aminocephalosporanic acid from direct hydrolysis of cephalosporin C.** *Anal Biochem* 2006, **350:**304-306.

Tables

Table 1. Effect of buffer concentration on fit parameters of the pH/Phase calibration curve (Equation 1) at 37°C

Buffer[a]	A_{max} (°)	A_{min} (°)	pK_a	x	R^2
50 mM PPB	31.1±0.7	20.2±0.23	5.80±0.05	1.26±0.08	0.9983
100 mM PPB	31.5±0.3	20.9±0.11	6.36±0.02	0.80±0.02	0.9997

[a]Ionic strength 50 mM PPB 0.139 M; Ionic strength 100 mM PPB 0.279 M

Table 2. Effect of luminophores labeling on protein loading and specific activity of immobilized CCA

Labeling	*Offered protein (mg/g dry)*	*Bound protein (mg/g dry)*	*Specific activity* [a] *(U/mg)*
Fluorescein	85	68	1.66±0.06
Fluorescein+ Ru(dpp)	85	68	1.50±0.09
None	82	64	1.74±0.17

[a] Specific activity was measured with the spectrophotometric assay: 40 mM CC-Na; 100 mM PPB pH 8.0; 37°C

Figures

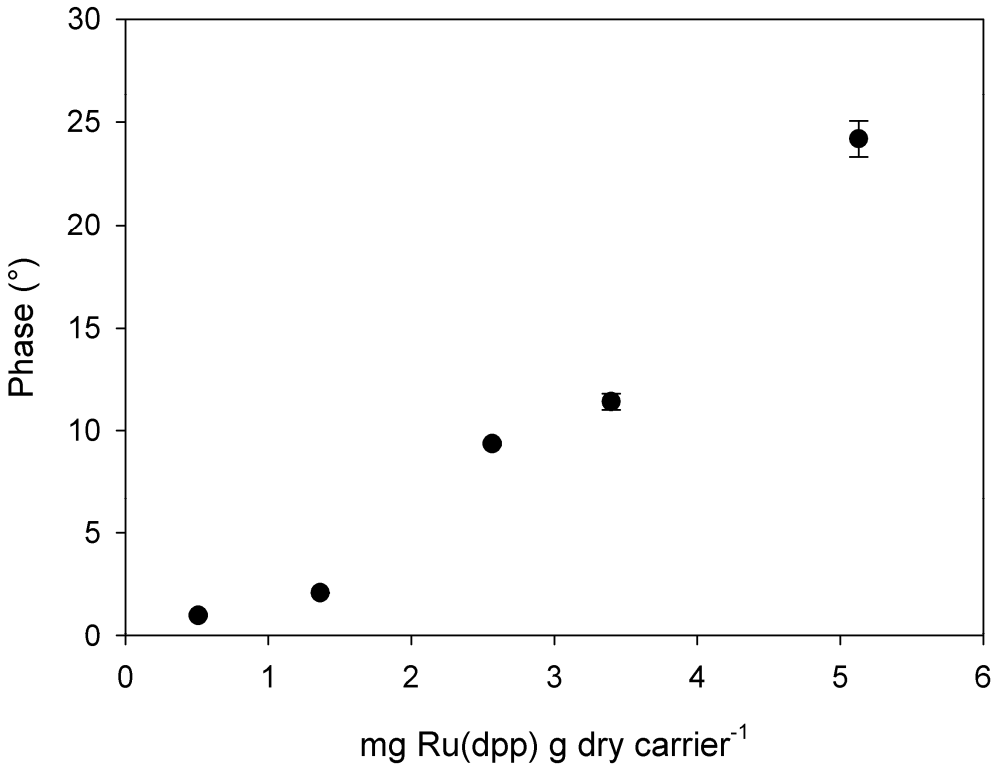

Figure 1. Effect on phase shift of Ru(dpp) amount in relation to fluorescein.

50 mM PPB pH 8.0; 37°C; Fluorescein 2.5 mg/g dry; modulation frequency 45 kHz.

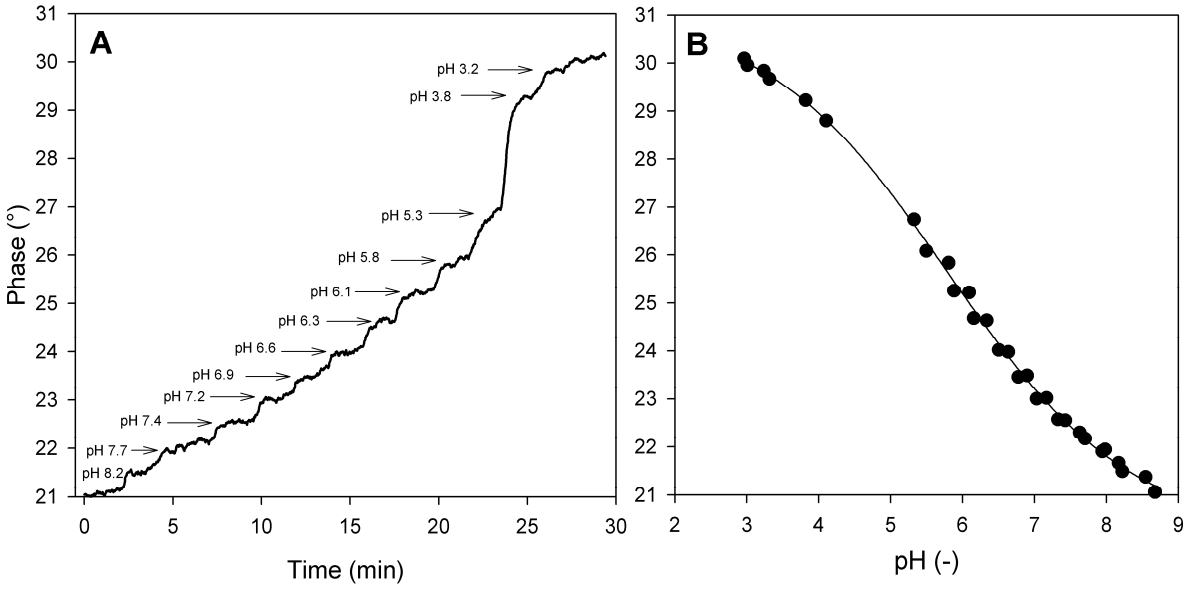

Figure 2. Response curve to pH (Panel A) and calibration curve (panel B).

50 mM PPB; 37°C.

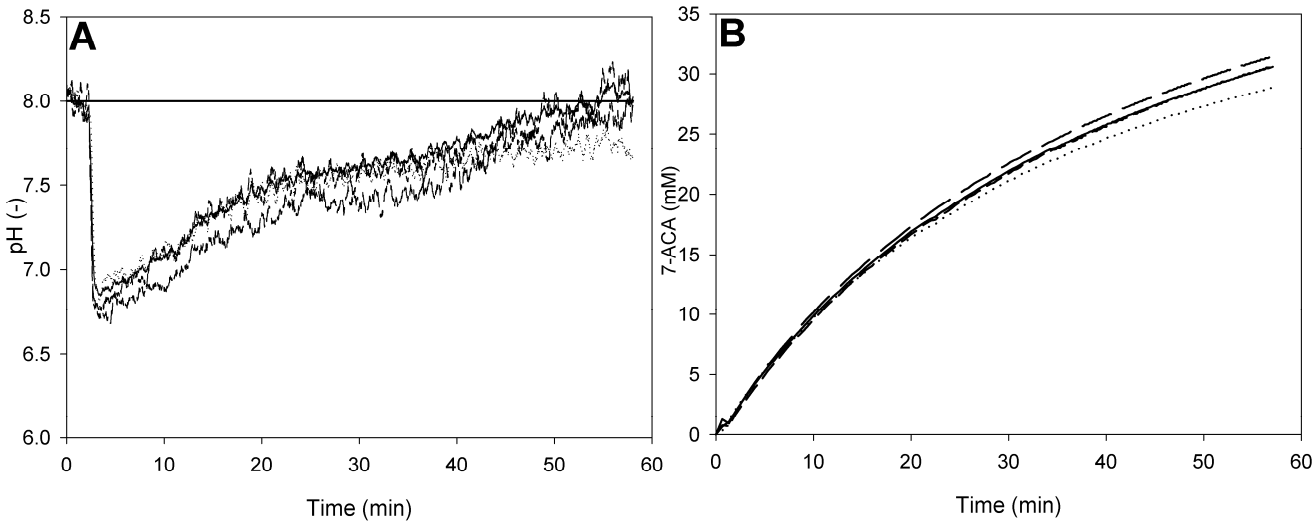

Figure 3. Panel A. Internal pH in immobilized CCA as result of 3 independent experiments. Panel B. 7-ACA concentration in the bulk liquid phase.

Long dashed line Exp A; Dotted Exp B; Short dashed Exp C; Solid average. pH in bulk is kept constant to pH 8.0 by titration with 0.1 NaOH. 0.65 mg/mL CCA; 50 mM CC-Na; 50 mM PPB pH 8.0.

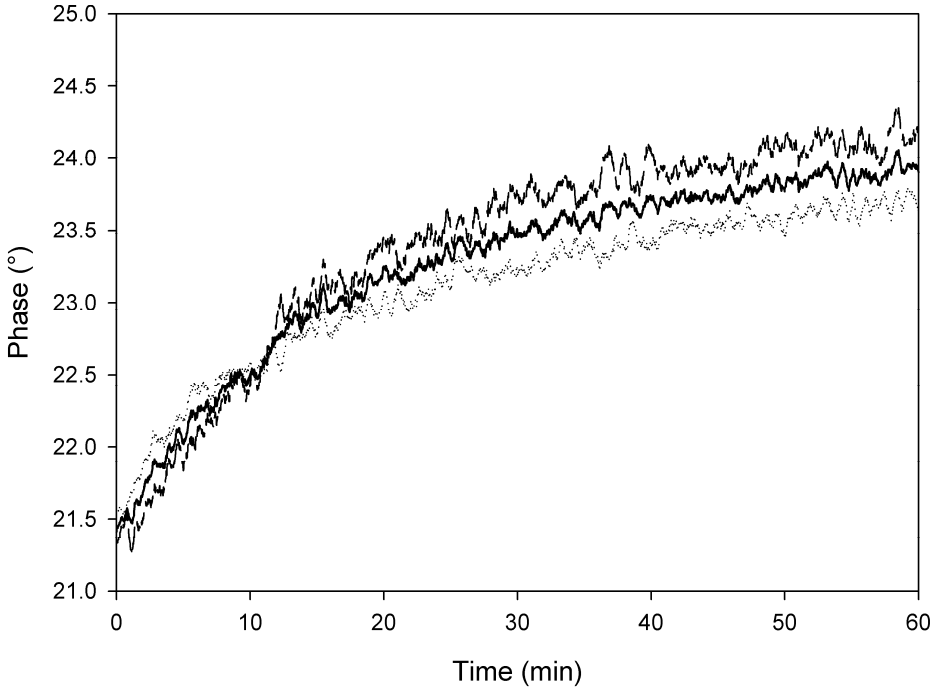

Figure 4. Phase drift as effect of light excitation.

Sampling rate every second; LED intensity 10%. Dashed line Exp A; Dotted line Exp B; Solid line average.

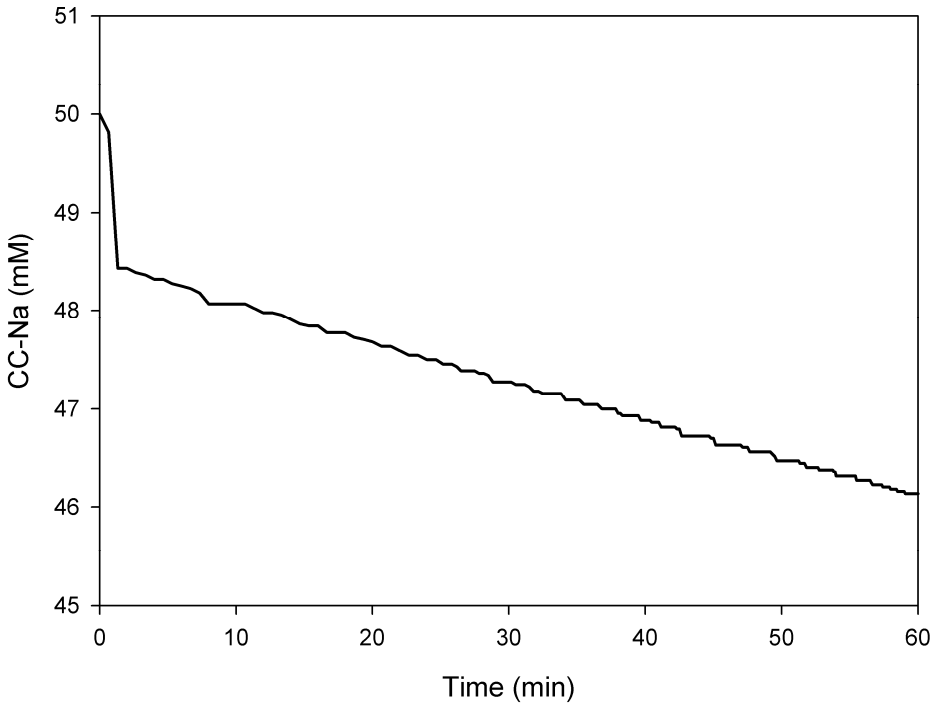

Figure 5. CC-Na self-hydrolysis.

800 µl 550 mM CC-Na pH 8.0 added to 8 mL 50 mM PPB pH 8.0; 37°C.

List of Publications

Measurement and Modeling of Mass Transfer Effects for Rational Design of Immobilized Biocatalysts

Caterina Boniello and Bernd Nidetzky

Manuscript in preparation

Intraparticle Concentration Gradients for Substrate and Acidic Product in Immobilized Cephalosporin C Amidase and Their Dependencies on Carrier Characteristics and Reaction Parameters

Caterina Boniello, Torsten Mayr, Ingo Klimant, Burghard Koenig, Waander Riethorst[1], and Bernd Nidetzky

Biotechnology and Bioengineering, Vol. 106, No. 4, 2010

Acidic Product Accumulation in Immobilized Cephalosporin C Amidase Characterized By Experiment and Modeling: Implications For Optimal Carrier Selection

Caterina Boniello and Bernd Nidetzky

Manuscript in preparation

Dual-lifetime Referencing (DLR) for On-line Monitoring of Immobilized Enzymes Microenvironmental pH in Stirred Batch Reactors

Caterina Boniello, Torsten Mayr and Bernd Nidetzky

Manuscript in preparation